

## RMIS View/Print Document Cover Sheet

This document was retrieved from the Documentation and Records Management (DRM) ISEARCH System. It is intended for Information only and may not be the most recent or updated version. Contact a Document Service Center (see Hanford Info for locations) if you need additional retrieval information.

Accession #: D196063543

Document #: SD-WM-ER-555

Title/Desc:

THERMAL HYDRAULIC BEHAVIOR EVALUATION OF TANK A101

Pages: 165

MAR 27 1995

ENGINEERING DATA TRANSMITTAL

1. EDT No 613544

2. To: (Receiving Organization) Distribution	3. From: (Originating Organization) Plant Engineering Analysis	4. Related EDT No.: N/A
5. Proj./Prog./Dept./Div.: W74A50	6. Cog. Engr.: D. M. Ogden	7. Purchase Order No.: N/A
8. Originator Remarks:  Approval/Release		9. Equip./Component No.: N/A
		10. System/Bldg./Facility: N/A
11. Receiver Remarks:		12. Major Assm. Dwg. No.: N/A
		13. Permit/Permit Application No.: N/A
		14. Required Response Date:

15. DATA TRANSMITTED					(F)	(G)	(H)	(I)
(A) Item No.	(B) Document/Drawing No.	(C) Sheet No.	(D) Rev. No.	(E) Title or Description of Data Transmitted	Approval Designator	Reason for Transmittal	Originator Disposition	Receiver Disposition
1	WHC-SD-WM-ER-555		0	Thermal Hydraulic Behavior Evaluation of Tank A-101	N/A	1	1	

16. KEY		
Approval Designator (F)	Reason for Transmittal (G)	Disposition (H) & (I)
E, S, O, D or N/A (see WHC-CM-3-5, Sec. 12.7)	1. Approval 2. Release 3. Information 4. Review 5. Post-Review 6. Dist. (Receipt Acknow. Required)	1. Approved 2. Approved w/comment 3. Disapproved w/comment 4. Reviewed no/comment 5. Reviewed w/comment 6. Receipt acknowledged

17. SIGNATURE/DISTRIBUTION (See Approval Designator for required signatures)										(G)	(H)
Reason	Disp.	(J) Name	(K) Signature	(L) Date	(M) MSIN	(J) Name	(K) Signature	(L) Date	(M) MSIN	Reason	Disp.
1	1	Cog. Eng.	<i>D. M. Ogden</i>	<i>3/25/95</i>	HO-34						
1	1	Cog. Mgr.	<i>D. M. Ogden</i>	<i>3/25/95</i>	HO-34						
		QA									
		Safety									
		Env.									
1	1	M. J. Thurgood	<i>mj Thurgood</i>	<i>3/25/95</i>	HO-34						

18. <i>D. M. Ogden</i> D. M. Ogden Signature of EDT Originator Date: <i>3/26/95</i>	19. _____ Authorized Representative for Receiving Organization Date	20. <i>D. M. Ogden</i> D. M. Ogden Cognizant Manager Date: <i>3/26/95</i>	21. DOE APPROVAL (if required) Ctrl. No. <input type="checkbox"/> Approved <input type="checkbox"/> Approved w/comments <input type="checkbox"/> Disapproved w/comments
--	---	--	---

# Thermal Hydraulic Behavior Evaluation of Tank A-101

D. M. Ogden

Westinghouse Hanford Company, Richland, WA 99352  
U.S. Department of Energy Contract DE-AC06-87RL10930

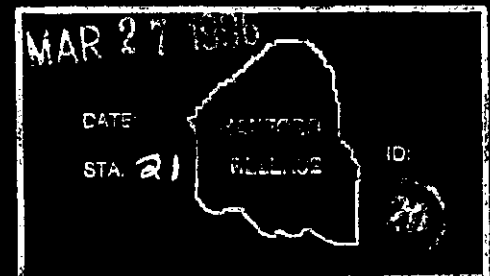
EDT/ECN: 613544 UC: 2020  
Org Code: 74A50 Charge Code: N2203  
B&R Code: EW3135040 Total Pages: 162

Key Words: Tank A-101, thermal hydraulic, temperature data, heatup, waste, conductivity, soil

Abstract: This report describes a new evaluation conducted to help understand the thermal-hydraulic behavior of tank A-101. Prior analysis of temperature data indicated that the dome space and upper waste layer was slowly increasing in temperature. This evaluation indicates that dome and upper waste temperature increases are due to increasing ambient temperatures and termination of forced ventilation. However, this analysis also indicates that other dome cooling processes are slowly decreasing, or some slow increase in heating is occurring at the waste surface. Dome temperatures are not decreasing at the rate expected as a consequence of radiolytic decay when ambient temperature changes and forced ventilation termination effects are accounted for.

TRADEMARK DISCLAIMER. Reference herein to any specific commercial product, process, or service by trade name, trademark, manufacturer, or otherwise, does not necessarily constitute or imply its endorsement, recommendation, or favoring by the United States Government or any agency thereof or its contractors or subcontractors.

Printed in the United States of America. To obtain copies of this document, contact: WHC/BCS Document Control Services, P.O. Box 1970, Mailstop H6-08, Richland WA 99352, Phone (509) 372-2420; Fax (509) 376-4989.



*Dennis Bishop* 3/27/96  
Release Approval Date

Release Stamp

Approved for Public Release

WHC-SD-WM-ER-555  
Rev. 0

THERMAL-HYDRAULIC BEHAVIOR EVALUATION  
OF  
TANK A-101

D. M. Ogden  
Westinghouse Hanford Company

by  
B. C. Fryer  
M. J. Thurgood  
JOHN MARVIN, INC.

March 1996

Issued by  
WESTINGHOUSE HANFORD COMPANY  
for the

U.S. DEPARTMENT OF ENERGY  
RICHLAND OPERATIONS OFFICE  
RICHLAND, WASHINGTON

## TABLE OF CONTENTS

1.	SUMMARY.....	1
2.	INTRODUCTION.....	4
2.1.	RELATED PRIOR ANALYSIS.....	4
2.2.	OVERVIEW OF POTENTIAL EXPLANATIONS FOR TANK A-101 THERMAL HYDRAULIC BEHAVIOR.....	6
3.	TANK A-101, TANK FARM A, AND VENTILATION SYSTEM DESCRIPTION.....	15
3.1.	TANK A-101 .....	15
3.2.	TANK FARM A AND VENTILATION SYSTEM.....	20
4.	TANK A-101 TEMPERATURE DATA.....	25
4.1.	DYNAMIC DATA.....	25
4.2.	TIME AVERAGED DATA.....	35
4.2.1.	Time Averaged Axial Temperature Difference.....	35
4.2.2.	Temperatures versus Time--Linear Fit.....	40
4.3.	TIME RATE OF CHANGE OF FIRST AND SECOND ORDER SPATIAL TEMPERATURE DIFFERENCES .....	48
4.3.1.	Second Order Calculation of Time Rate of Change in Heat Generation.....	49
4.3.2.	First Order Calculation of Time Rate of Change in Temperature Differences and Heat Generation Rate.....	56
4.3.2.1.	Time Rate of Change of Spatial Temperature Differences 1990-1/1996..	59
4.3.2.2.	Time Rate of Change in Spatial Temperature Differences, Linear Fits, and Half Lives 1993-1/1996.....	66
4.3.2.3.	Time Rate of Change in Heat Generation Rate Based on First Order Spatial Temperature Differences.....	74
5.	MODELING AND ANALYSIS METHODOLOGY AND GOTH MODEL DESCRIPTIONS.....	79

5.1.	GOTH MODEL DESCRIPTION.....	79
5.2.	ESTIMATES OF THERMOPHYSICAL PROPERTIES AND OPERATING CONDITION PARAMETERS.....	84
6.	HUB SCOPEING AND ANALYTICAL CALCULATION RESULTS....	101
6.1.	SIMPLE ANALYTICAL MODEL ESTIMATE OF THERMAL CHARACTERISTICS .....	101
6.2.	EFFECT OF ANNUAL METEOROLOGICAL CYCLE ON WASTE AND DOME GAS TEMPERATURE .....	108
6.3.	ESTIMATED EFFECT OF ADJACENT TANKS .....	115
6.4.	HEAT REMOVAL AND SLURRY DRYOUT RATES VIA EVAPORATION .....	122
7.	GOTH SIMULATION RESULTS.....	130
7.1.	CONSTANT DOME COOLING MECHANISM .....	132
7.1.1.	Constant Meteorological Conditions.....	132
7.1.2.	Annual Cyclic Meteorological Conditions..	134
7.2.	DECREASING DOME COOLING MECHANISM .....	136
7.2.1.	Constant Meteorological Conditions.....	136
7.2.2.	Annual Cyclic Meteorological Conditions..	139
7.3.	DECREASING DOME COOLING MECHANISM COMBINED WITH FORCED VENTILATION PERIOD IN 1990.....	141
7.3.1.	Constant Meteorological Conditions.....	141
7.3.2.	Annual Cyclic Meteorological Conditions..	143
8.	CONCLUSIONS.....	150
9.	REFERENCES.....	152

## LIST OF FIGURE

2.1 Tank A-101 Temperature Rate of Change Location--Linear Term of Fourier Series Fit (1/93-9/95) .....	5
2.2 Annual Average Temperature .....	10
3.1 Tank A-101 Basic Dimensions, Thermocouple Elevations Relative to Tank Bottom Inside, and Approximate Thermocouple Tree Radial Location .....	16
3.2 Tank A-101 Level Versus Time .....	17
3.3 Various Level Measurements and Estimates for Hanford Waste Tank A-101 .....	19
3.4 A Tank Farm--Relative Location of Tanks and Thermocouple Tree in Tank A-101 .....	22
3.5 A Tank Farm Distance to Groundwater .....	24
4.1 Tank A-101 Thermocouples 1-10 Temperature Data Versus Time .....	28
4.2 Tank A-101 Thermocouples 9-18 Temperature Data Versus Time (upper waste layer, waste/gas interface, dome gas).....	29
4.3 Tank A-101 Thermocouples 9-18 Temperature Data Versus Time (upper waste layer, waste/gas interface, dome gas).....	32
4.4 Tank A-101 Thermocouples 1-10 Lower Waste Temperature Data Versus Time .....	33
4.5 Tank A-101 Thermocouples 1-10 Lower Waste Temperature Data Versus Time .....	34
4.6 Tank A-101 Temperature versus Location-- Constant Term of Fourier Series Fit (Essentially time average temperature, 1/93-9/95, versus location)...	37
4.7 Tank A-101 Time Averaged Axial Temperature Distribution Comparison--Prior Analysis and Current Evaluation .....	39

4.9 Temperature vrs Time and Linear Fits TC-5 through TC-8 .....	42
4.10 Temperature vrs Time and Linear Fits TC-9 through TC-12 .....	43
4.11 Temperature vrs Time and Linear Fits .....	44
4.12 Temperature vrs Time and Linear Fits TC-16 through TC-18, and Ambient Monthly Average .....	45
4.13 Tank A-101 Temperature Rate of Change versus Axial Location--Reference and Current Analyses .....	47
4.14 Relative Magnitude of Volumetric Heat Generation Rate and Stored Energy Change Rates.....	52
4.15 Volumetric Heat Generation Rates vrs Time, Linear Fits, and Half Lives .....	54
4.16 Volumetric Heat Generation Rates vrs Time, and Linear Fits and Half Lives.....	55
4.17 Tank A-101 Thermocouples 1-5 Temperature Data Differences Versus Time.....	60
4.18 Tank A-101 Thermocouples 5-9 Temperature Data Differences Versus Time.....	61
4.19 Tank A-101 Thermocouples 9-16 Temperature Data Differences Versus Time.....	62
4.20 Tank A-101 Thermocouples 16-18 Temperature Data Differences Versus Time.....	63
4.21 Tank A-101 Thermocouples 1, 9, 16 and Ambient Temperature Difference Data Versus Time .....	65
4.22 Temperature Differences vrs Time, Linear Fits, and Half Lives .....	68
4.23 Temperature Difference vrs Time, Linear Fits, and Half Lives .....	69
4.24 Temperature Difference vrs Time, Linear Fits, and Half Lives .....	70
4.25 Temperature Difference vrs Time, Linear Fits, and Half Lives .....	71
4.26 Temperature Difference vrs Time, Linear Fits, and Half Lives .....	72
4.27 Temperature Difference vrs Time, Linear Fits, and Half Lives .....	73
4.28 Volumetric Heat Generation Rates vrs Time, Linear Fits, and Half Lives .....	75

4.29 Volumetric Heat Generation Rates vrs Time, Linear Fits, and Half Lifes .....76

4.30 Volumetric Heat Generation Rates vrs Time, Linear Fits, and Half Lifes .....77

4.31 Volumetric Heat Generation Rate vrs Time, Linear Fits, and Half Lifes .....78

5.1 Tank A-101 1-D GOTH Nodalization Diagram .....81

5.2 Variable Meteorology Dry Bulb Temperature History Assumed .....83

5.3 Energy Transport Processes and Parameters Under No Air Inleakage Conditions .....86

5.4 Energy Transport Processes and Parameters Under Air Inleakage Conditions .....87

5.5 Time Averaged Parameter Compatibility Requirements .....89

5.6 Dynamic Parameter Compatibility Requirements .....90

5.7 Two Layer Classical Conduction Solution Approximation for the Temperature Distribution ....95

5.8 Comparison of GOTH Steady State Temperature Distribution to Data and Classical Approximation ..96

5.9 Estimated Tank A-101 Radiolytic Heat Load Versus Year for 30 Year Half Life .....98

5.10 Decreased Dome Cooling or Increased Waste Surface Heating Required to Compensate for Radiolytic Heat Load Decay .....100

6.1 Simple Analytical Thermal Model--Estimate of Temperature Response of Upper Waste Layer .....104

6.2 Comparison of Temperature Data and Simple Analytical Model Calculated Temperatures .....107

6.3 1-D Classical Solution to Temperature versus time and distance from soil surface.....110

6.4 Amplitude of Temperature Oscillation versus Distance Downward from the Soil Surface.....111

6.5 Phase Shift of Temperature Oscillation versus Distance Downward from the Soil Surface.....112

6.6 Comparison of Simple Analytical Solution to Data--Ambient and Dome Gas Temperature .....114

6.7 A Tank Farm--Relative Location of Tanks and Thermocouple Tree in Tank A-101 .....116

6.8	Amplitude of Temperature Oscillation versus Horizontal Distance from the Soil Surface.....	118
6.9	Phase Shift of Temperature Oscillation versus Horizontal Distance from the Soil Surface.....	119
6.10	Temperature Versus Location and Time .....	121
6.11	Low Heat Tanks with Natural Inflow Leakage--Dome Ventilation Heat Removal versus Inflow and Outlet Relative Humidity at 98.3 F Outlet Temperature...	124
6.12	Low Heat Tanks with Natural Inflow Leakage--Tank Heat Load Partitioning versus Inflow and at 98.3 F Outlet Temperature and 100% Relative Humidity....	125
6.13	Low Heat Tanks with Natural Inflow Leakage--Tank Heat Load Partitioning versus Inflow and at 98.3 F Outlet Temperature and 100% Relative Humidity....	126
6.14	Low Heat Tanks with Natural Inflow Leakage--Tank Evaporation Rate versus Inflow Rate and Outlet Relative Humidity at a 98.7 F Outlet Temperature.....	127
6.15	Low Heat Tanks with Natural Inflow Leakage--Tank Level Change Rate Due to Evaporation Versus Inflow and Outlet Relative Humidity.....	128
6.16	Low Heat Tanks with Natural Inflow Leakage--Tank Level Change Due to Evaporation Versus Inflow and Outlet Relative Humidity.....	129
7.1	Data versus Model--Historical Average Meteorology, Fixed Inleakage Flow, 30 Year Half Life Radiological Heat Load .....	133
7.2	Data versus Model--Annual Cycle Meteorological Conditions, Fixed Inleakage Flow, 30 Year Half Life Radiological Heat Load .....	135
7.3	Data versus Model--Historical Average Meteorology, Variable Inleakage Flow, 30 Year Half Life Radiological Heat Load .....	138
7.4	Data versus Model--Annual Cycle Meteorological Conditions, Variable Inleakage Flow, 30 Year Half Life Radiological Heat Load .....	140
7.5	Data versus Model--Historical Average Meteorology, Variable Inleakage Flow, 30 Year Half Life Radiological Heat Load, Late 1990 Forced Ventilation Period .....	142

7.6 Data versus Model--Annual Cycle Meteorology,  
 Variable Inleakage Flow, 30 Year Half Life  
 Radiological Heat Load, Late 1990 Forced  
 Ventilation Period .....144

7.7 Data versus Model--1989 to present, upper axial  
 waste region. ....146

7.8 Data versus Model--1989 to present, intermediate  
 lower axial waste region .....148

7.9 Data versus Model--1989 to present, bottom axial  
 waste region .....149

## 1. SUMMARY

A new evaluation of the thermal hydraulic behavior of Tank A-101 to resolve concerns that heat generation in the upper layers of waste in Tank A-101 may be increasing is described in this report. Prior analysis of tank temperature data indicated that temperatures in the dome and upper waste were increasing at a rate of the order of .5-1.4 F/year.

Mathematical fits of the temperature data conducted in this evaluation indicates that between January 1993 and January 1996 that time averaged dome gas space and waste/dome gas space interface temperatures are increasing on a time averaged at approximately at 1.25-1.45 F/year. There are several factors that have contributed to this increase. These include increases in the ambient average temperature of 1.85 F/year, plus cooldown and reheat of the dome space and waste due to operation of the ventilation system during late 1990 or possibly early 1991. Mathematical fits of the time rate of change of axial temperature differences within the waste over several recent years indicate these gradients are decreasing and therefore that the heat generation rate within the waste is decreasing.

These conclusions are supported by dynamic thermal hydraulic simulations of the tank contents and adjacent soil. However these dynamic thermal hydraulic simulations also indicate that simultaneously matching calculated waste and dome space temperature values with data requires the occurrence of changes in one of two thermal factors. Either, (1) dome cooling processes are decreasing; or (2) some increasing heat generation is occurring at the surface of the waste. One or the other, or combinations thereof, is required to maintain the dome gas and dome gas/waste interface temperatures at their measured levels under conditions of decreasing waste heat load.

Decreased cooling could be occurring due to decreased

inleakage air flow, decreased evaporation due to slurry dryout near the surface, or decrease in soil overburden conductivity due to soil dry out. Increased heat load due to chemical reaction or heat of precipitation are possibilities. Increased heat load at the surface due to chemical reactions is questionable, however, as depletion of reactants would lead to decreasing heat load. Increased heat load due to heat of precipitation is questionable due to decreased heat of precipitation as evaporation decreases due to dryout. Because evaporation cooling would always be directly coupled to any precipitation heating, and since the cooling effect of evaporation would likely be significantly larger than the precipitation heating effect, the precipitation heating effect would also be masked.

In the future, if the forced ventilation system is not operated, the following thermal hydraulic behavior of Tank A-101 could be anticipated. Simulation results indicate that time averaged tank dome gas and waste/dome gas interface temperatures would be expected to remain nearly constant or begin to decrease slightly in the future. This assumes annual time averaged ambient temperatures do not exceed historical averages (53.3 F), and the rate of decrease in dome cooling continues at its present rate or alternatively the rate of increase of surface heating continues at its present rate. If the rate of decrease in dome cooling decreases (e.g. inleakage air flow decreases at the same rate but finally stops for example) then the rate of temperature decrease at all locations within the tank will be expected to increase.

If there is significant inleakage to the dome, and if this is suddenly stopped, then waste temperatures will rise to a new equilibrium level, then start decreasing as the radiolytic heat load decreases. Since inleakage is not likely to be very large, the expected increase in temperature from a sudden inleakage stoppage would be small.

There is no evidence that decreasing evaporative cooling due to dryout will lead to larger increases in waste temperature than stopping inleakage, since they are both coupled to the maximum expected inleakage rate. Bounds on the maximum expected inleakage rate could be defined through further analysis if required. Once defined, upper bounds on the maximum expected temperature increase due to complete shutoff of inleakage could be estimated--however, these increases in temperature cannot be large.

There is no evidence of a decrease in waste conductivity due to dryout. However, soil overburden dryout with a reduction in conductivity could be occurring. This process could be extended over many years into the future and would be altered by the year to year dry and wet bulb temperatures and precipitation (i.e. rain and snow). Large temperature increases via this process would not be expected as the soil above Tank A-101 is likely not different from other tanks which have similar total heat loads, and operating temperatures, and which do not experience tank heat ups. In addition, the soil dryout process if it is occurring, is as slow or slower than the radiolytic decay process and there is no way to suddenly shut off conduction through the soil due to decreasing soil conductivity.

Tank A-101 temperatures should continue to be monitored. After at least a year has passed a simulation with the existing dynamic model incorporating the 1996 meteorology should be made and the results compared to the temperature data to verify the above expectations. No other actions are recommended at this time.

## **2. INTRODUCTION**

This report briefly overviews related prior analysis and documents the results of a new evaluation of the thermal hydraulic behavior of Tank A-101. The analysis was initiated by a concern that heat generation in the upper layer of waste in Tank A-101 may be increasing.

### **2.1. RELATED PRIOR ANALYSIS**

A prior regression analysis of Tank A-101 temperature data [Crowe, 1993], conducted for other purposes, indicated that the time averaged temperature in the dome space gas was increasing, rather than decreasing as might be expected due to decay of the tank's radiolytic heat load. This previous analyses calculated the dome gas was increasing at an average rate of .9 F/year over the 1/88-3/93 time period

A second analysis [Crowe, 1995] calculated the rate of temperature change for the dome gas/waste interface and for the waste at elevations corresponding to thermocouple locations, in addition to the dome gas, for a more recent time period, 1/93-9/95. The rate of temperature increase for the dome gas was calculated to be .52-.57 F/year, or lower than for the previous period. For this more recent time period, temperatures at the dome gas/waste interface were calculated to be increasing at 1.37 F/year. Temperatures of the top 7 feet of waste were also calculated to be increasing, but waste temperatures below this region and the tank floor were calculated to be decreasing. The axial distribution of the rate of temperature change is reproduced in Figure 2.1.

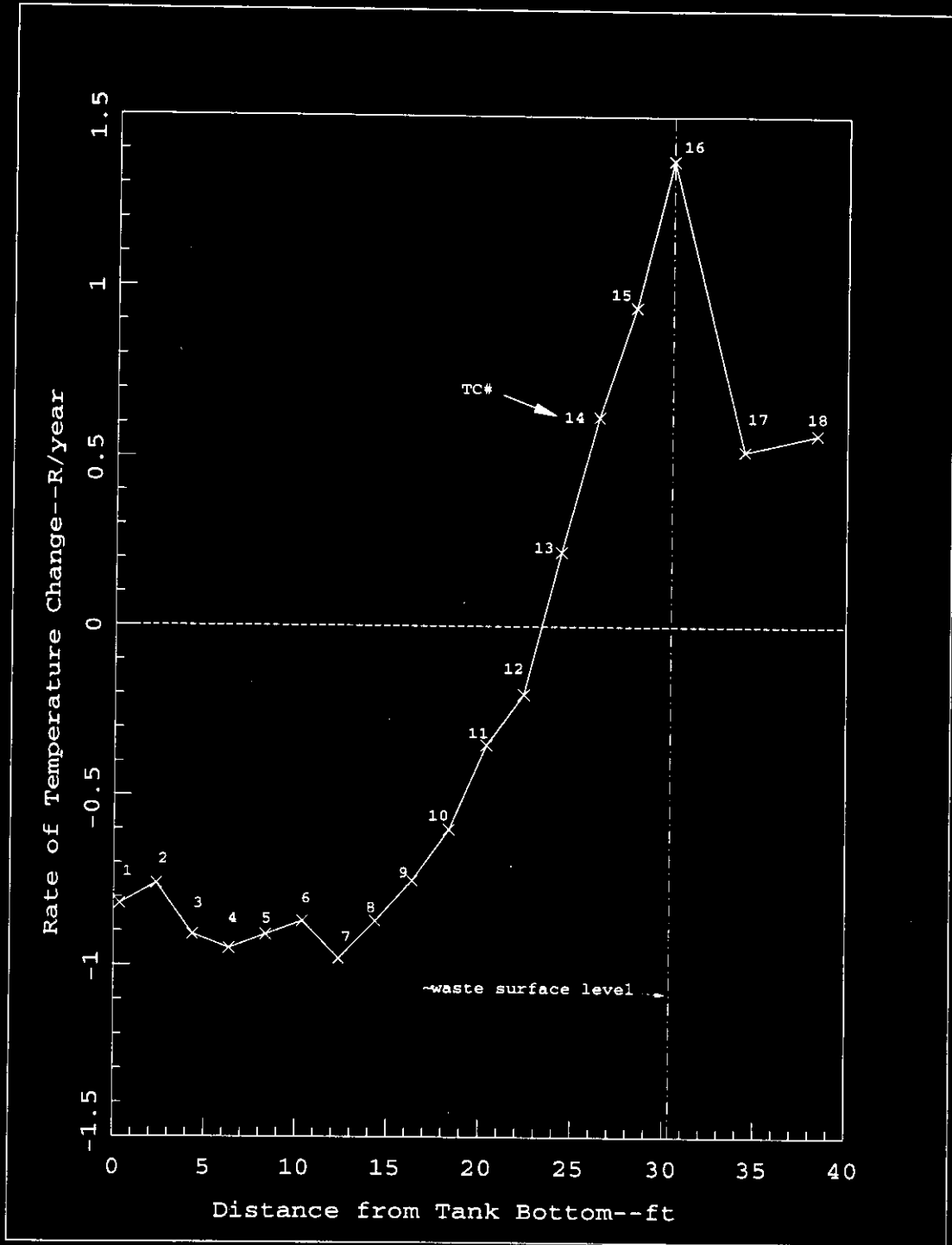


Figure 2.1 Tank A-101 Temperature Rate of Change versus Axial Location--Linear Term of Fourier Series Fit (1/93-9/95)

## 2.2. OVERVIEW OF POTENTIAL EXPLANATIONS FOR TANK A-101 THERMAL HYDRAULIC BEHAVIOR

The following potential itemized causes of Tank A-101 thermal hydraulic behavior were considered in this evaluation. With exception of item 1. and 3.d, each item in whole or in part either contributes to the behavior, or could potentially contribute and cannot therefore be ruled out. Evaluation of the time rate of change of temperature gradients between thermocouple locations provides no evidence that heat generation within the waste is increasing, or that thermal conductivity in the waste near the surface is changing significantly.

1. Non nuclear heat source with increasing heat generation within the upper layer, combined with radiolytic decay in both Upper and lower layers:

- a. Chemical heat sources
- b. Endothermic heat of solution resulting in heat release upon salt precipitation and dryout.

2. Non nuclear heat source with increasing heat generation at the waste surface, combined with radiolytic decay in both Upper and lower layers:

- a. Chemical heat sources
- b. Endothermic heat of solution resulting in heat release upon salt precipitation and dryout.

3. Change in cooling processes:

- a. Forced ventilation flow turned on followed by shutdown of ventilation during late 1990 or early 1991.
- b. Decreasing natural circulation ventilation (or

inleakage) due to line plugging, or cool down of other tanks which are coupled to Tank A-101 via cascade lines.

c. Soil heat conduction effects associated with long term thermal wave effects from other tanks.

d. Reduction in top layer waste thermal conductivity due to dry out.

e. Reduction in evaporative cooling at waste surface due to dry out.

f. Reduction in tank overburden soil conductivity due to soil dry out.

g. Reduction in convective heat transfer coefficients between waste surface and dome gas, and dome gas and tank dome.

4. Temperature data for time periods selected for mathematical correlation or fit of temperature data are skewed upwards.

a. More frequent operation of ventilation system 1980-88, followed by less frequent operation during 1989 and early 1990, followed by no operation from 1991 to the present.

a. Skew due to 1990/91 ventilation operation--and exceptional hot summer weather in 1994.

5. Actual Time average increases in ambient temperature over the periods of time considered.

If it is assumed that the waste cooling mechanisms have not changed, that the average ambient temperature over each annual cycle is constant, and that there are no sources of thermal energy in addition to radiolytic heating, it would

be expected that the time averaged waste and dome gas temperatures would be decreasing as the radiolytic heating decays. If the dome temperature were maintained constant by some means, it would be expected that the time average waste temperatures would decrease, but not as fast as if the dome were allowed to cool. The primary radiolytic heat sources in Tank A-101 are Cesium 137 and Strontium 90 with half lives of 30.2 and 28.6 years respectively. Since Tank A-101 is currently believed to be cooled primarily by conduction through the soil to the atmosphere at the soil surface, the temperature difference between the sludge and ambient should also be decreasing with a 28.6-30.2 year half life (equivalent to a 41.3-43.6 year thermal time constant), increased somewhat due to thermal inertia effects of the waste and adjacent soil.

The referenced data analyses considered two different time periods, the first analysis for dome gas only, 1/88-3/93, and the second analysis for the dome gas, dome/sludge interface, and sludge, 1/93-9/95. The temperature changes included the superimposed effect of time averaged changes in ambient temperature. The time periods selected for data analysis of the ambient temperature were somewhat different than for the sludge and dome. For the first study the time period used for ambient temperature data analysis was 1/90-1/93 and resulted in a calculated ambient temperature increase of .5 F/year. For the second analysis the time period selected was 1/89-1/95 and resulted in an ambient temperature increase rate of .06 F/year. If the differences in time periods selected for the dome gas, interface, and waste, versus the ambient are ignored, when the ambient rate of change is backed out of the dome gas, interface, and waste temperature changes, net increases in dome gas, interface, and waste temperature near the surface are still computed.

The history of average annual temperature for 1980-95 is graphed in Figure 2.2 [Hoitink, 1994], [Burk, 1996]. Mathematical fits of the rate of change in the annual

temperature obviously depend on the period of time selected. Although this does provide some guidance regarding whether the waste should be heating or cooling due to ambient changes, a dynamic thermal hydraulic model is needed to more clearly evaluate the dynamic effects of ambient changes.

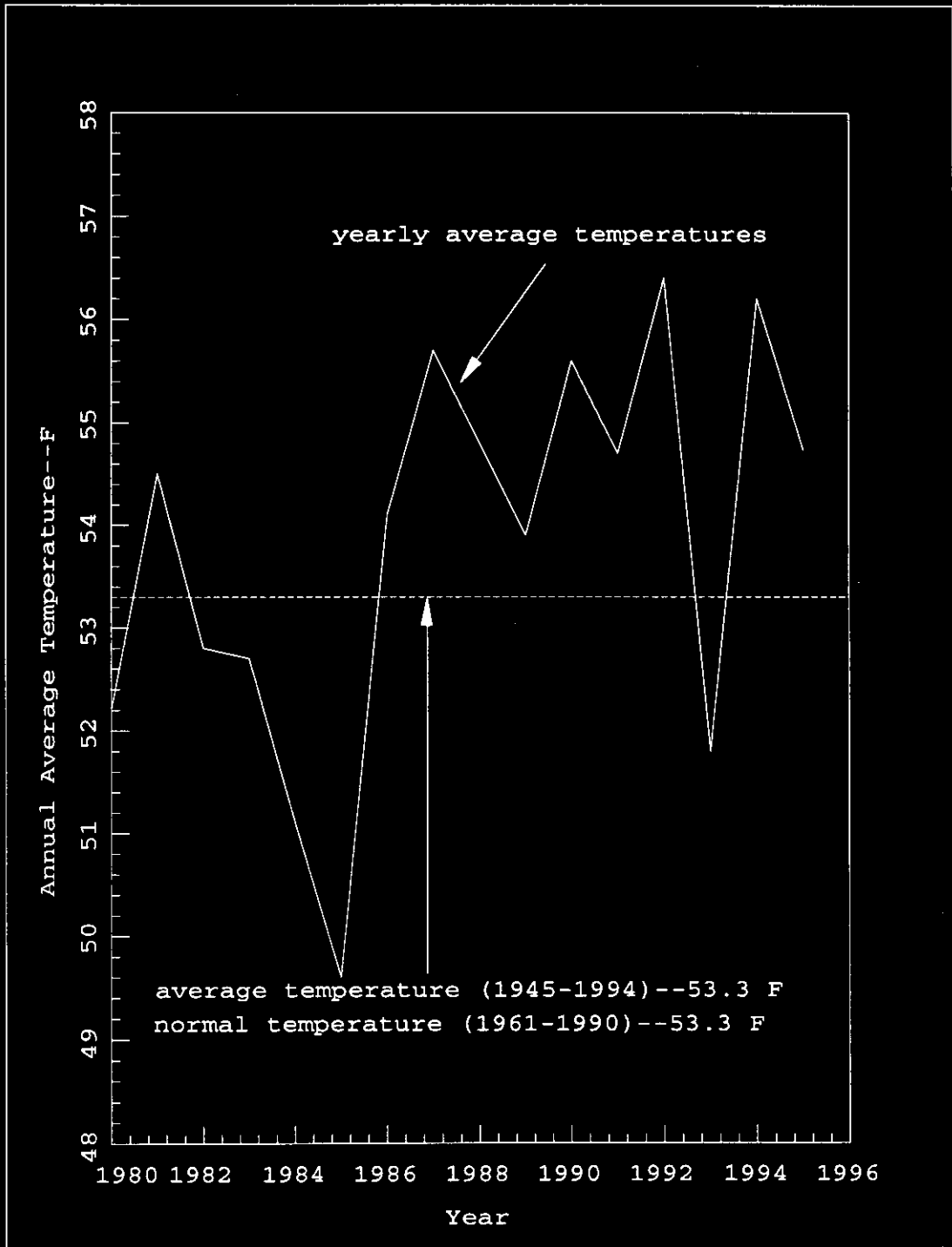


Figure 2.2 Annual Average Temperature

Various types of regression analysis over various periods of time may indicate that the dome gas, interface, and upper sludge time averaged temperatures are increasing slightly even when ambient time averaged temperature effects are backed out. However it cannot be conclusively determined from regression analysis of the absolute temperature data if there is an increasing heat load in Tank A-101 from chemical or other sources, nor can other possibilities be easily eliminated. A new indepth evaluation of the thermal behavior of Tank A-101 including all parameters which could effect the thermal behavior of this tank has been conducted. The thermal behavior of the tank can be explained by any one of four hypotheses, or combinations thereof. These hypothesis were developed by additional evaluation of the data, classical steady state and transient thermal analysis, and the use of the GOTH<sup>1</sup> thermal hydraulic code to conduct transient simulations of possible tank operating scenarios.

Only one of the four hypothesis developed is based on increased heating due to some non radiolytic heat source, and this source if it exists, must be present at the waste surface, or in the dome--but not within the body of the waste. The other hypothesis are based on changes in the cooling mechanisms between the waste surface and the ambient heat sink.

The order of magnitude of the decrease in heat generation rate within the waste is compatible with the ~30 year half life decay of Sr and Cs based on the decrease in temperature differences between thermocouples at different axial elevations within the waste. However, it can be concluded that the waste surface temperature and the dome gas temperature are not decreasing at a rate compatible with the ~30 year radiolytic decay half life. Even if the cooldown and subsequent heatup effects of the 1990 ventilation operating period, and the effects of different annual meteorological cycles from 1990-1995 are considered, these temperatures are higher than expected based on

---

<sup>1</sup>GOTH is a trademark of JMI, which is derived from GOTHIC - a registered trademark of the EPRI Corp., CA 11

dynamic thermal hydraulic simulations which assume a 30 year half life for the tank heat load. Either continually reducing cooling effects between the dome and the ambient, or continually increasing heating at the waste/dome gas interface, must be occurring to maintain interface and dome gas temperatures constant, or slightly increase them, under a decaying radiolytic heat load in the waste.

Accounting for the temperature behavior of the waste surface and the dome gas requires at least one of the following hypothetical situations to be present, or a combination of partial effects from one or more of the following to be present:

A. non radiolytic heat load (chemical, heat of solution, or other) at the waste surface, or in the dome must be increasing, at the same rate the radiolytic tank heat load is decreasing, this includes chemical heat or heat of precipitation (reverse of heat of solution);

B. convective cooling from sensible temperature change of dome inleakage ventilation flow must be decreasing at a rate that compensates for the decay in radiolytic heat load. Various scenarios are thermally compatible with the data. Inleakage rates of 60 ft<sup>3</sup>/min in 1990 decreasing to zero by 1997 is one compatible with the data.

C. evaporative cooling due to evaporation from the salt cake surface must be decreasing at a rate that compensates for the decay in radiolytic heat load and there must be a compatible air in leakage rate. A constant air inleakage rate of 24 ft<sup>3</sup>/min combined with adequate evaporation to saturate the air in 1990, but with evaporation dropping to zero due to salt cake dryout by 1997 is one scenario compatible with the data.

D. soil conductivity above the tank must decrease at the same rate as the radiolytic heat decays.

Although regression analysis of the data indicates the interface and dome gas time averaged temperatures have increased over the last several years, even when the changes in the time averaged ambient temperature is subtracted out, regression analysis does not back out the effect of the cooldown and reheat that occurred due to the operation of the forced ventilation system in 1990. Nor does it include the detailed effects of significant variations in the annual meteorological cycle during recent years.

Dynamic thermal hydraulic simulations which include these effects indicate that even if any one of items A-B, or combinations of partial effects thereof are present, and the time averaged annual meteorological cycle temperature is at or below the time averaged temperature for the last several decades, then no increase in the time averaged waste/dome gas interface, or dome gas temperatures will be expected to occur. However, these simulations do indicate that if the behavior is based on items B or C, then in the near future the interface and dome gas temperatures will start decreasing since decreases in the convective or evaporative cooling will cease once the inleakage flow drops to zero, or the evaporation rate drops to negligible levels due to salt cake dry out. At that time the rate of decrease in sludge temperature at all axial levels will begin to increase. Item D, effects of soil dryout on soil conductivity, could prolong the reduction in cooling over many more years into the future than appear reasonable for items B and C.

If heat generation near the surface due to precipitation of salt as the waste slurry dries out is occurring, it should be occurring at a decreasing, not increasing rate, as evaporation and therefore precipitation should be decreasing with time. In addition precipitation cannot occur under nearly isothermal conditions without evaporation occurring. Evaporation removes heat from the

waste making it difficult to determine the net heating or cooling effect due to combined evaporation plus heat of solution effects. Chemical reactions at an increasing rate seem questionable since the consumption of reactants would lead to a decrease in the total chemical reaction heat load over time. In addition since there has been no large change in temperatures in the tank contents since being filled in 1980, reactions accelerated by increasing temperatures don't appear to be a plausible explanation. Since the physical appearance and color of the waste surface seems to be changing due to dryout since 1980, it is not unreasonable to assume that these visual changes may be indicators of chemical reaction, which may be exothermic. Although significant increasing chemical reactions cannot be totally ruled out, they appear unlikely.

The analysis conducted to arrive at these conclusions is described below. Background information required to form a basis for this analysis is first described.

### **3. TANK A-101, TANK FARM A, AND VENTILATION SYSTEM DESCRIPTION**

#### **3.1. TANK A-101**

Hanford waste Tank A-101 is illustrated in Figure 2.1 [Drawing Set 1]. Major dimensions of the tank, depth of burial, and thermocouple numbers and locations are illustrated there.

The tank currently contains 953,000 gallons of waste of which 413,000 gallons is estimated to be drainable interstitial liquid. The liquid is contained within 3000 gallons of sludge located at the bottom of the tank, 403000 gallons of salt slurry immediately above the sludge, and 547000 gallons of saltcake overburden located at the top of the tank [Hanlon, 1995], [Gaddis, 1994]. The salt slurry may contain significantly more liquid than the salt cake, however, this is not known with certainty. Tank A-101 was sluiced and emptied in 1975-76 and subsequently filled with its current contents between that time and the beginning of 1981. Slurry added at the beginning of 1981 has a higher heat generation rate and lower conductivity than the slurry added earlier as discussed in following sections of the report. Some mixing likely occurred between these layers at their interface. The level history since 1975 is shown in Figure 3.2.

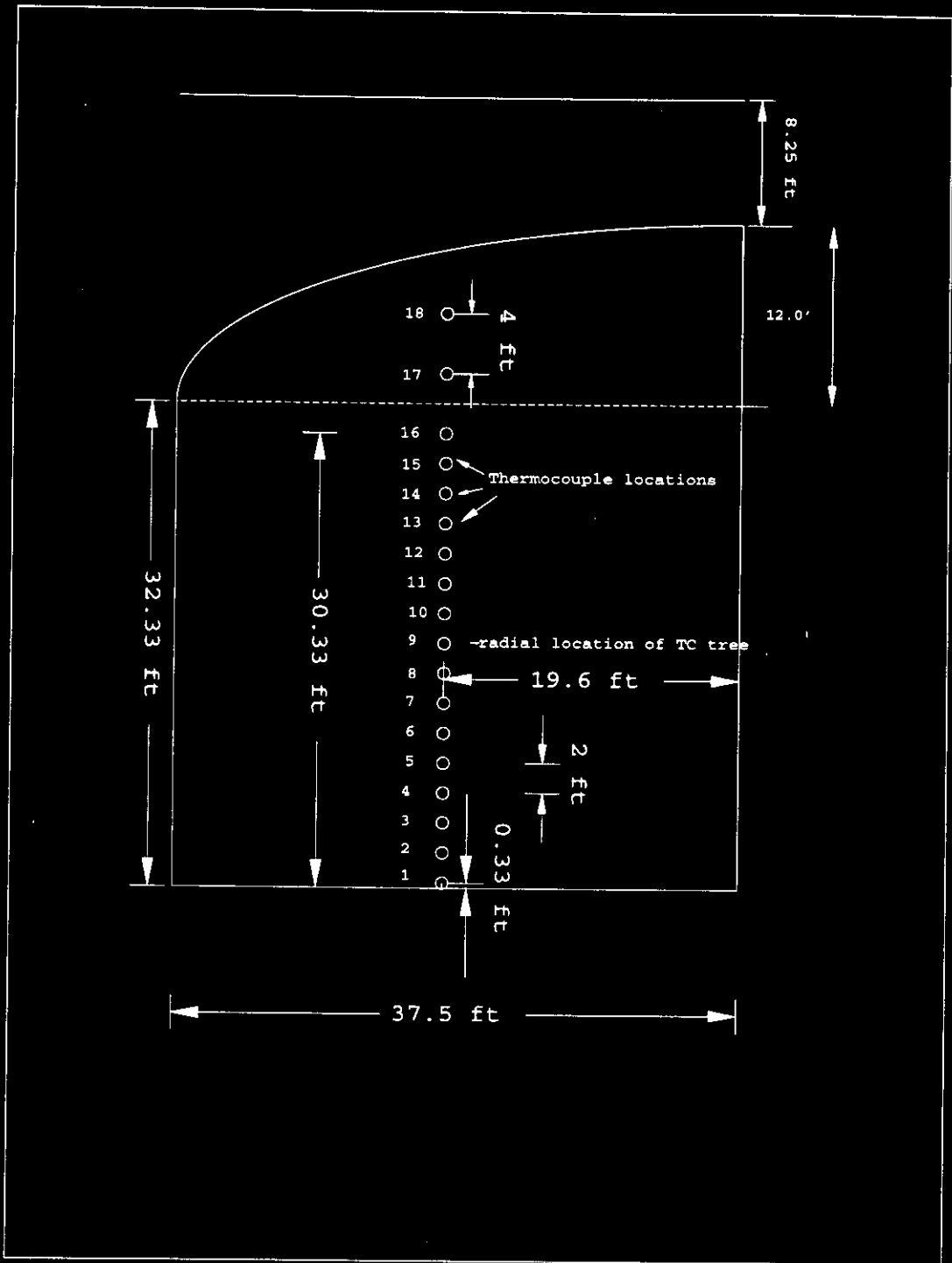


Figure 3.1 Tank A-101 Basic Dimensions, Thermocouple Elevations Relative to Tank Bottom Inside, and Approximate Thermocouple Tree Radial Location

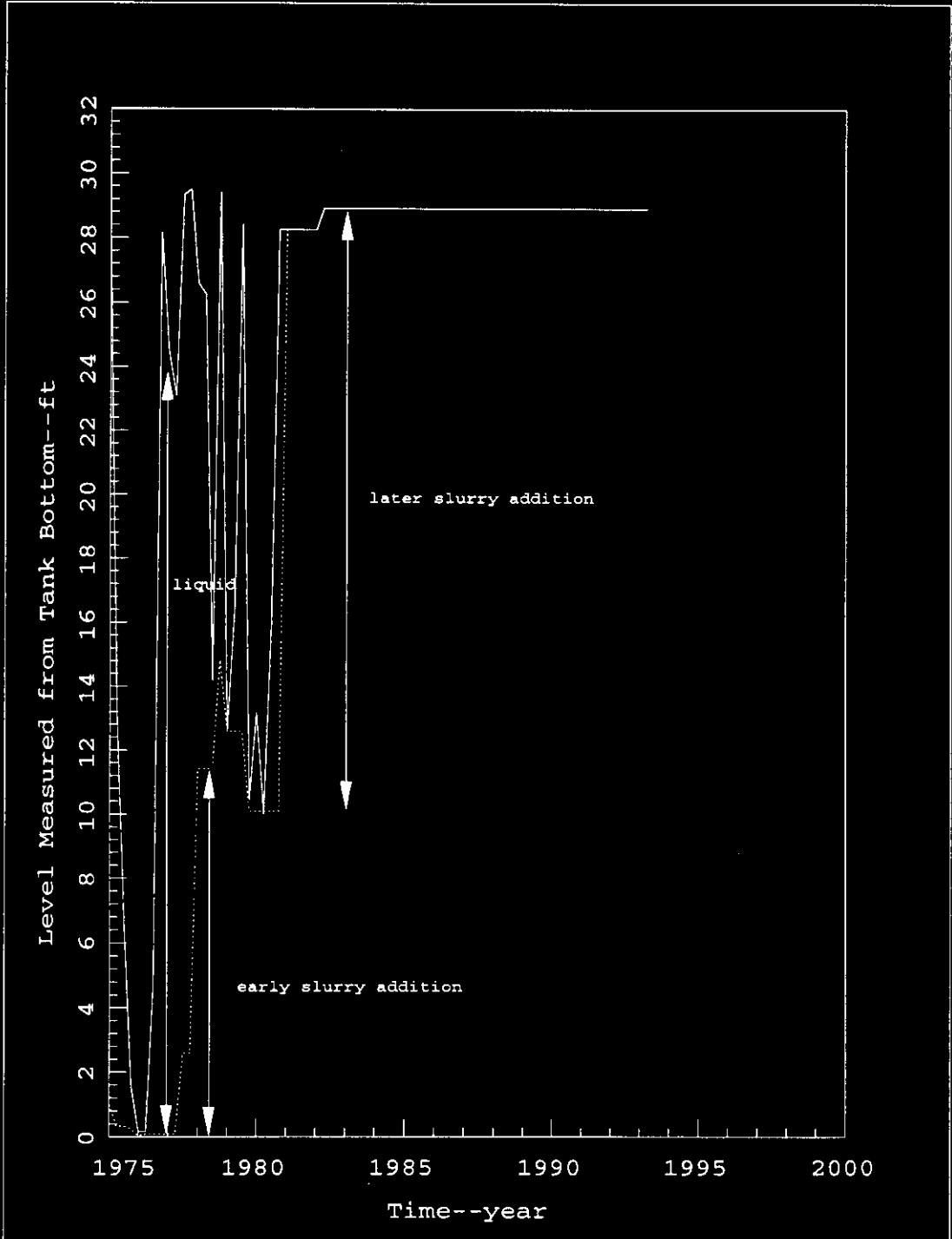


Figure 3.2 Tank A-101 Level Versus Time

There are various level measurements and estimates made in Tank A-101 and recent values associated with these measurement methods are provided in Figure 3.3. These measurements coupled with the temperature distribution measurements suggest that the level, at least near the radial and azimuthal vicinity of the thermocouple tree, is near the elevation of thermocouple 16. Apparently no significant change in level has occurred since the end of 1981 [Gaddis, 1994].

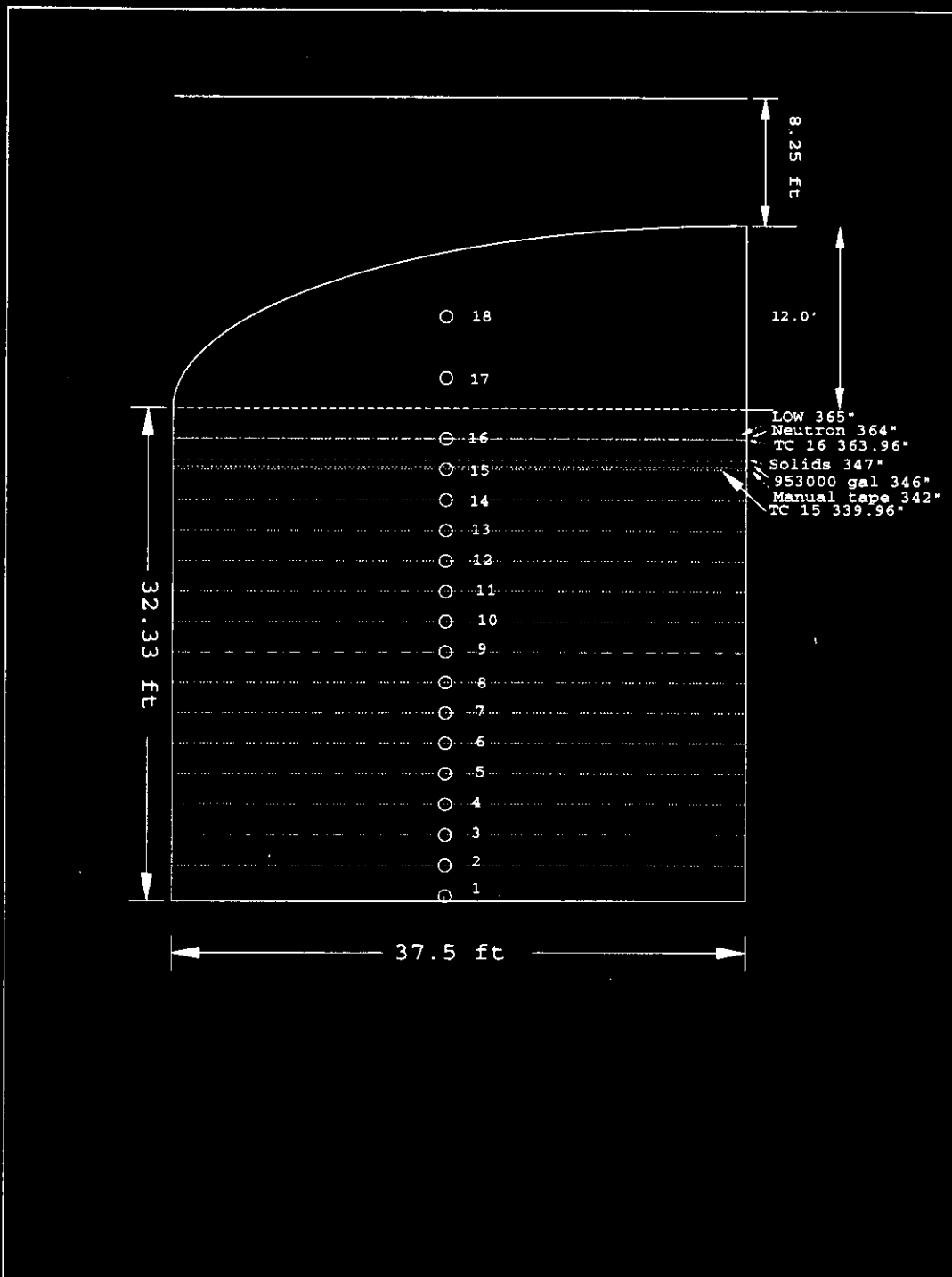


Figure 3.3 Various Level Measurements and Estimates for Hanford Waste Tank A-101

Shortly after filling the tank with evaporator slurry at about 125 F at the beginning of 1981, axial temperature gradients developed throughout the 30 ft depth of waste and a crust formed on the surface. The rapid development and continued existence of axial temperature gradients, the development of the crust, and lack of observable liquid suggest that precipitated salt solids have not settled nor left a convective layer of supernatant.

### **3.2. TANK FARM A AND VENTILATION SYSTEM**

The A Tank farm includes 6 tanks, A-101 through A-106, and their relative positions are shown in Figure 3.4 [Drawing Set 2]. The adjacent tanks 102, 104, and 105 are essentially empty, containing only a few inches of solids. There is limited temperature instrumentation inside these tanks. Tanks 104 and 105 apparently are at elevated gas and tank wall temperatures of 180-190 F and 130-155 F respectively. Temperatures in lateral wells located below Tank A-105 are as high as 230-250 F. Tank 102 is operating with a dome temperature of about 90-95 F, slightly lower than the dome gas temperature in Tank A-101. One primary ventilation system with one exhaust fan serves all six tanks, when operational. The position of Tank A-101 and its single active thermocouple tree relative to the other tanks is illustrated in Figure 3.4. As indicated there the thermocouple tree is quite isolated from the influence of the other tanks. Also shown are the exhaust fan, and normal flow direction when the forced ventilation system is active. Ventilation air flows through a 6 inch cascade overflow piping system that couples the tanks together. Although the ventilation system has not been operational for any extended period of time since the summer of 1991, coupling of the tanks could result in large natural circulation flows than might otherwise occur. During much earlier operation periods 20 inch ventilation lines and 24 inch vapor headers connected Tank A farm to the Tank AY/AZ farm primary ventilation system. Seal loops in this piping system were grouted to isolate

Tank Farm A. It has been speculated that the grout may not completely seal any particular A farm tank from this ventilation system.

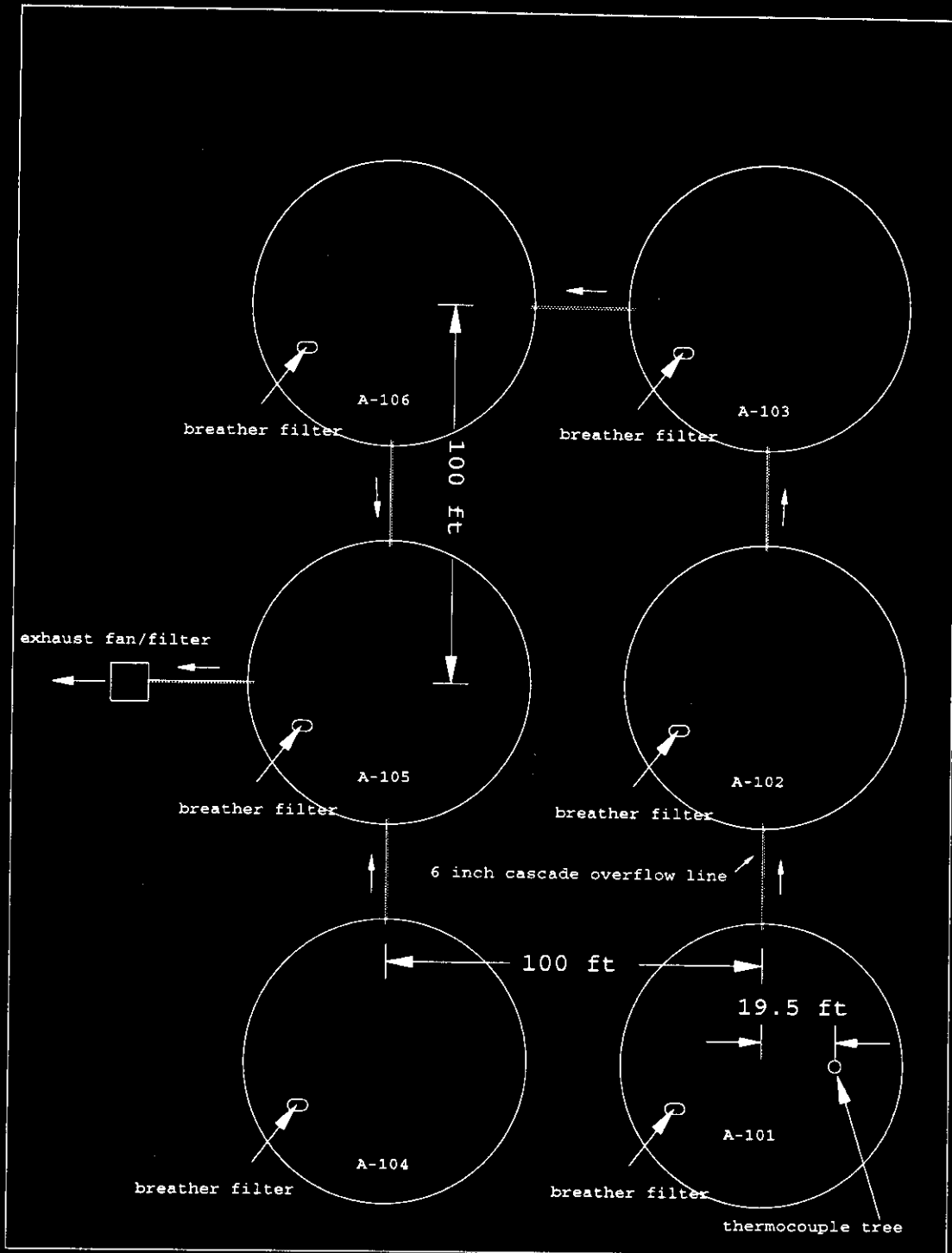


Figure 3.4 A Tank Farm--Relative Location of Tanks and Thermocouple Tree in Tank A-101

The tanks in the A farm are closer to each other than to groundwater as is illustrated in Figure 3.5.

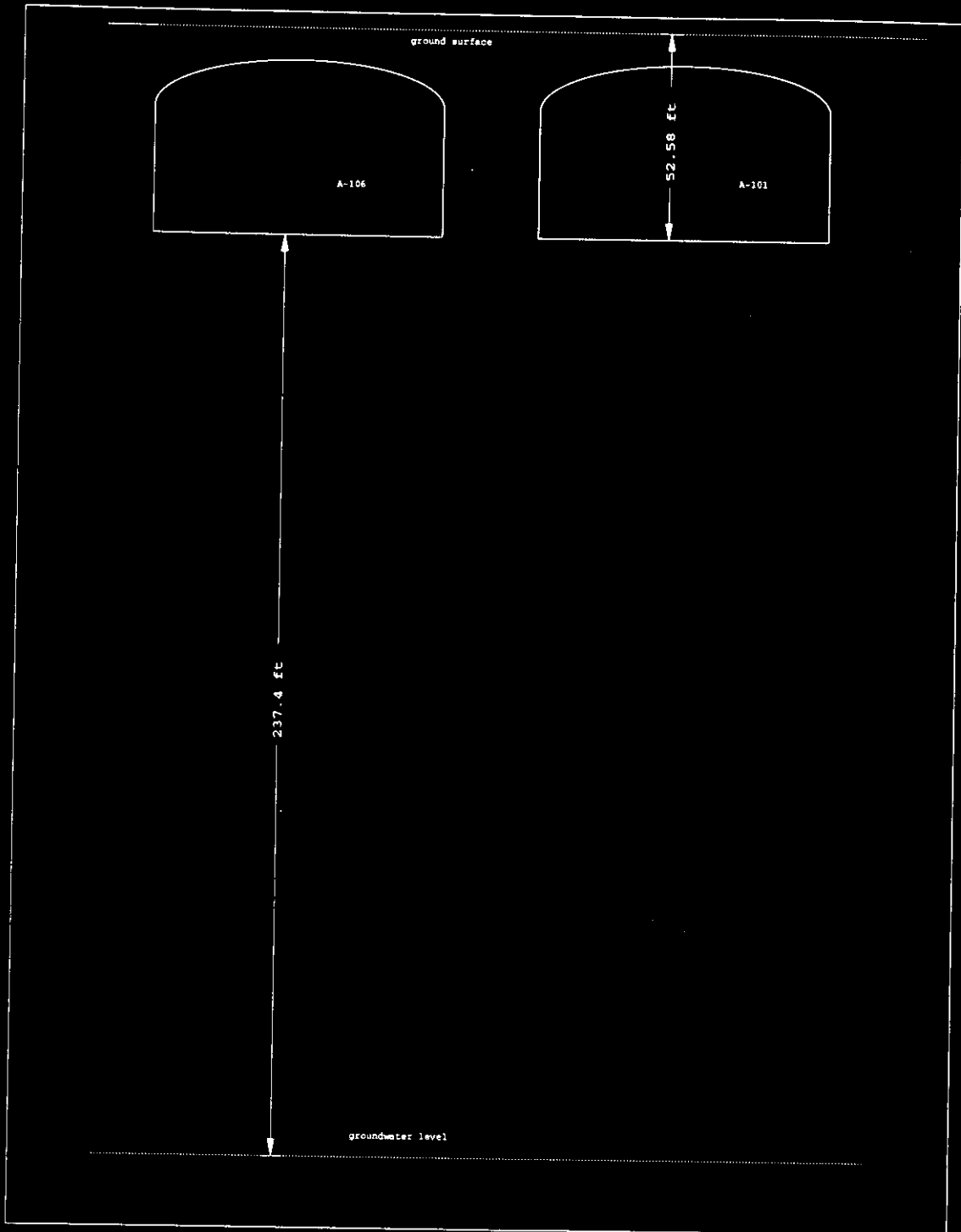


Figure 3.5 A Tank Farm Distance to Groundwater

#### 4. TANK A-101 TEMPERATURE DATA

##### 4.1. DYNAMIC DATA

Temperature Data for all 18 thermocouples over the period of time for which data is available is provided in Figures 4.1 and 4.2. Following filling of Tank A-101 in 1980 with salt precipitated slurry from the evaporator, the ventilation system was apparently operated intermittently, and temperature measurements were relatively infrequent. Just prior to 1990 the forced ventilation was turned off and waste temperatures increased a few degrees. During late 1990, or possibly early in 1991 the forced ventilation was operated for a short period of time cooling the waste a few degrees, then the ventilation was shut off and the waste temperatures subsequently increased a few degrees. Up to the beginning of 1991 the data acquisition frequency was low and erratic, and little is known about ventilation flow rates or periods of operation. Temperature data suggests the ventilation system operated intermittently.

Beginning in 1991 the frequency of temperature data acquisition was increased to weekly and forced ventilation apparently was permanently discontinued. Temperature data preceeding and following January 1991 clearly shows the cooldown and reheat associated with the last operating period of the forced ventilation system. The propagation of the annual meteorological temperature cycle from the soil surface, down to the dome gas and waste, is also clear for the dome gas and waste near the surface. However low in the waste the amplitude attenuation and phase shift of the oscillation are obscured by the high frequency "hash" in the temperature data which is likely due to a non stable reference junction common to all 18 thermocouples. Photographs of the tank surface indicate that evaporation of the liquid at the surface has occurred leaving a surface layer of salt cake. The depth to which the salt slurry has been dried to salt cake, the quantity of interstitial liquid in the waste versus depth, or the rate at which

evaporation occurred or when it occurred is apparently not known.

As indicated there, prior to 1990 the temperature swings are larger than which would occur due to the annual meteorological cycle suggesting the ventilation system was run intermittently, and that convective cooling due to sensible air change may have been augmented by evaporative cooling at the wet slurry surface which would also dry the waste surface. Transpiration or wicking effects could have been present to dry the waste below the surface.

High frequency oscillations with quite large amplitudes are observed in the temperature data, even near the bottom of the tank. These are not likely due to rapid changes in the tank heat load, its distribution, cooling effects, or actual waste temperature changes. These are more likely due to a non constant thermocouple reference junction, common to all 18 thermocouples, since differences between thermocouples at different axial locations do not show as large an effect as that observed for the absolute temperatures. These oscillations tend to obscure the actual thermal behavior of the tank contents, and increase the difficulty of explaining the thermal behavior.

If the primary heat removal mechanism is conduction through the waste and soil, then the effect of large oscillatory daily and weekly meteorological changes will be damped out deep in the soil and also in the waste due to thermal diffusivity effects. Although the effect of annual meteorological cycles is felt in the dome and top layers of waste, deep in the waste the effect is so highly attenuated it is almost imperceptible, particularly with the high frequency "hash" in the data which has been superimposed on the actual temperature. Cooling effects due to air inleakage, with or without evaporation from the waste, will increase the amplitude of the dome gas temperature and

waste surface temperature annual oscillations.

Thermal diffusivity effects not only cause the amplitude of temperature oscillations at the soil surface to be attenuated deep in the soil and the waste, it also causes a phase shift between the ambient annual temperature oscillation at the soil surface and at some depth into the soil or waste. Inleakage cooling effects will decrease the phase shift. Forced ventilation can significantly increase the amplitude of the dome gas and waste surface temperature annual oscillations, and decrease the phase shift.

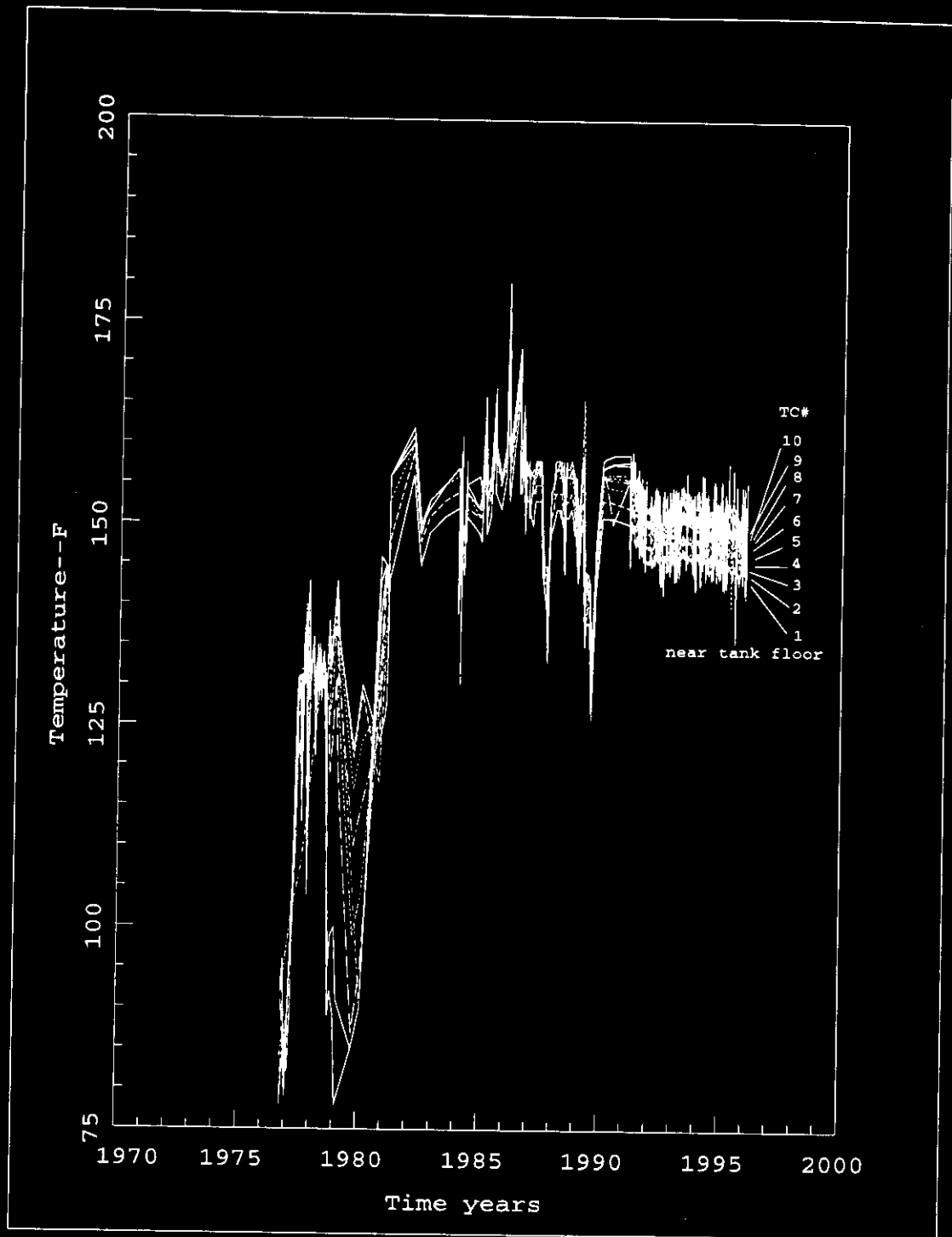


Figure 4.1 Tank A-101 Thermocouples 1-10 Temperature Data Versus Time

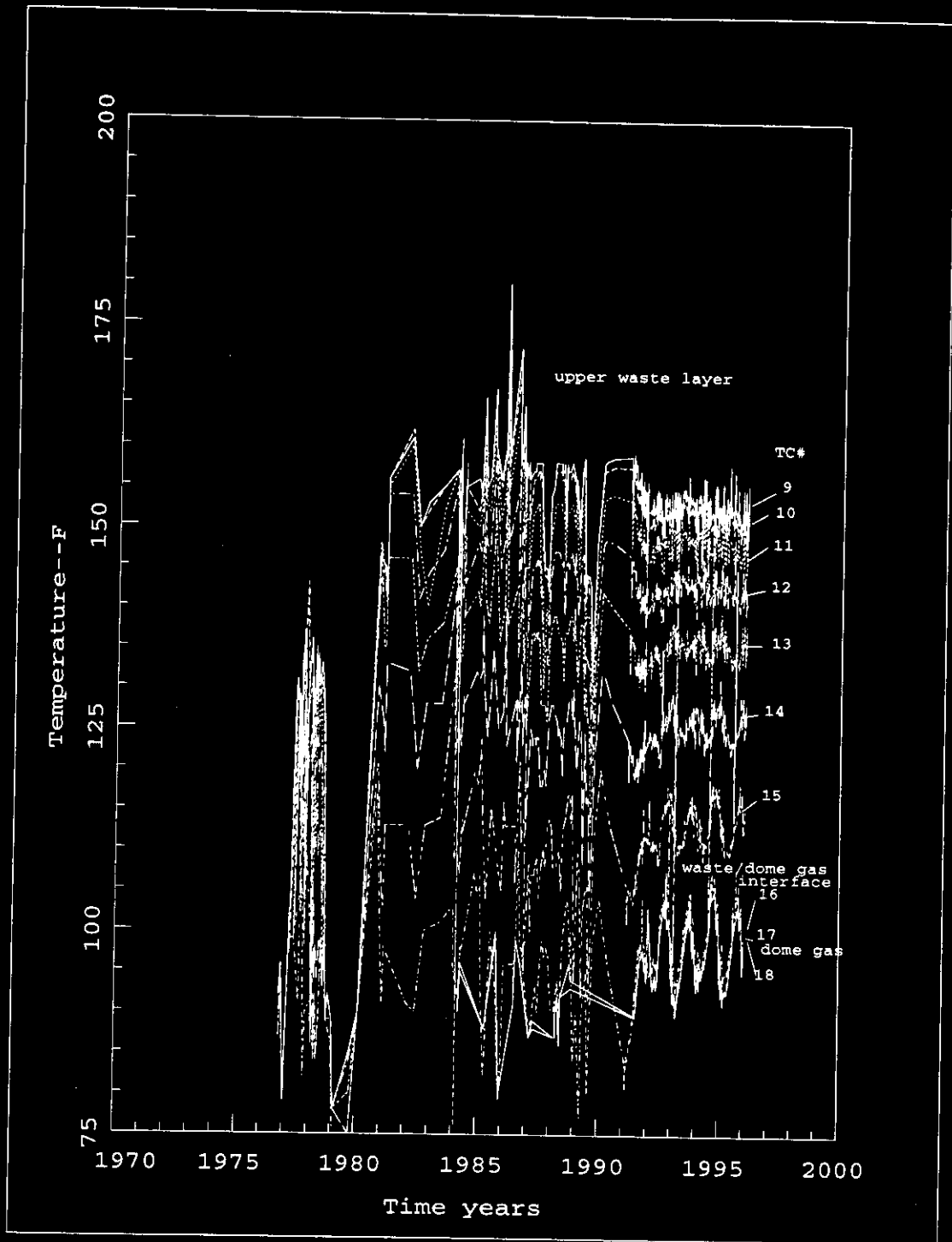


Figure 4.2 Tank A-101 Thermocouples 9-18 Temperature Data Versus Time (upper waste layer, waste/gas interface, dome gas)

Temperature and ventilation data prior to 1991 is too infrequent and erratic to draw many detailed conclusions. Data acquisition frequency since 1991 has been weekly, and the ventilation system has been off. The concern about potential increases in tank heat load is an issue for future operation, not the distant past. Therefore most of the effort for this new analysis has concentrated on the thermal behavior between 1990 and the present, which is both most relevant, and for which the best data base is available. Figures 4.1 and Figures 4.2 are therefore replotted as Figures 4.3-4.5 over this more recent time period to allow better resolution of the data. Although the measured data for this period exhibits considerable high frequency "hash", it does clearly show the effects of the annual meteorological cycle, the effects of variations in the annual cycle between 1990 and 1995, the effect of the forced ventilation being on during late 1990, and the effect of depth on amplitude attenuation and phase shift resulting from thermal inertia. The high frequency "hash" appears to be the result of a thermocouple reference junction common to all thermocouples that has erratic behavior, since differences between thermocouple measurements do not exhibit as severe a behavior as discussed below.

Also plotted in Figures 4.3 and 4.4 is the monthly average ambient temperature which shows the annual meteorological temperature cycle and its effect on the waste. The oscillating temperature amplitudes and phase shifts or lags relative to the ambient cycle are clearly evident for the dome gas (TC-17 & 18), the waste/dome gas interface (TC-16), and about 10 feet below the surface of the waste (TC-15 through TC-11). However, below this depth (TC-1 through TC-10) propagation of the annual cycle into the waste is obscured by the "hash" as well as damped out by the thermal inertia of the waste.

Deep in the waste, TC-1 through TC-10, the difference in temperatures between axial locations is not large, due

apparently to low radiolytic heat generation in the lower layer of waste. Although the actual temperatures between these thermocouple locations would be expected to change very little over a years time, the data show up to 7 F swings in temperature over periods as short as the acquisition frequency (7 days), likely due to the thermocouple reference junction problem noted above.

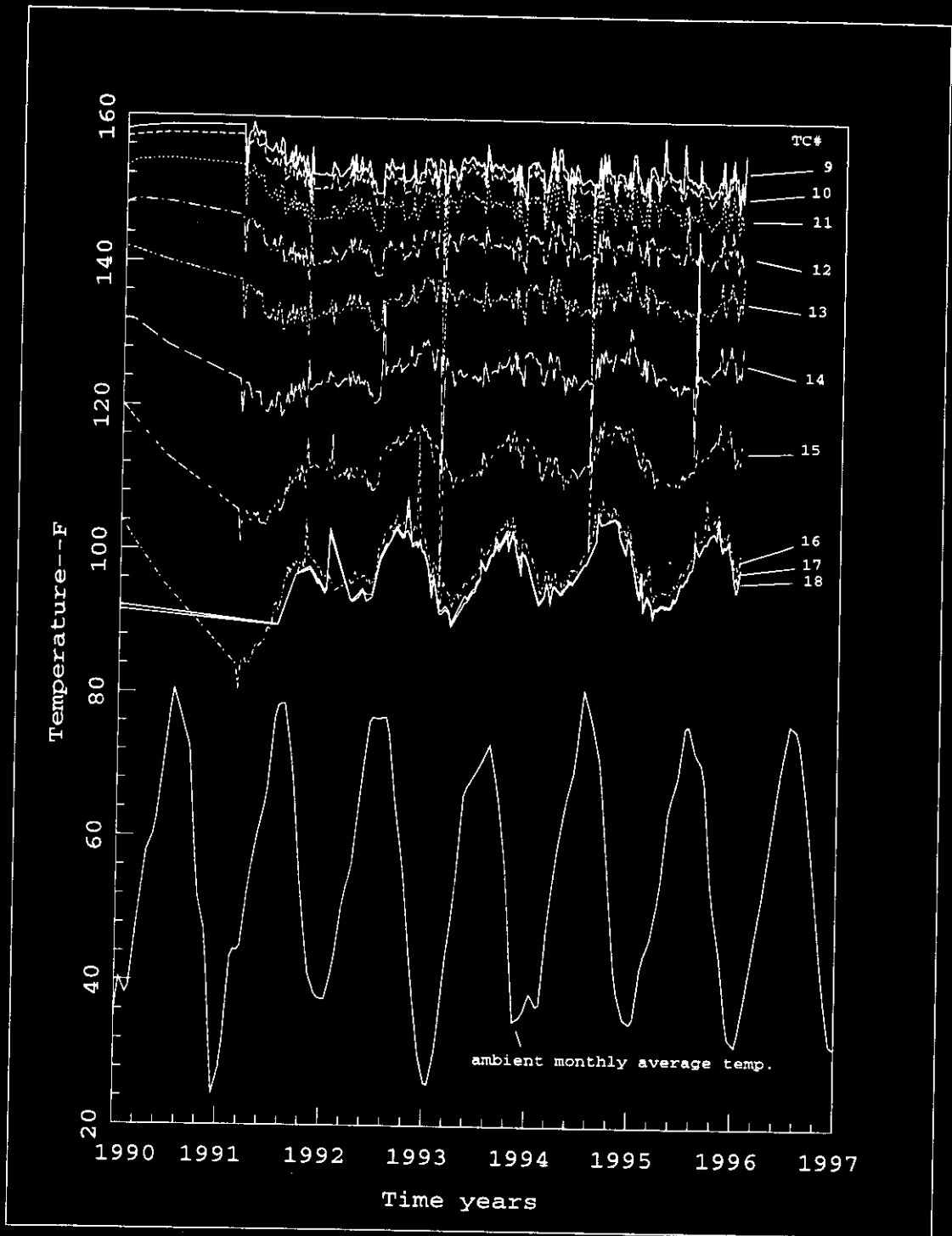


Figure 4.3 Tank A-101 Thermocouples 9-18 Temperature Data Versus Time (upper waste layer, waste/gas interface, dome gas)

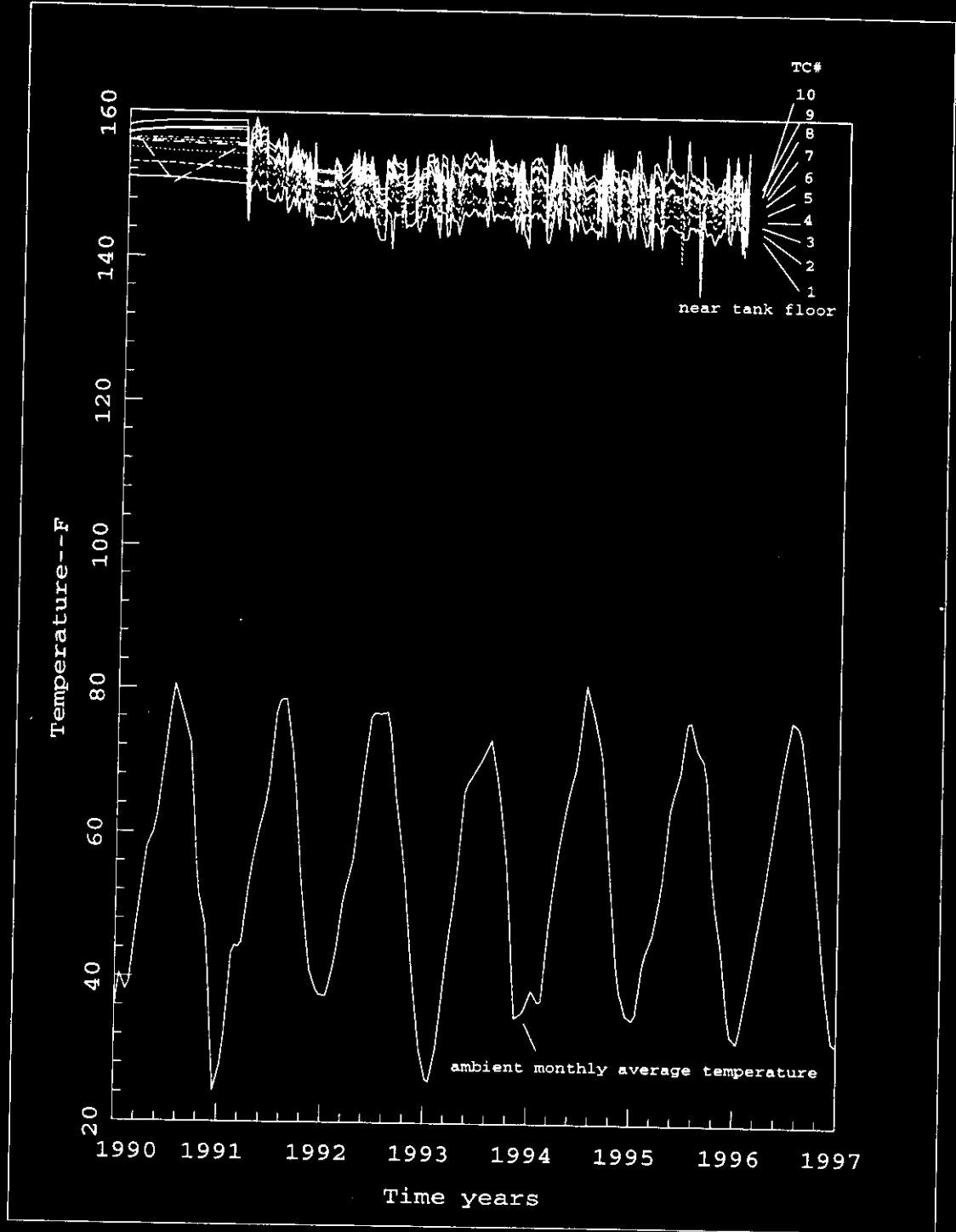


Figure 4.4 Tank A-101 Thermocouples 1-10 Lower Waste Temperature Data Versus Time

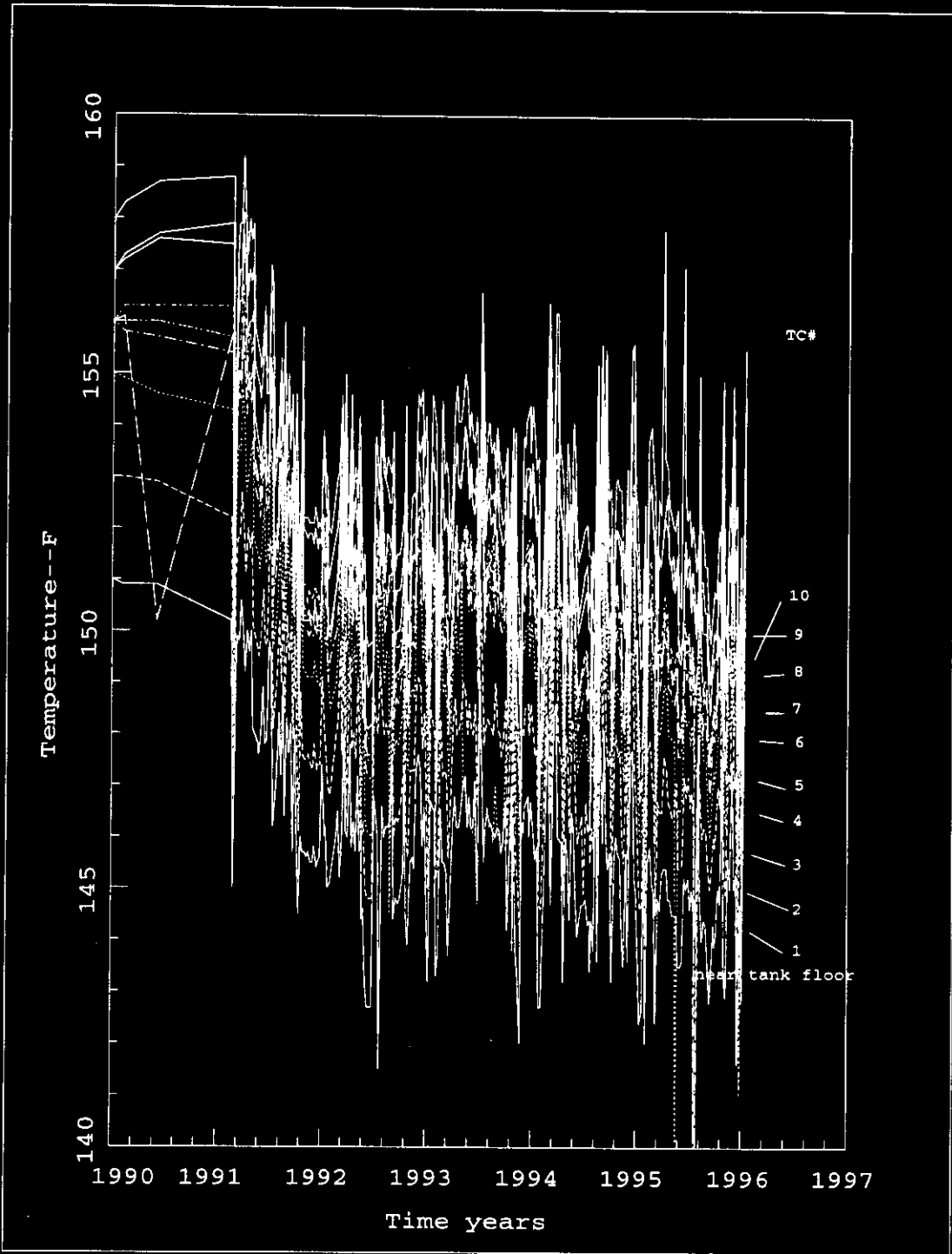


Figure 4.5 Tank A-101 Thermocouples 1-10 Lower Waste Temperature Data Versus Time

#### **4.2. TIME AVERAGED DATA**

Tank A-101 waste temperature has never reaches a steady state condition since being filled in 1980. Initial filling of the tank with warm slurry at ~125 F slurry from the evaporator in late 1980, annual cycle weather conditions, decaying radiolytic heat load, and varying active primary ventilation have resulted in the temperature history graphed above. Other factors which could augment the tanks transient thermal behavior include gradual changes in the annual average ambient temperature, varying natural circulation driven ventilation due to changing weather conditions and coupling of Tank A-101 to other tanks, changes in ventilation flow path resistance over time, changes in evaporation cooling due to slurry dryout, changes in soil conductivity due to dryout, and possibly changes in tank heat load due to chemical reactions, or heat of solution.

Tank A-101 temperatures may also change as a result of temperature changes in nearby tanks A-102, A-105, and A-106. The temperature may also not be uniform in the azimuthal direction due to the proximity of the neighboring tanks.

In spite of these issues, the temperature data provides a valuable basis from which to understand and evaluate the thermal hydraulic behavior of this particular tank. Time averaging the temperature data can provide some very useful and direct insights into the thermal hydraulic behavior of Tank A-101. The time averaged results also provided a rational basis for the modeling methodology employed in this evaluation.

##### **4.2.1. Time Averaged Axial Temperature Difference**

Essentially a time averaged axial temperature distribution was developed in prior analysis [Crowe, 1995] for the

beginning of 1993 using a Fourier Series regression approach applied to the time varying temperature data. This axial distribution is reproduced here as Figure 4.6 together with the corresponding thermocouple numbers for the thermocouple tree illustrated in Figures 3.1 and 3.4. Between thermocouples 9 and 16 the distribution can be characterized as parabolic, suggesting uniform heat generation and uniform conductivity within the waste, and heat removal primarily by axial 1-D conduction with little effect of multi-dimensional conduction effects. The temperature distribution between thermocouples 1 and 9 is somewhat more complicated to interpret, but when combined with the poor conductance through the soil below the tank to ultimate heat sinks, it can be concluded that the heat generation rate in this region is very low, rather than the conductivity being high.

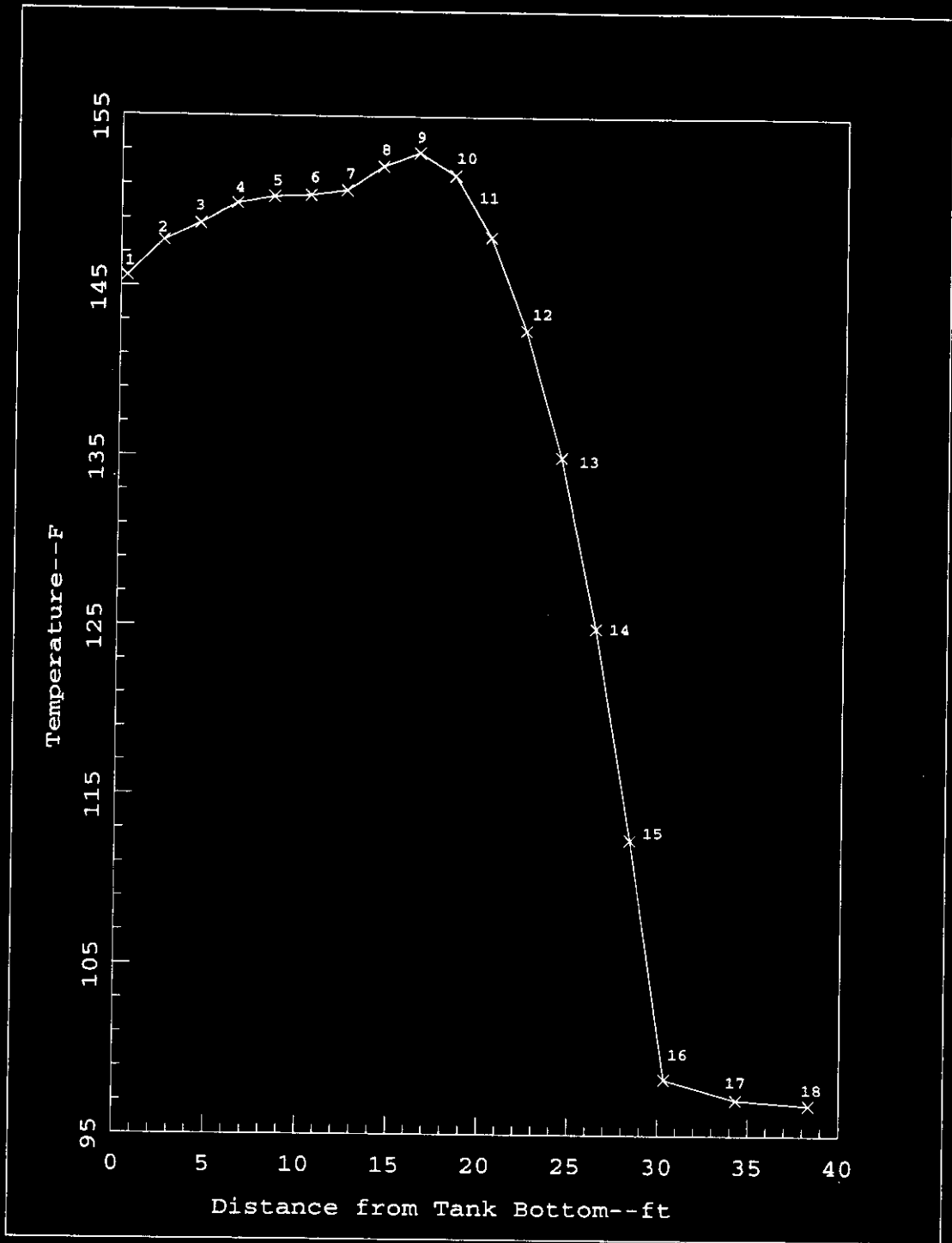


Figure 4.6 Tank A-101 Temperature versus Location--  
 Constant Term of Fourier Series Fit (Essentially time  
 average temperature, 1/93-9/95, versus location).

In the course of this evaluation linear regression fits of the temperature data over a slightly different time period were developed for both the axial distribution, as well as for time averaged temperature versus time. The time period selected for this evaluation was 1/93-1/96. The resulting axial temperature distribution is compared to that of Figure 4.6 in Figure 4.7. There are no major differences.

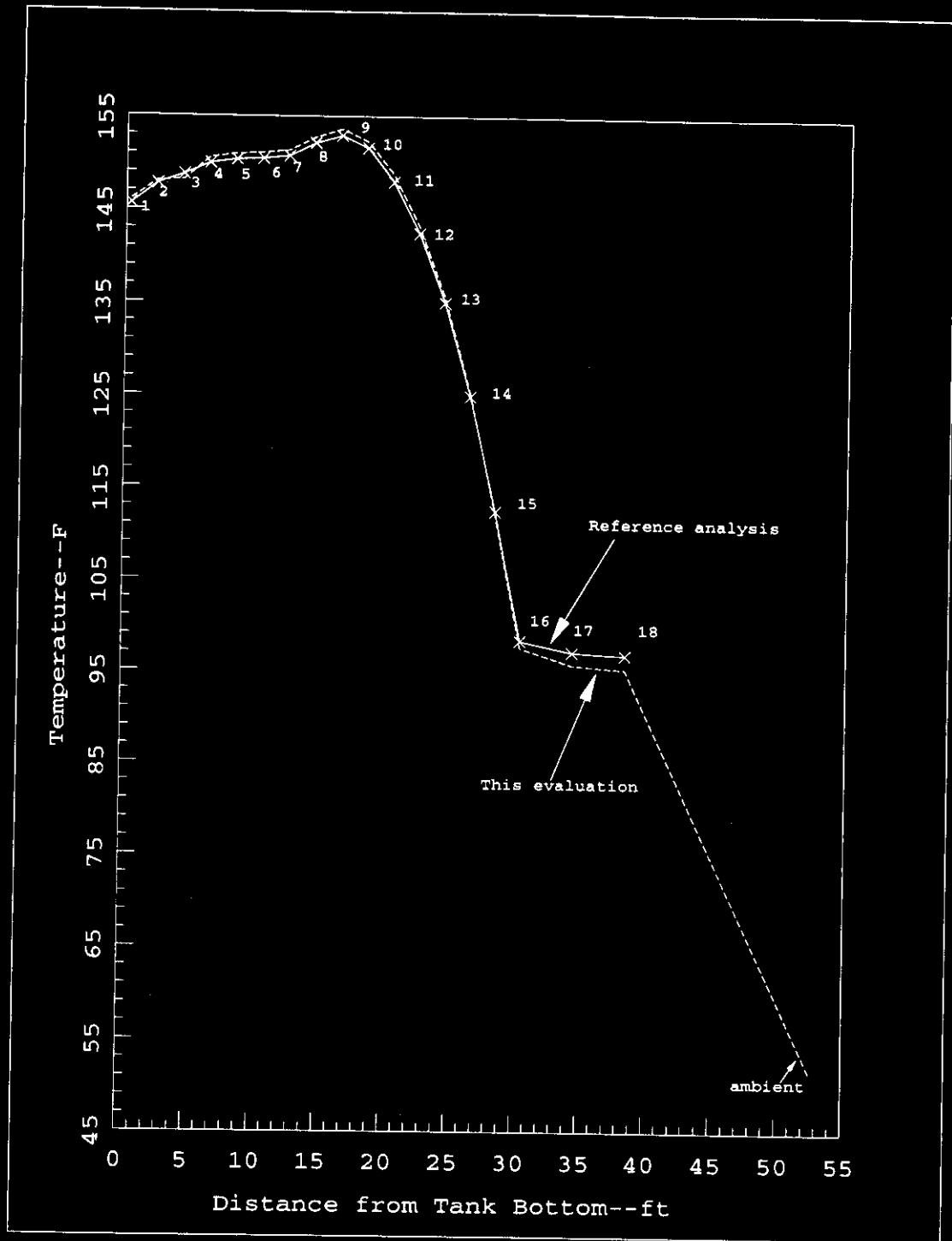


Figure 4.7 Tank A-101 Time Averaged Axial Temperature Distribution Comparison--Prior Analysis and Current Evaluation

#### 4.2.2. Temperatures versus Time--Linear Fit

As indicated in the previous section linear fits of the temperature at each thermocouple over time as well as the monthly average ambient over the 1/93-1/96 time period were made to clarify the temperature trends which were somewhat skewed by the "hash" in the data. The data for this time period and linear fits are provided in Figures 4.8-4.12. The time rate of temperature change, or slope, of the linear fit is also shown.

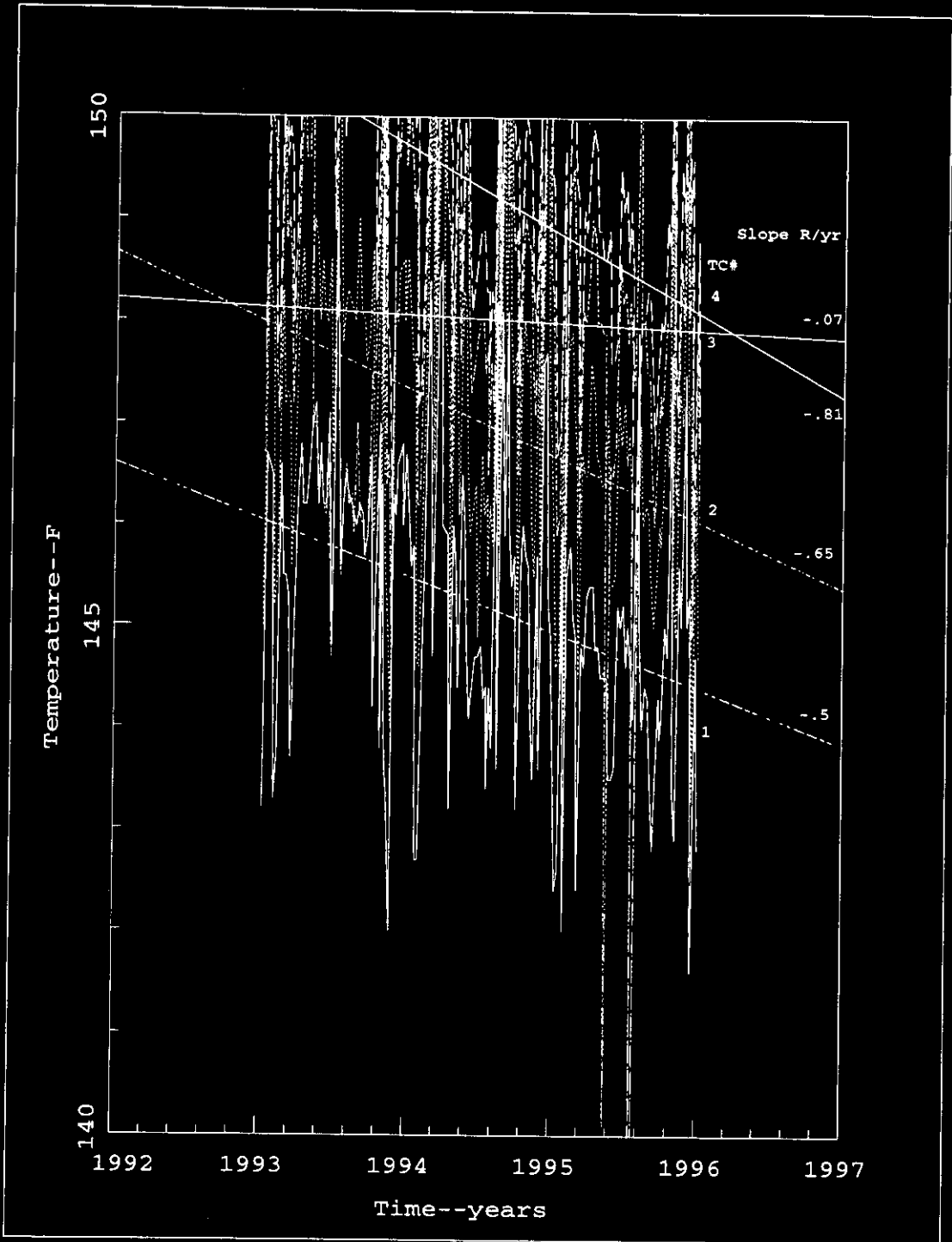


Figure 4.8 Temperature vrs Time and Linear Fits TC-1 through TC-4

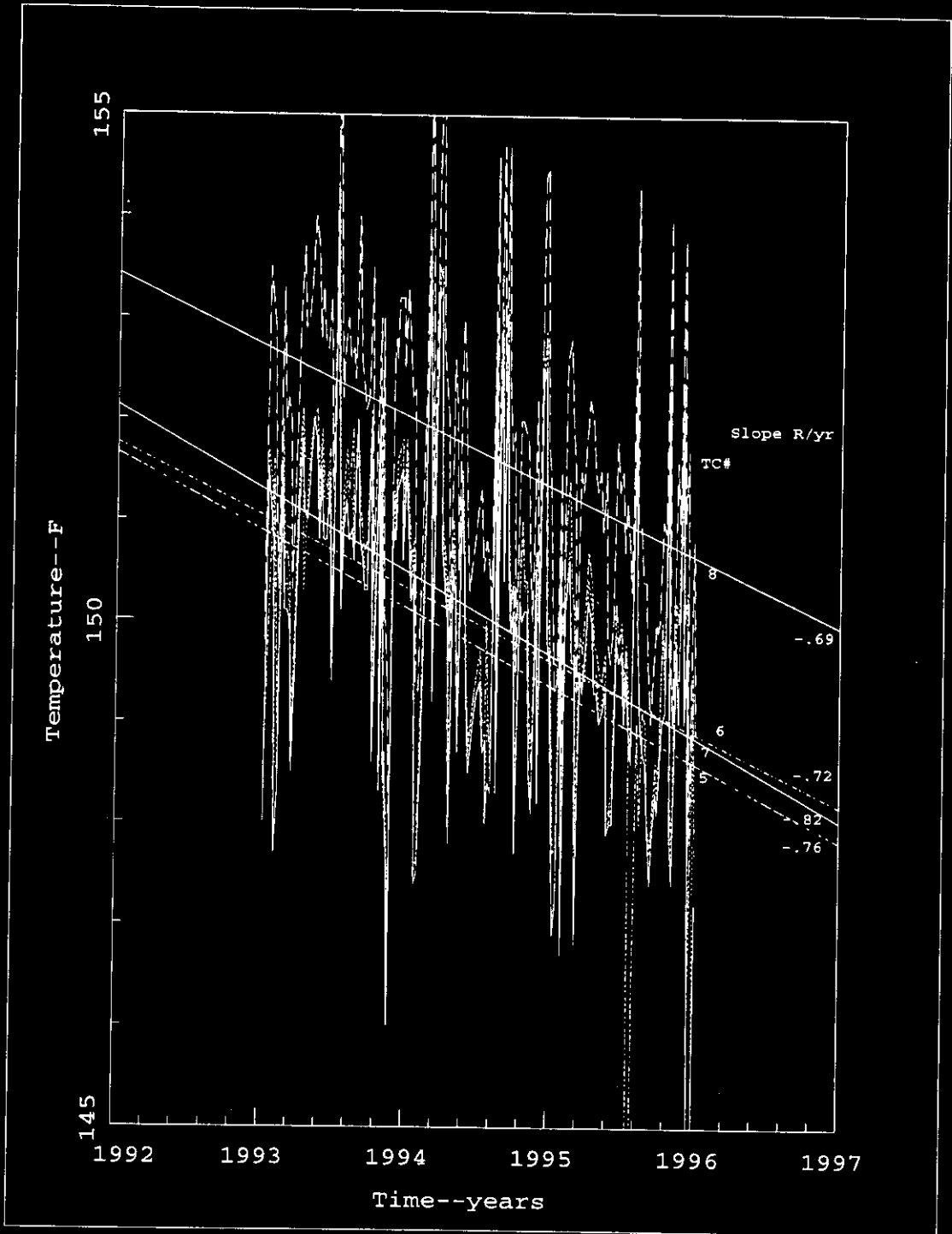


Figure 4.9 Temperature vrs Time and Linear Fits TC-5 through TC-8

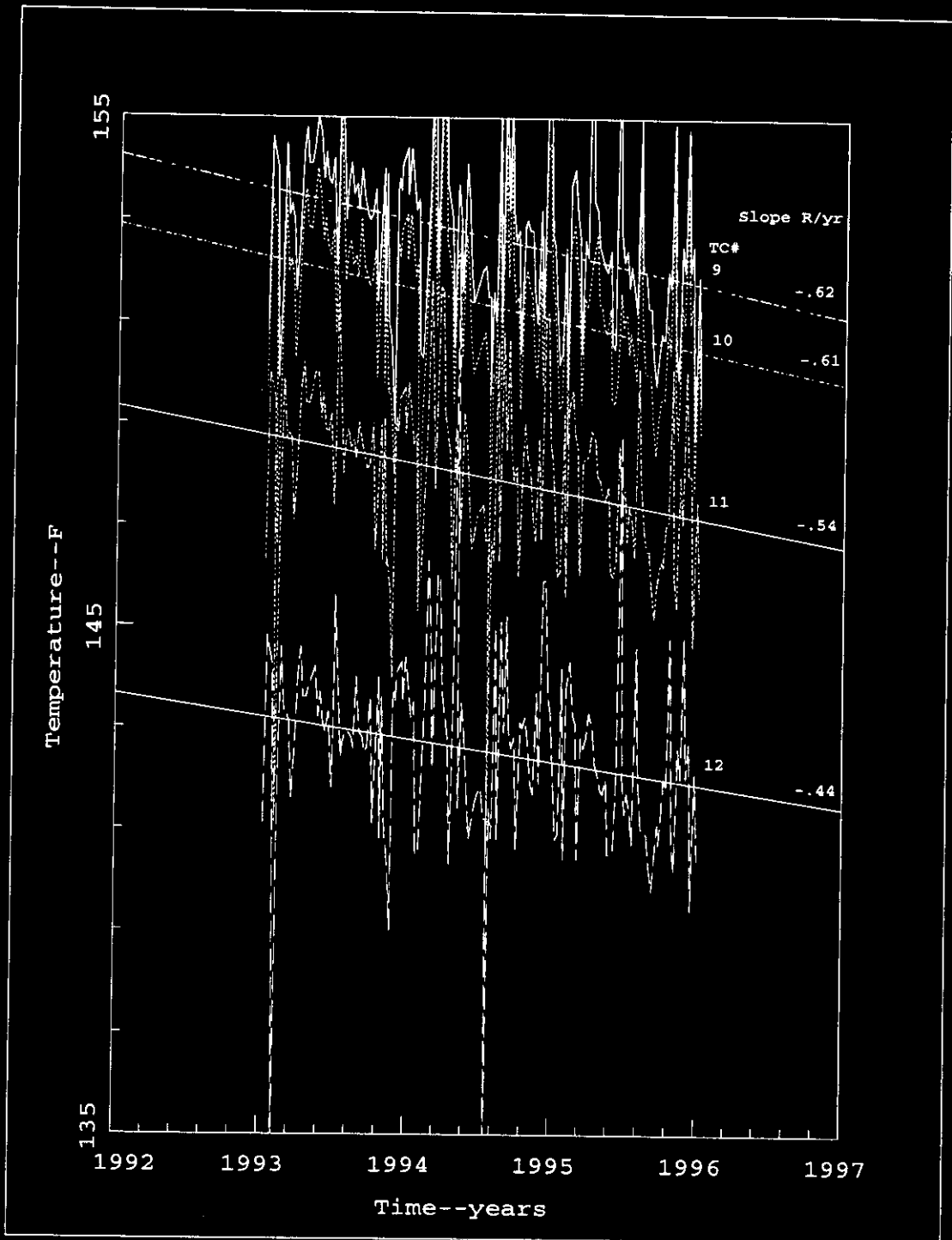


Figure 4.10 Temperature vrs Time and Linear Fits TC-9 through TC-12

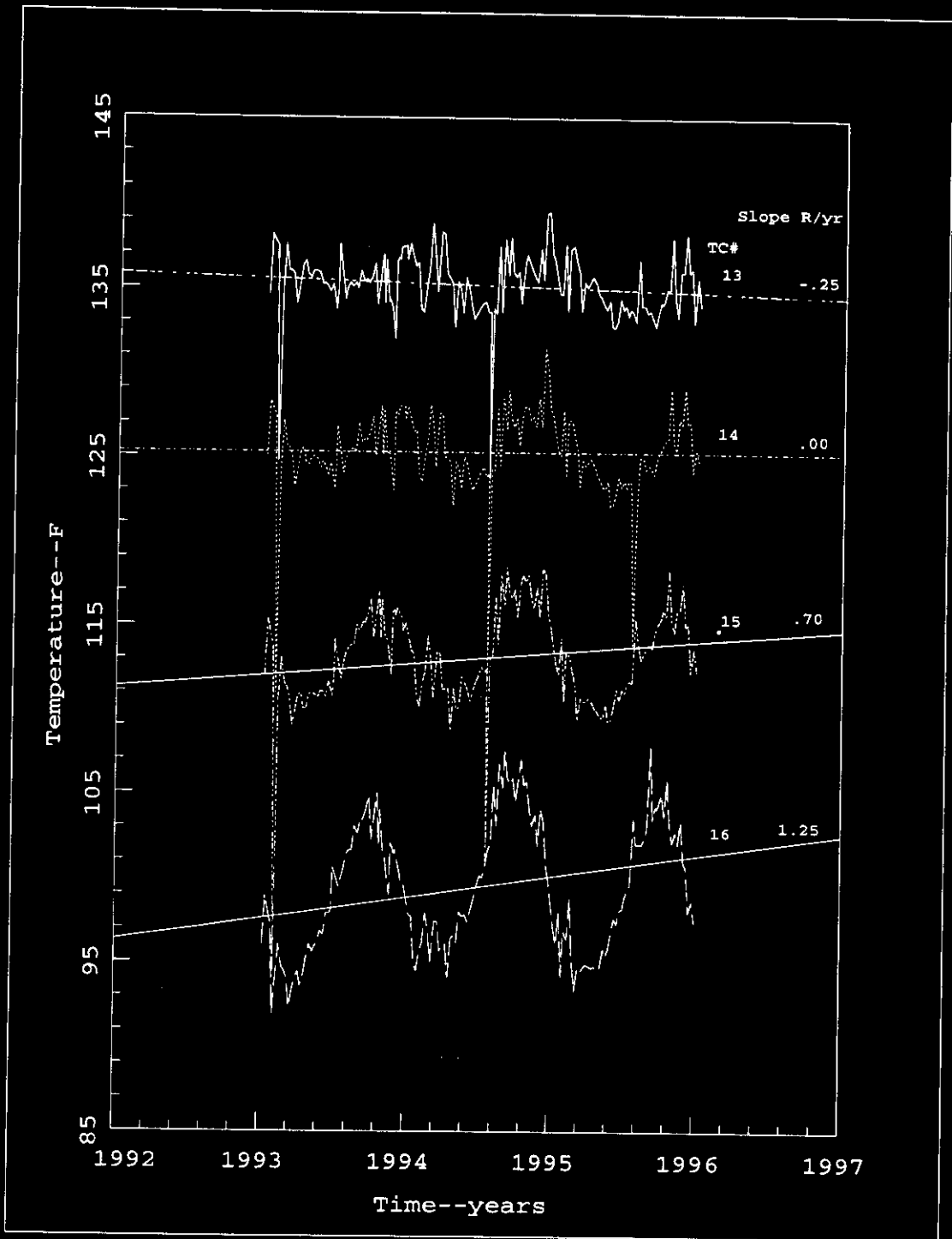


Figure 4.11 Temperature vrs Time and Linear Fits

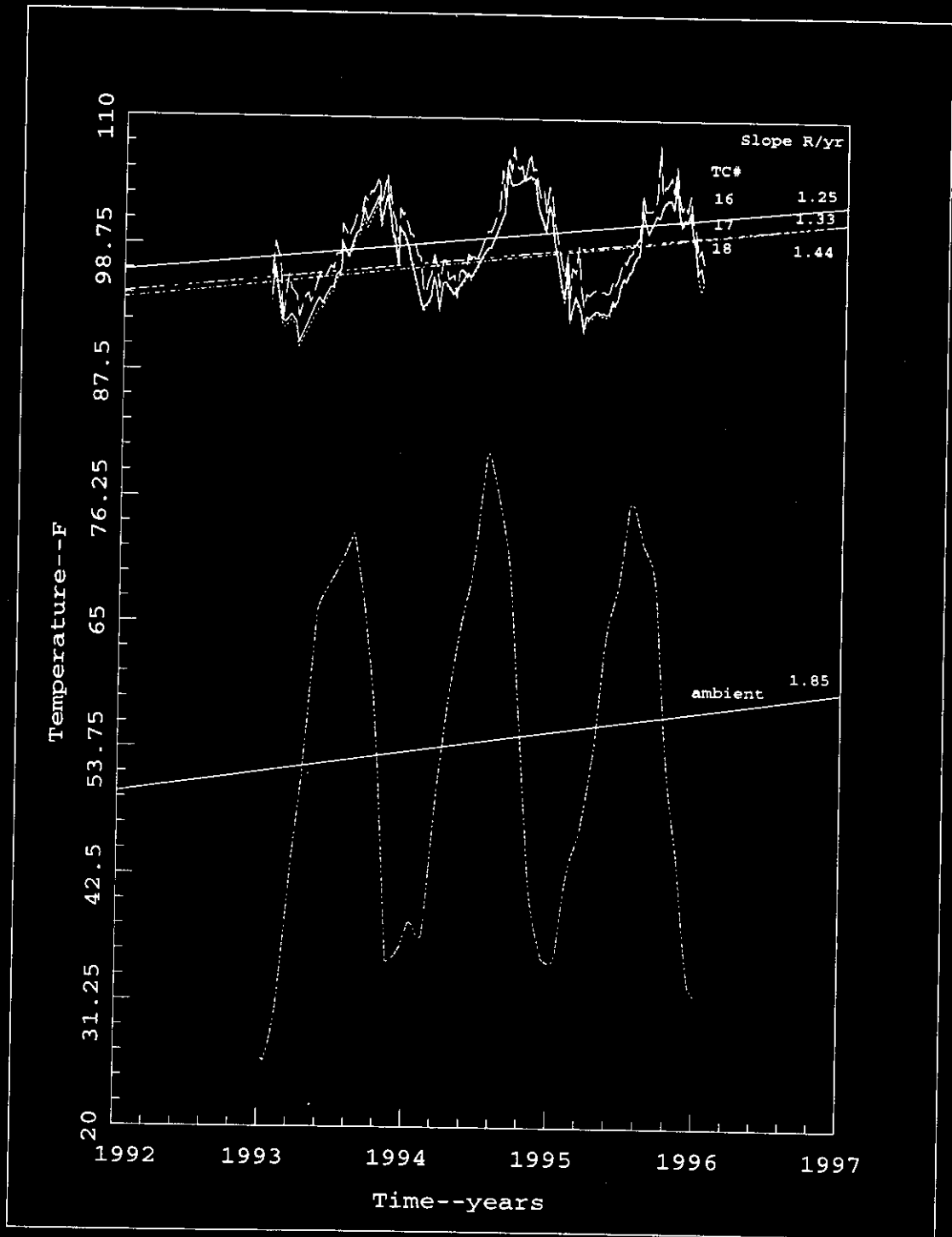


Figure 4.12 Temperature vrs Time and Linear Fits  
 TC-16 through TC-18, and Ambient Monthly Average

A comparison of the Reference analysis and the current evaluation rates of temperature change are provided in Figure 4.13. All data points were included in the current evaluation, whereas some culling of the data was done in the Reference analysis which may account for the difference at TC-3. It is not clear what the cause of the difference in the dome region is, TC-17 and TC-18. In this evaluation the dome temperature rise appears to track the rise in the ambient time averaged temperature. The rise in the ambient time average temperature will cause the temperature in the dome and the upper regions of the sludge to rise. The extent this temperature increase propagates into the waste depends upon the rate of rise in temperature of the ambient, and the decrease in heat generation rate in the waste.

Examination of the absolute temperatures and their rate of change cannot resolve the issue of whether heat generation is increasing in the dome, or waste. Evaluation of spatial temperature gradients versus time can help in this regard. Both first and second order spatial temperature gradients were evaluated in this analysis. This is discussed in the following section.

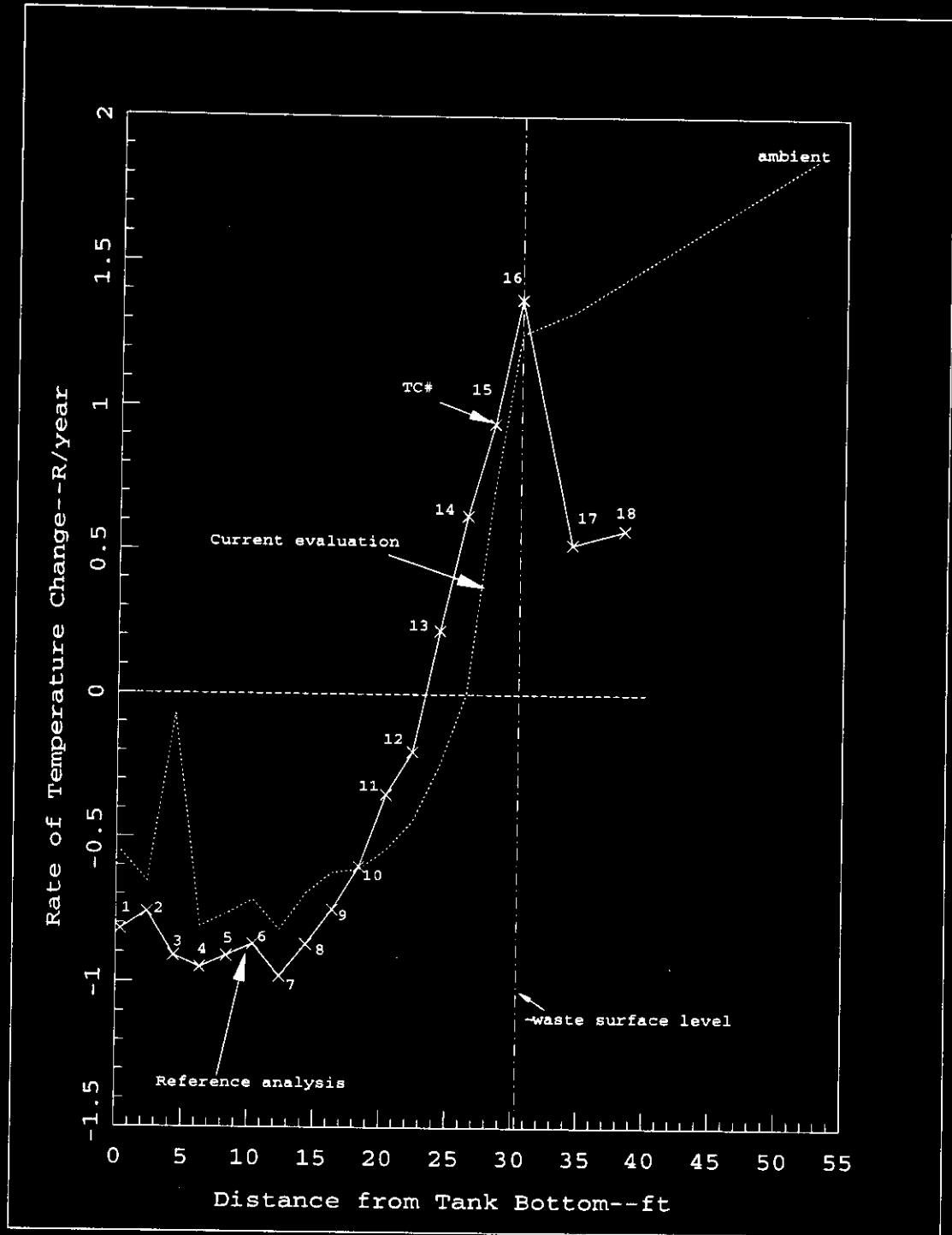


Figure 4.13 Tank A-101 Temperature Rate of Change versus Axial Location--Reference and Current Analyses

#### 4.3. TIME RATE OF CHANGE OF FIRST AND SECOND ORDER SPATIAL TEMPERATURE DIFFERENCES

Although temperatures may be holding steady or slowly rising within the waste or dome space on a time averaged basis, there does not need to be an increase in the heat generation rate, since rising time averaged ambient temperature conditions, or operation of the forced ventilation system followed by termination of operation can cause temperatures to rise for a period of time. Ultimately these effects will diminish and the temperatures should decrease due to decreasing radiolytic heat load, if no other heat sources (chemical, etc.) are present at an increasing rate, and assuming cooling mechanisms are not changing. Although the trends in heating or cooling can be noted visually by graphing the temperature data over very long periods of time, for shorter periods of time (even including several years) mathematical regression may be required and here care must be taken in selecting the time periods of evaluation.

On a shorter term basis the annual cyclic meteorology cause all temperatures to rise and fall annually within the waste and dome, although the amplitude of oscillation is exponentially attenuated with depth.

Besides evaluating the absolute temperatures and their trends, some insight can be gained by evaluating the temperature differences between axial positions within the tank. If all heat generation sources are uniformly distributed and decreasing over time, if all cooling mechanisms are not changing on a time averaged basis, then time averaged temperature differences between any two axial locations within the waste/dome and surrounding soil should be decreasing with time also.

The general differential equation describing the relationship between temperature, heat generation rate, conductivity, and diffusivity for one dimensional heat

conduction is [Kreith, 1973]:

$$\frac{\partial^2 T}{\partial x^2} = \left( \frac{1}{\alpha} \right) \left( \frac{\partial T}{\partial t} \right) - \frac{q}{k} \quad (4.1)$$

where,

T = Temperature

x = distance from arbitrary reference location

t = time

q = volumetric heat generation rate

k = conductivity

$\alpha$  = thermal diffusivity

$$\alpha = \frac{k}{\rho C_p} \quad (4.2)$$

where,

$\rho$  = density

$C_p$  = specific heat

#### **4.3.1. Second Order Calculation of Time Rate of Change in Heat Generation**

The rate of heat generation at any point in the waste material in terms of the other terms is:

$$\frac{q}{k} = \frac{-\partial^2 T}{\partial x^2} + \left(\frac{1}{\alpha}\right) \left(\frac{\partial T}{\partial t}\right) \quad (4.3)$$

$$q = -k \frac{\partial^2 T}{\partial x^2} + \left(\frac{k}{\alpha}\right) \left(\frac{\partial T}{\partial t}\right) \quad (4.4)$$

$$q = -k \frac{\partial^2 T}{\partial x^2} + (\rho C_p) \left(\frac{\partial T}{\partial t}\right) \quad (4.5)$$

Since  $q$  and  $T$  are functions of time:

$$q(t) = -k \frac{\partial^2 T(t)}{\partial x^2} + (\rho C_p) \left(\frac{\partial T(t)}{\partial t}\right) \quad (4.6)$$

If the time rate of change in  $q(t)$  is based only upon the first term,

$$q(t) = k \frac{\partial^2 T(t)}{\partial x^2} \quad (4.7)$$

by ignoring the second term,

$$(\rho C_p) \left(\frac{\partial T(t)}{\partial t}\right) = 0.0 \quad (4.8)$$

then the calculated time rate of change will be too fast if the local temperature is rising (calculated half life will be too short). The calculated time rate of change of  $q(t)$  will be too slow if the local temperature is falling (calculated half life will be too long).

If this approximate method is used to determine the rate of decrease in heat generation in the lower part of the tank during the 1992-1996 time period, calculated half lives will be too long since temperatures there are decreasing.

Near the waste surface this approximate method will lead to calculated half lives that are too short since temperatures at that location are increasing.

If the rate of temperature change is slow, however, as shown in Figure 4.14 the order of magnitude of the stored energy term is small relative to the spatial derivative term. Therefore ignoring the stored energy term and using only the time averaged value for the spatial derivative term to compute the local volumetric heat generation term and its rate of change with time, or decay, should not result in significant error. A difficulty arises when the data has considerable "hash" as will be seen in the following, and the time averaging process results in skewed time averaged fits of the spatial temperature derivatives, which do not really represent the time averaged conditions in the tank. For locations low in the tank this makes determination of the rate of change in power at these locations difficult to determine.

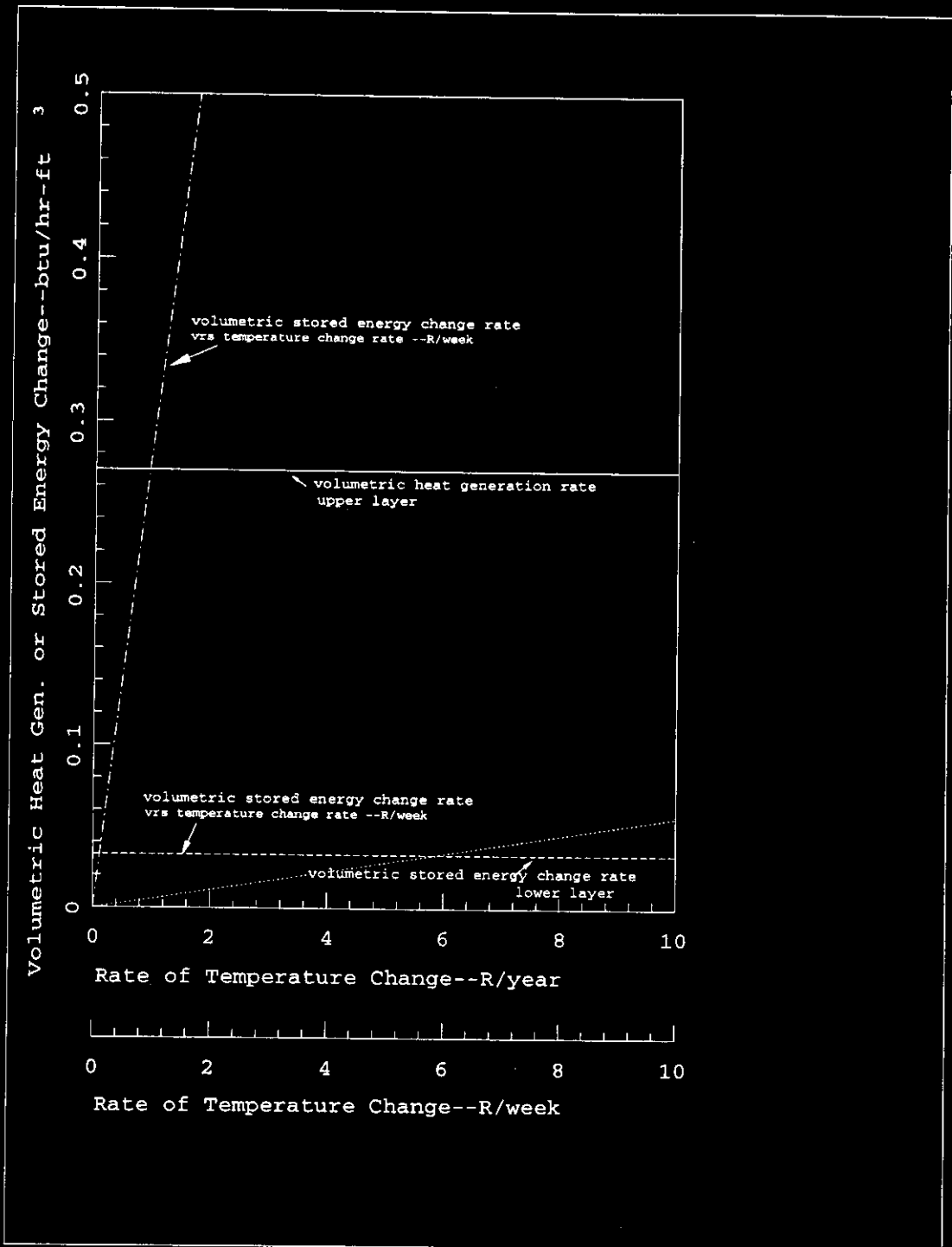


Figure 4.14 Relative Magnitude of Volumetric Heat Generation Rate and Stored Energy Change Rates

Figures 4.15 and 4.16 illustrate the results of computing local heat generation rates as a function of time based on second order spatial derivatives of temperature. These were then fitted with a linear curve and the equivalent half life computed. Each heat generation rate curve was based on the temperature differences between the thermocouple locations noted. Results are only shown for locations between thermocouples 10-16 in the upper waste regions. Although some of the results are in the expected half life range, the "hash" in the data becomes magnified when processed with this procedure, producing only marginally useful results in the upper regions of the waste. In the lower regions the effect of the "hash" becomes so amplified that the results are of little value. More useful results were obtained by considering the first order temperature differences as discussed in the following.

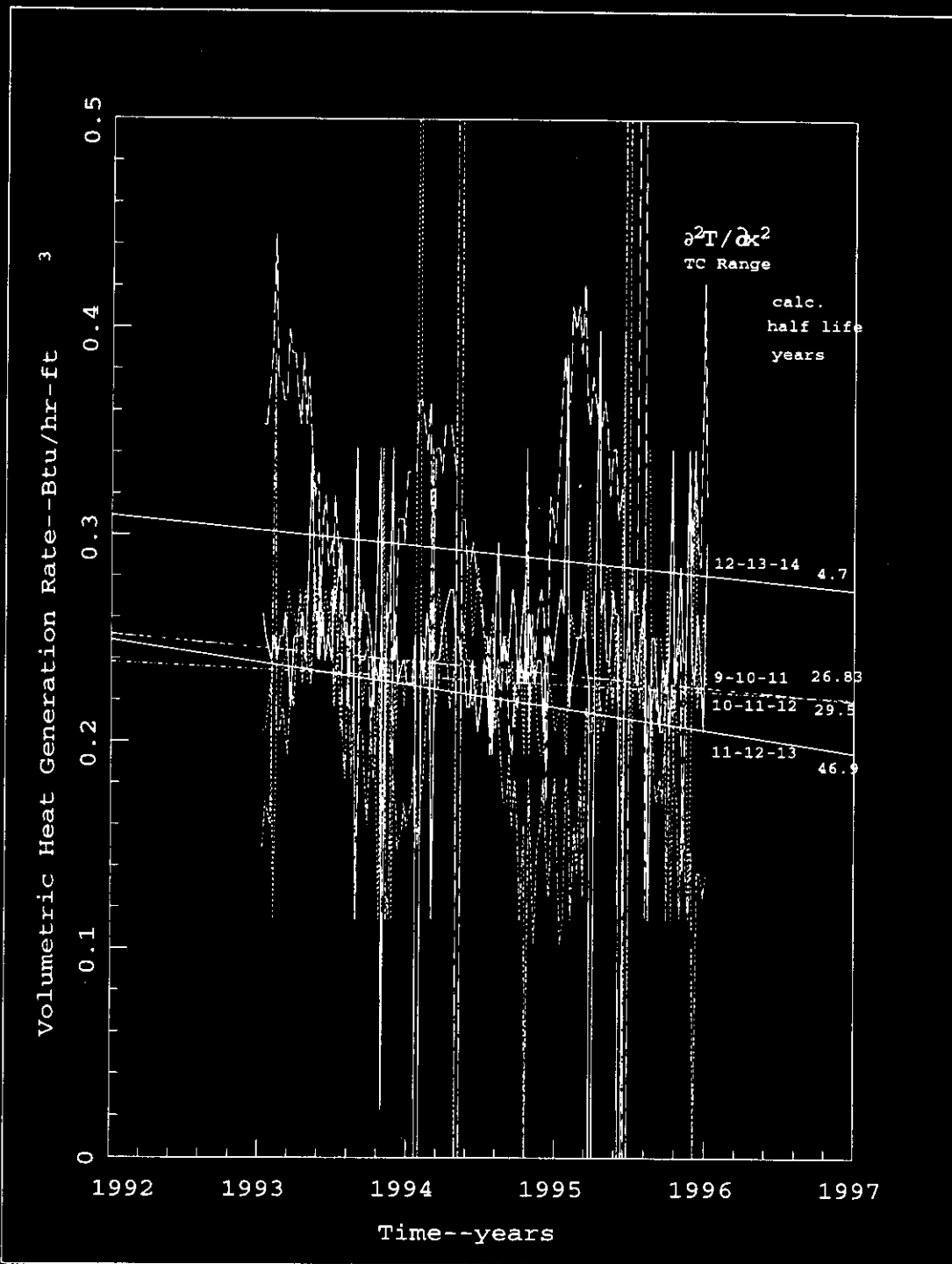


Figure 4.15 Volumetric Heat Generation Rates vrs Time, Linear Fits, and Half Lives

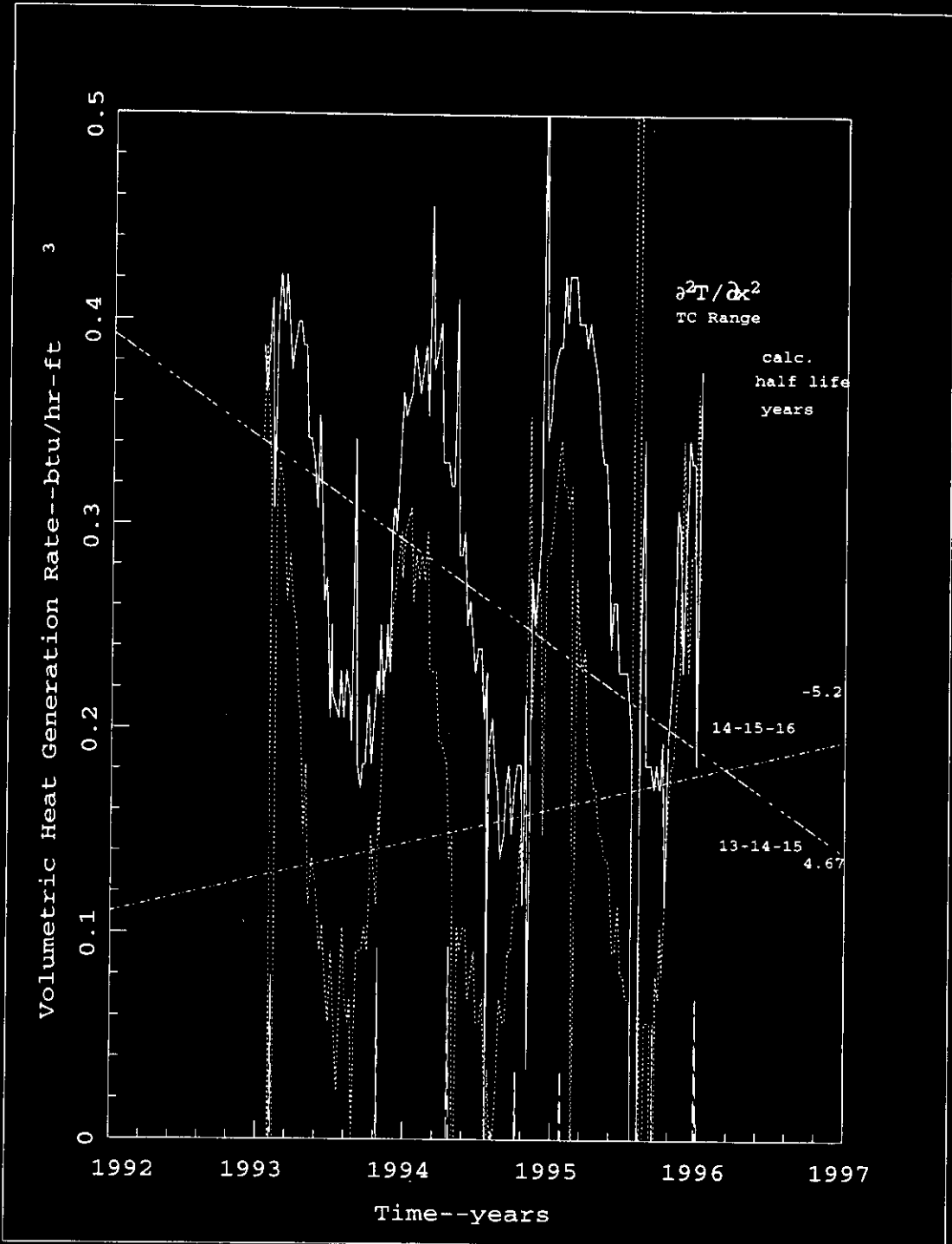


Figure 4.16 Volumetric Heat Generation Rates vrs Time, and Linear Fits and Half Lives

**4.3.2. First Order Calculation of Time Rate of Change in Temperature Differences and Heat Generation Rate**

The first order spatial temperature difference at any location, can be obtained by integrating:

$$\frac{\partial^2 T}{\partial x^2} = \left(\frac{1}{\alpha}\right) \left(\frac{\partial T}{\partial t}\right) - \frac{q}{k} \quad (4.9)$$

to obtain:

$$\frac{\partial T(t)}{\partial x} = \int_0^L \left(\frac{1}{\alpha}\right) \left(\frac{\partial T(t)}{\partial t}\right) dx - \int_0^L \frac{q(t)}{k} dx \quad (4.10)$$

$\partial T(t)/\partial x$  = Time rate of change of temperature difference (as a function of time) with space at any location within the tank waste.

Where,

$$\frac{\partial T(t)}{\partial x} = \frac{-q_{flux}}{k} \quad (4.11)$$

= Time varying heat flux,  $q_{flux}$ , divided by conductivity,  $k$ , at any location,

and,

$$\int_0^L \left(\frac{1}{\alpha}\right) \left(\frac{\partial T(t)}{\partial t}\right) dx = \int_0^L \left(\frac{\rho C_p}{k}\right) \left(\frac{\partial T(t)}{\partial x}\right) dx \quad (4.12)$$

= Time rate of change of heat stored within the soil/waste (as a function of time) between an adiabatic location,  $x=0$ , and the location,  $L$ , where  $\partial T(t)/\partial x$  is defined, divided by the conductivity,

and,

$$\int_0^L \frac{q(t)}{k} dx \quad (4.13)$$

= Time rate of change of heat being generated within the soil/ waste between an adiabatic location,  $x=0$ , and the location,  $L$ , where  $\partial T(t)/\partial x$  is defined, divided by the conductivity.

Therefore the heat flux at any location at any time,  $k\partial T(t)/\partial x$ , at any location, equals the rate of heat being generated between that location and an adiabatic location at that time, plus the rate of heat storage or draining between that location and the same adiabatic location.

If  $k$  and  $q(t)$  are uniform over the thickness considered:

$$\frac{\partial T(t)}{\partial x} = \int_0^L \left( \frac{1}{\alpha} \right) \left( \frac{\partial T(t)}{\partial t} \right) dx - \int_0^L \frac{q(t)}{k} dx \quad (4.14)$$

can be transformed after integrating the  $q(t)$  term to:

$$q(t) \frac{L}{k} = \int_0^L \left( \frac{1}{\alpha} \right) \left( \frac{\partial T(t)}{\partial t} \right) dx - \frac{\partial T(t)}{\partial x} \quad (4.15)$$

$$q(t) = \left( \frac{k}{L} \right) \int_0^L \left( \frac{1}{\alpha} \right) \left( \frac{\partial T(t)}{\partial t} \right) dx - \left( \frac{k}{L} \right) \frac{\partial T(t)}{\partial x} \quad (4.16)$$

$$q(t) = \left( \frac{\rho C_p}{L} \right) \int_0^L \left( \frac{\partial T(t)}{\partial t} \right) dx - \left( \frac{k}{L} \right) \frac{\partial T(t)}{\partial x} \quad (4.17)$$

From these relationships it could be concluded that if the temperature difference between any two points in the slurry were decreasing with time on a time average basis, then the average heat generation rate between an adiabatic location and midway between the two points would have to be decreasing--with one exception. Before this conclusion can be drawn the term involving the time rate of change of heat stored term must be considered.

If T is rising with time, and the time rate of change of

$$-\left(\frac{k}{L}\right) \frac{\partial T(t)}{\partial x} \quad (4.18)$$

alone is used as the basis for determining  $q(t)$ 's half life, then the calculated half life will be too small.

And if T is decreasing with time, and the time rate of change of  $(k/L) * \partial T / \partial x$  alone is used as the basis for determining  $q(t)$ 's half life, then the calculated half life will be too large.

If this approximate method is used to determine the rate of decrease in heat generation in the lower part of the tank during the 1992-1996 time period, calculated half lifes will be too long since temperatures there are decreasing. Near the waste surface this approximate method will lead to calculated half lifes that are too short since temperatures at that location are increasing.

As with the second order derivative approach, it can be shown however that the order of magnitude of the stored energy term is small relative to the spatial derivative term for time averaged values for both terms. The same can be shown for the time derivatives of both of these terms,

based on their time averaged values. Therefore ignoring the stored energy term and using only the time averaged value for the spatial derivative term to compute the local volumetric heat generation term and its rate of change with time, or decay, will not result in significant error.

#### 4.3.2.1. Time Rate of Change of Spatial Temperature Differences 1990-1/1996

The temperature differences between successive axial locations in the tank versus time are plotted below in Figures 4.17-4.20 from 1/90 through 1/96. Visual observation indicates the general trend is downward suggesting decreasing heat generation between all thermocouple locations.

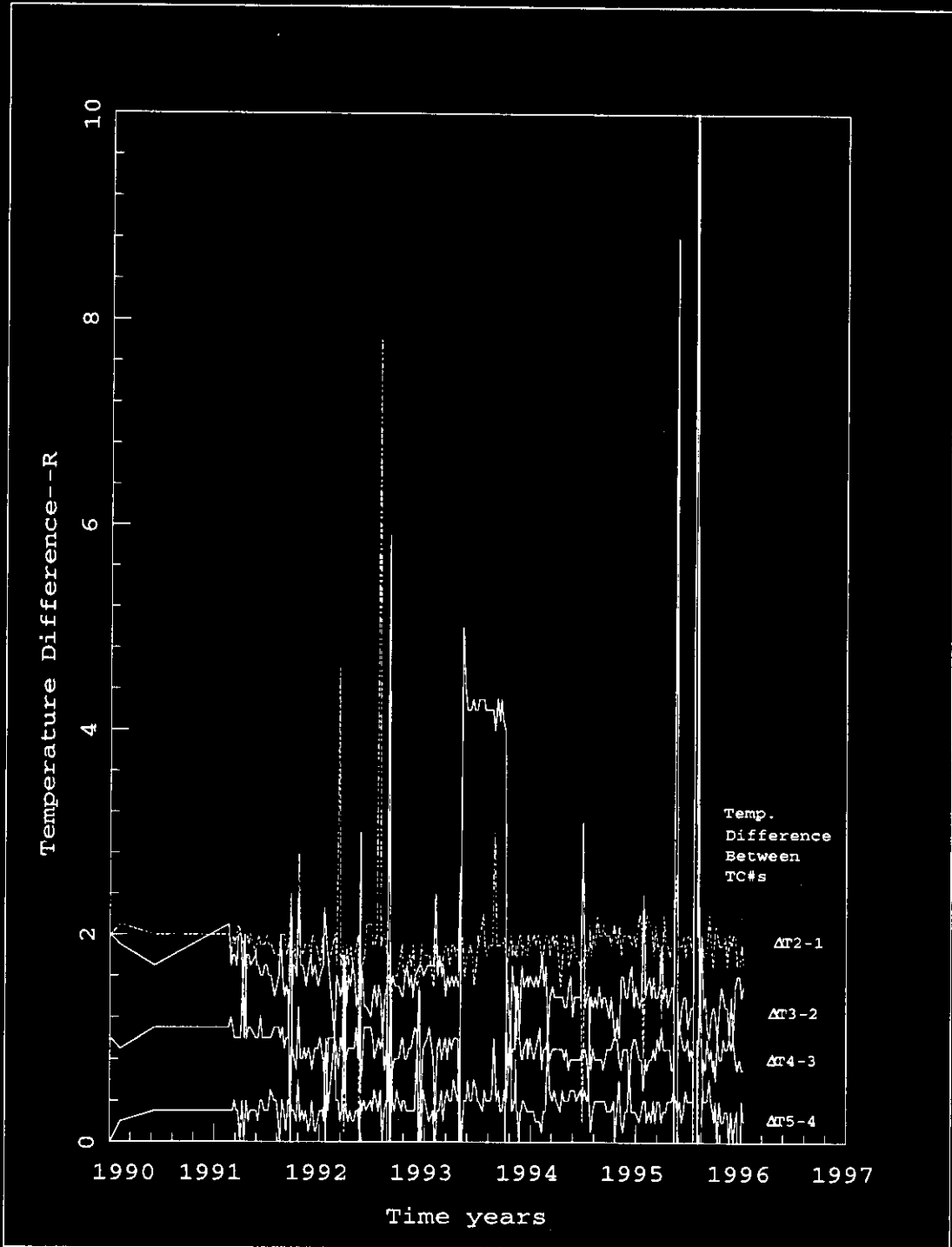


Figure 4.17 Tank A-101 Thermocouples 1-5 Temperature Data Differences Versus Time

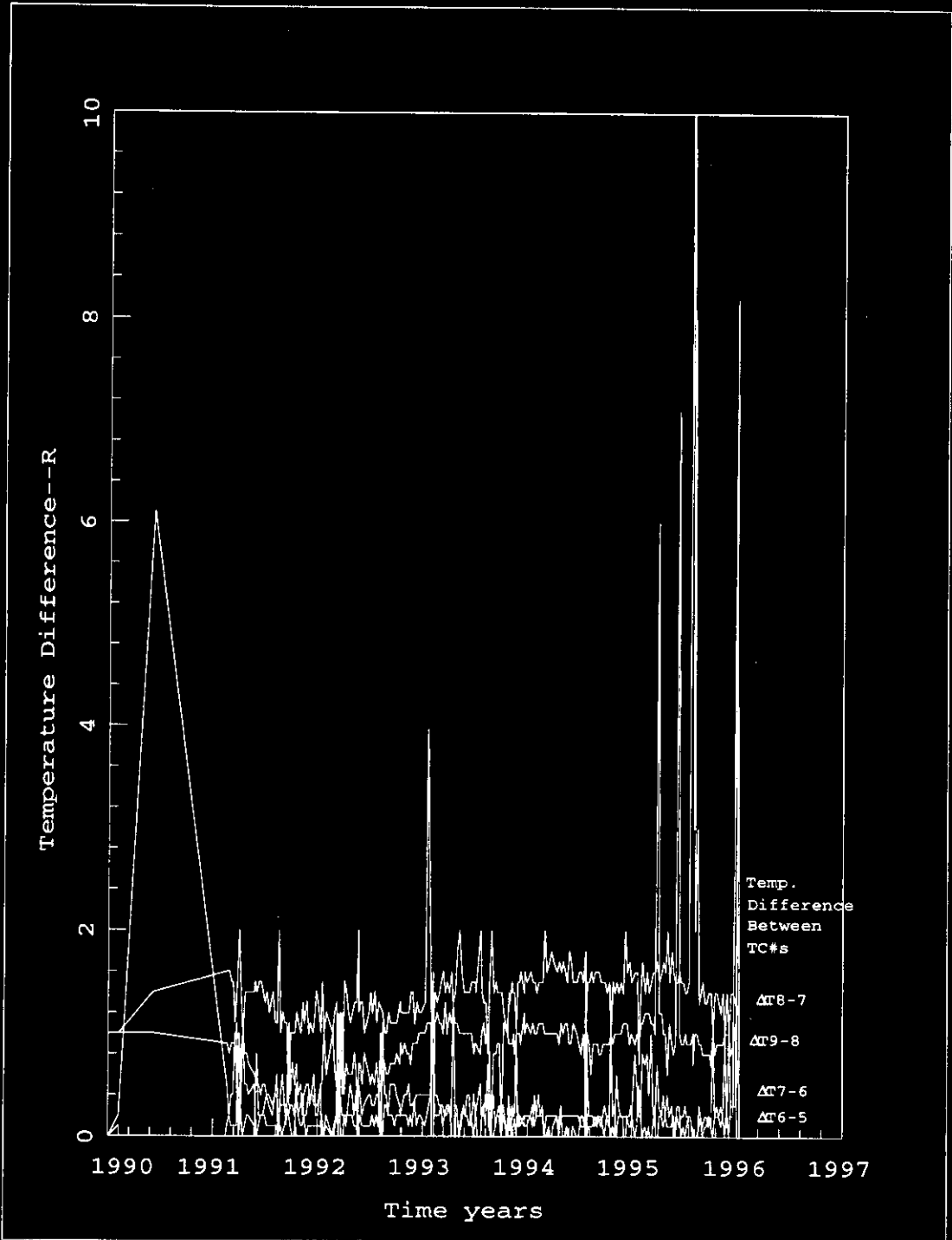


Figure 4.18 Tank A-101 Thermocouples 5-9 Temperature Data Differences Versus Time

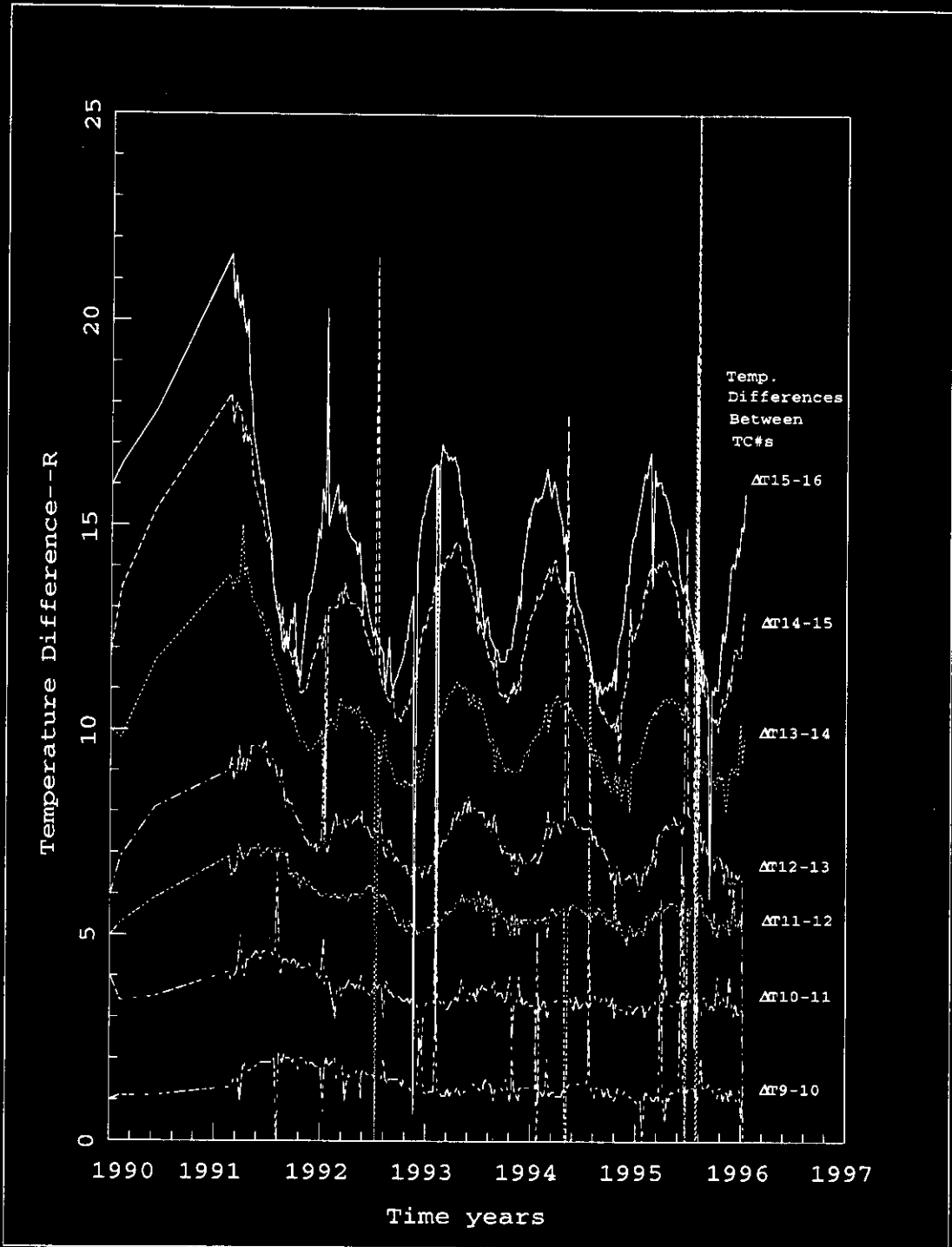


Figure 4.19 Tank A-101 Thermocouples 9-16 Temperature Data Differences Versus Time

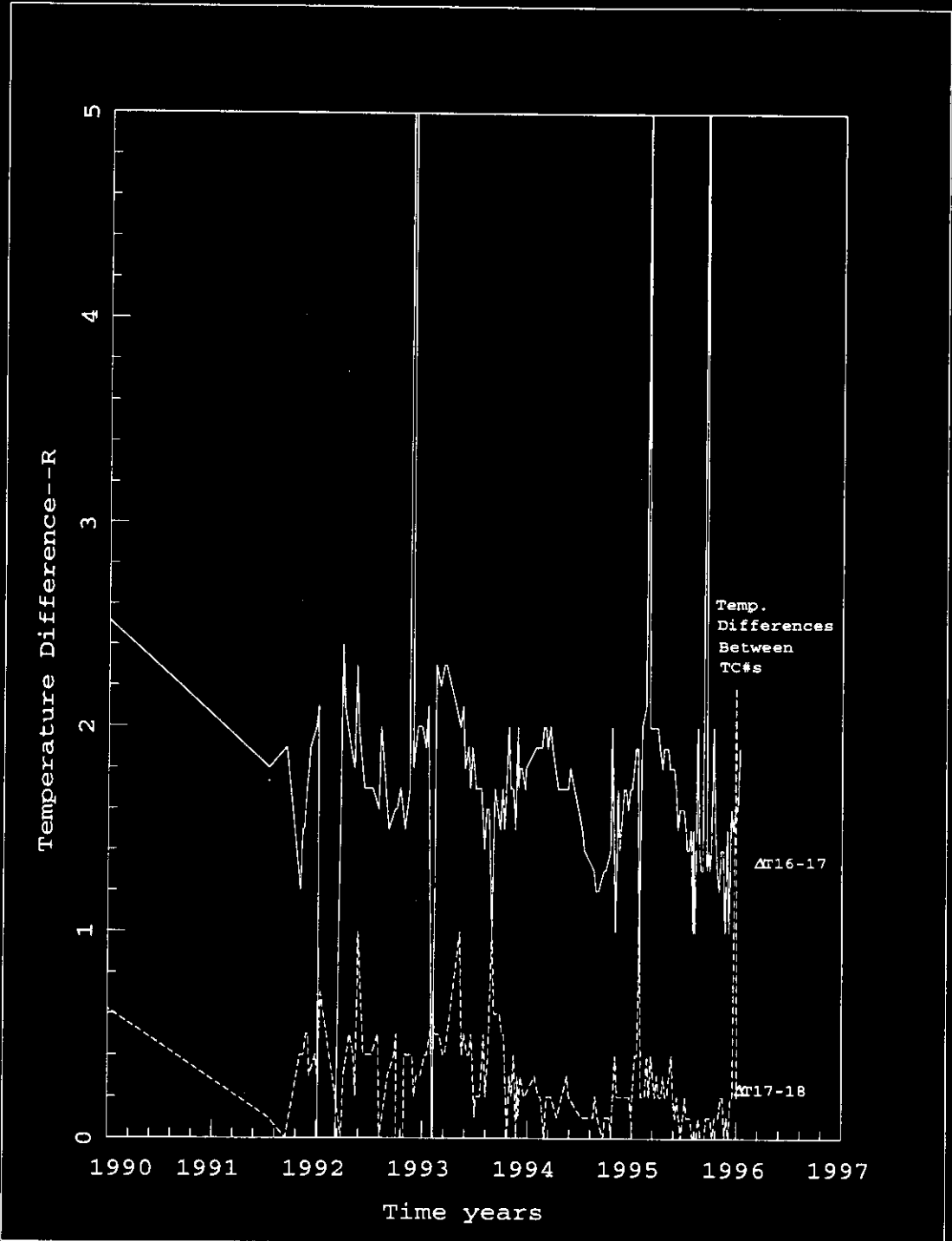


Figure 4.20 Tank A-101 Thermocouples 16-18 Temperature Data Differences Versus Time

Temperature differences between the bottom of the tank and the peak temperature location, TC-1 to TC-9, between the peak temperature location and the dome gas/ waste interface, TC-9 to TC-16, and between the dome gas/waste interface and the ambient, TC-16 to ambient, are plotted in Figure 4.22. Visual observation indicates a downward trend, particularly during the last 3 years.

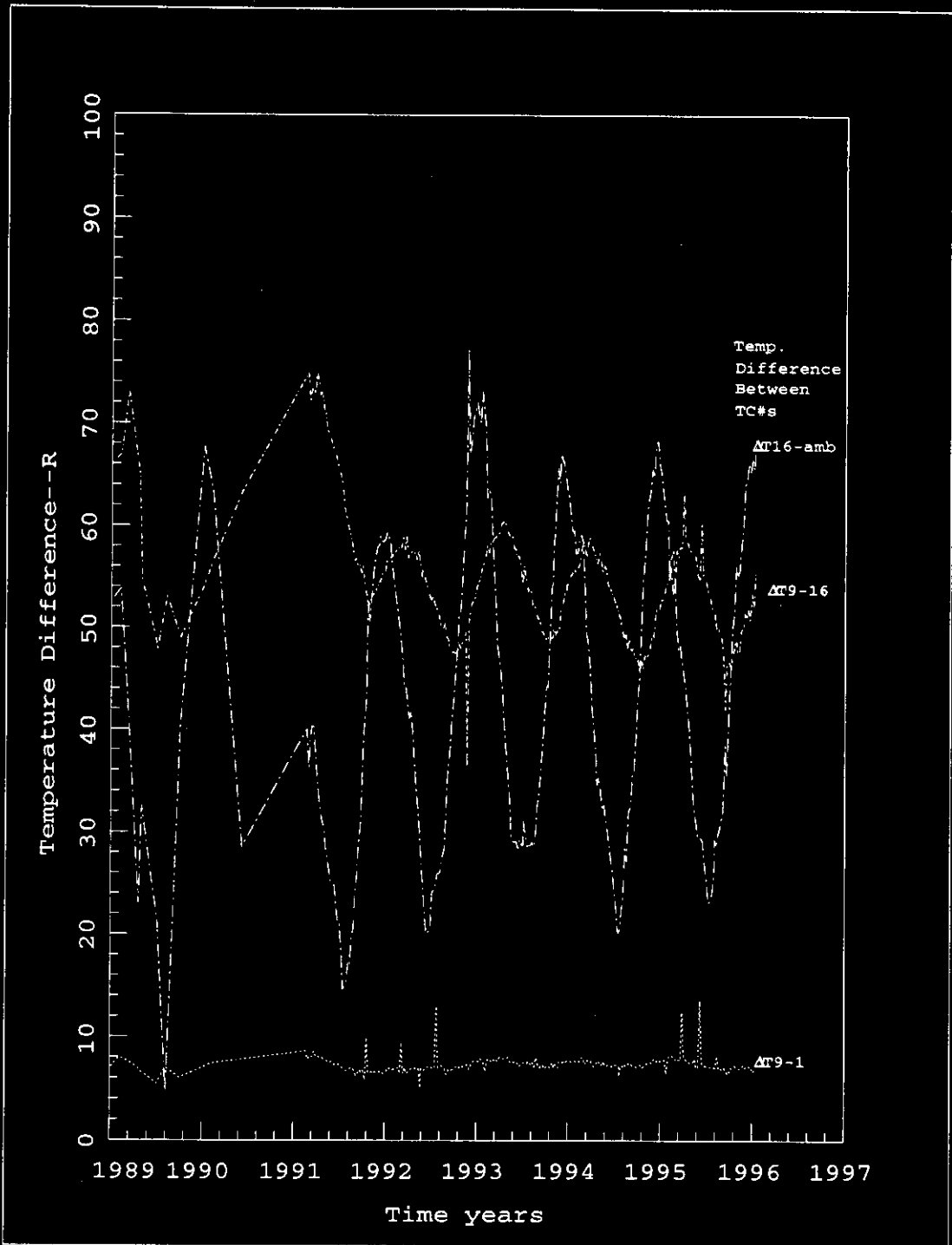


Figure 4.21 Tank A-101 Thermocouples 1, 9, 16 and Ambient Temperature Difference Data Versus Time

#### 4.3.2.2. Time Rate of Change in Spatial Temperature Differences, Linear Fits, and Half Lives 1993-1/1996

Axial temperature difference change rate versus time and axial location, linear fits of these rates, and half lives were calculated based on differences in temperature between thermocouple locations. The results are graphed in Figures 4.23-4.26. Temperature differences in the upper regions of the tank are decreasing somewhat faster than the 30 year half life expected. In the lower tank waste regions the axial temperature differences are small since the heat generation is low and heat fluxes are low, and as a result their rate of decay is more difficult to ascertain. Although it appears by visual observation that the temperature differences are decreasing in the bottom of the tank, linear fits of the unculled data have a positive slope at some locations. This appears to be due to the "hash" problem discussed earlier. Clearly there is nothing in these results that would indicate any significant increase in heat load at any location within the waste.

Figure 4.27 provides the temperature differences across the lower waste layer, upper waste layer, dome gas/waste interface to ambient, and peak waste temperature to ambient differences. Fortunately these differences eliminate much of the "hash" problem and show more clearly what appears to be occurring. First the total temperature difference across the lower layer, taken as a whole, is decreasing with a half life of about 75.6 years. Second the total temperature difference across the upper layer taken as a whole is decreasing with a half life of about 20.8 years. The temperature difference between the dome gas/waste interface and the ambient is decreasing with a 52.9 year half life. The peak waste temperature location to ambient temperature difference is decreasing with a half life of 28.6 years. Although it is coincidentally close to 30 years, it is a composite result of the 20.8 year half life in the upper waste layer, and the equivalent 52.9 year half life across the soil. The soil has no half life per se, however,

the temperature difference will drop off as the heat transferred across the soil drops off. The amount of heat conducted across the upper soil layer depends on the total heat load of the upper waste layer, minus that which is carried out by inleakage air due to sensible air temperature change and evaporation at the waste surface.

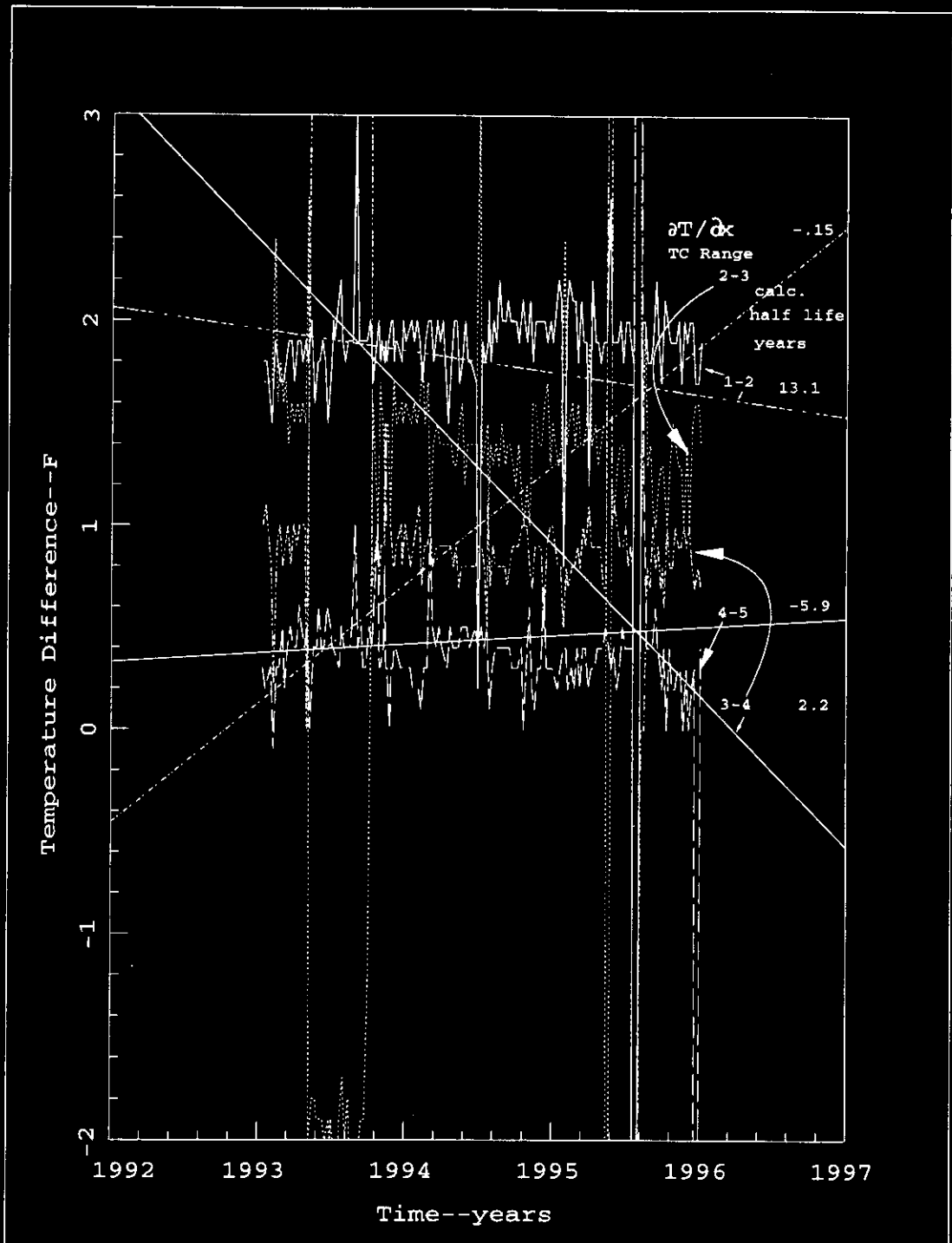


Figure 4.22 Temperature Differences vrs Time, Linear Fits, and Half Lives

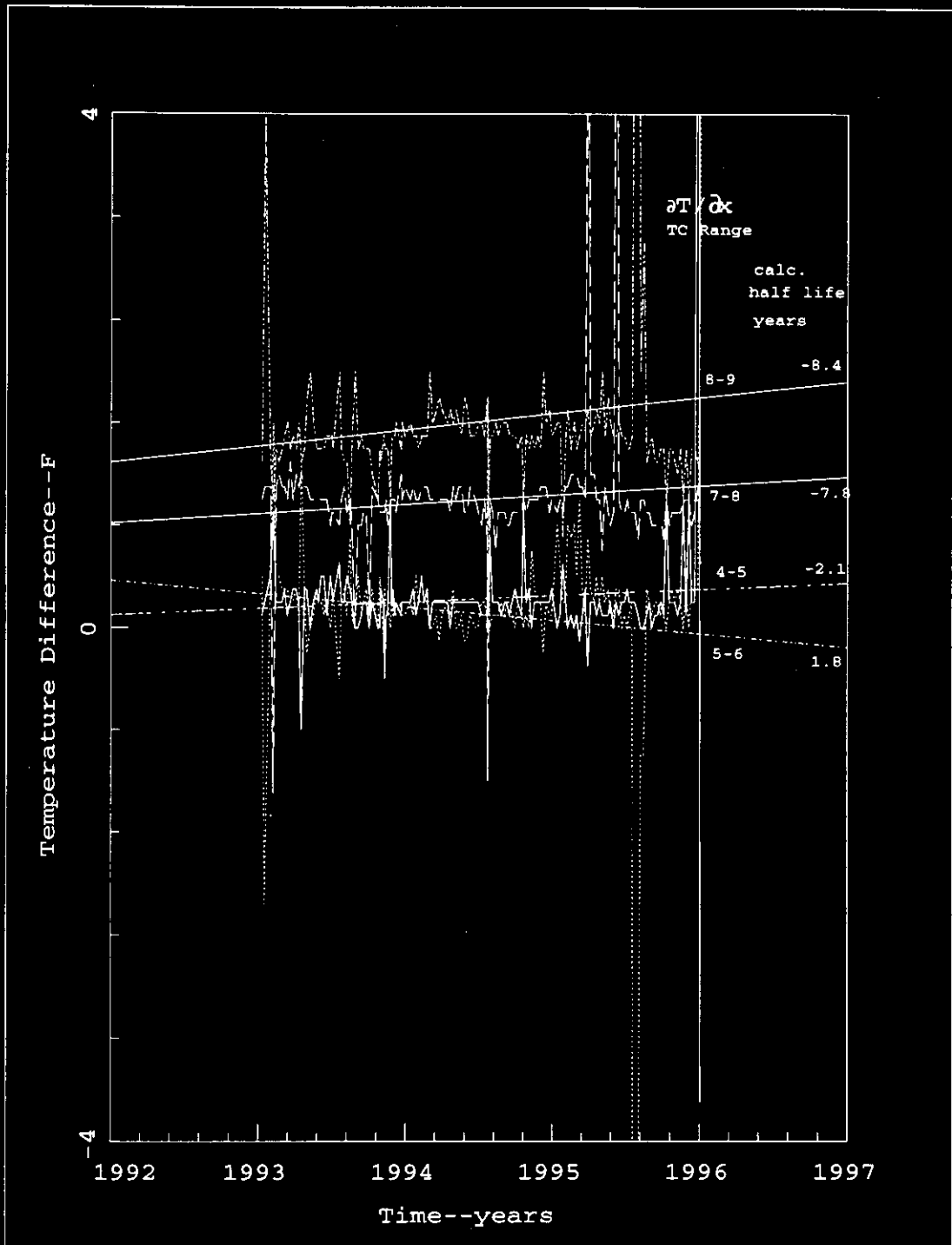


Figure 4.23 Temperature Difference vrs Time, Linear Fits, and Half Lives

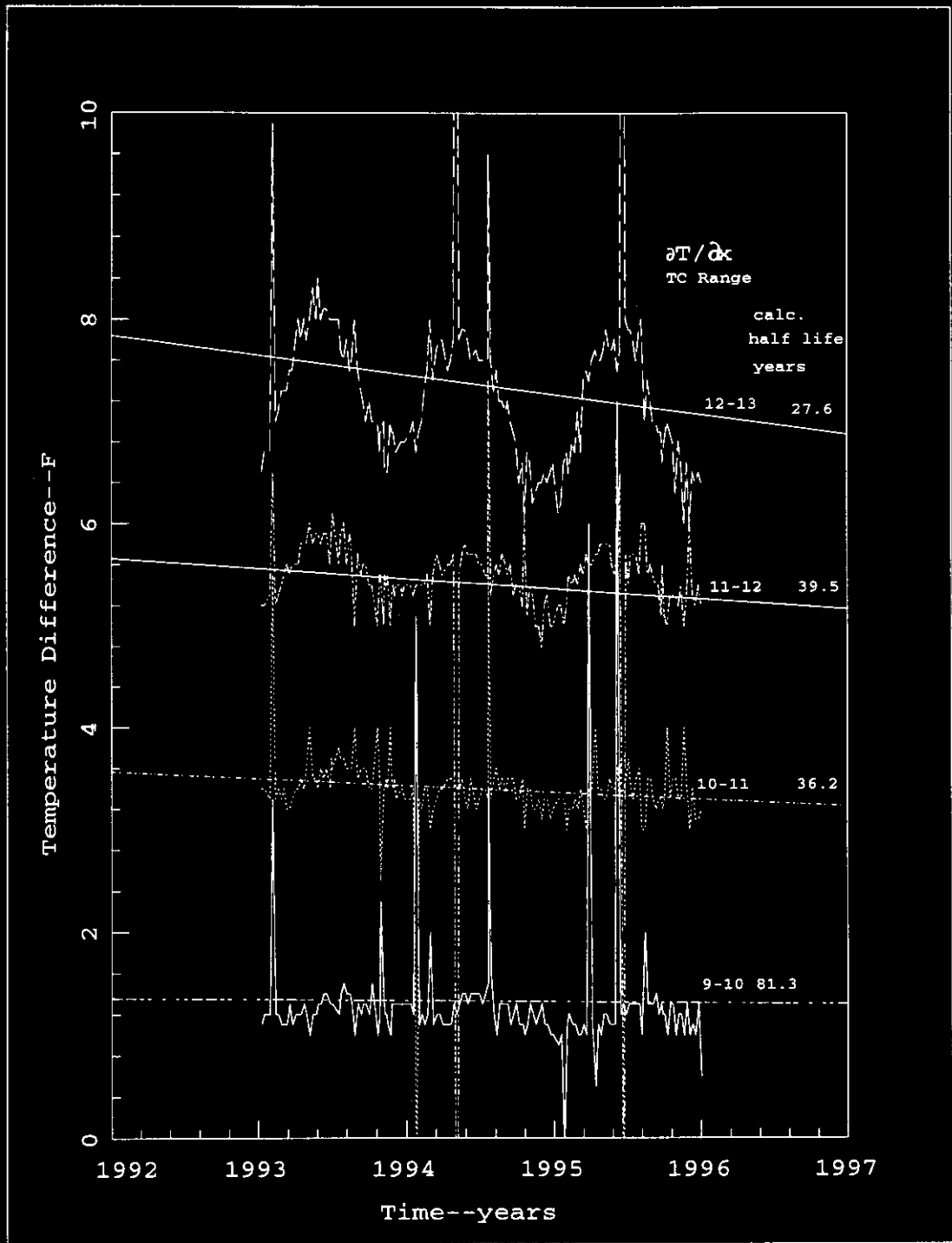


Figure 4.24 Temperature Difference vrs Time, Linear Fits, and Half Lives

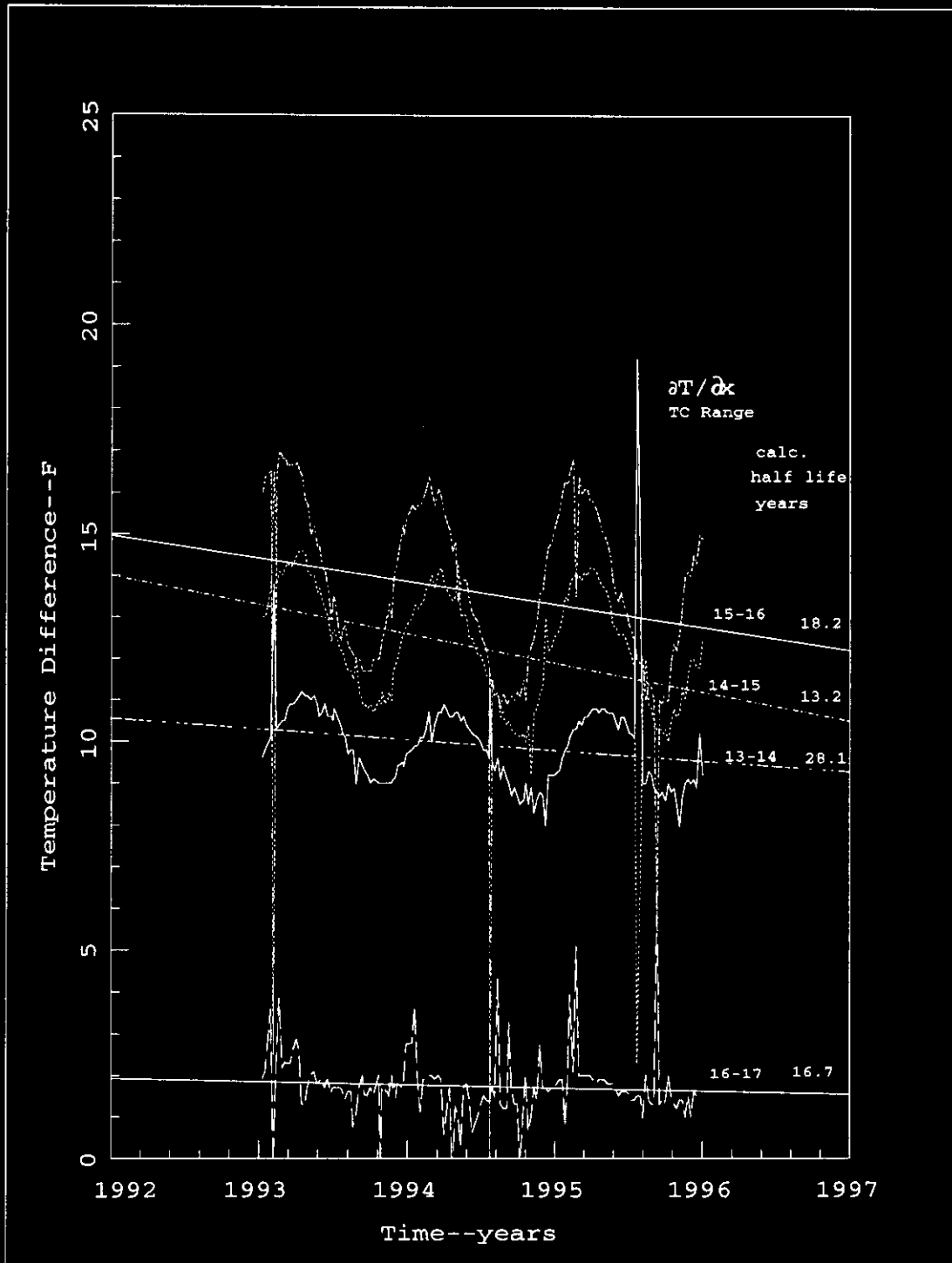


Figure 4.25 Temperature Difference vrs Time, Linear Fits, and Half Lives

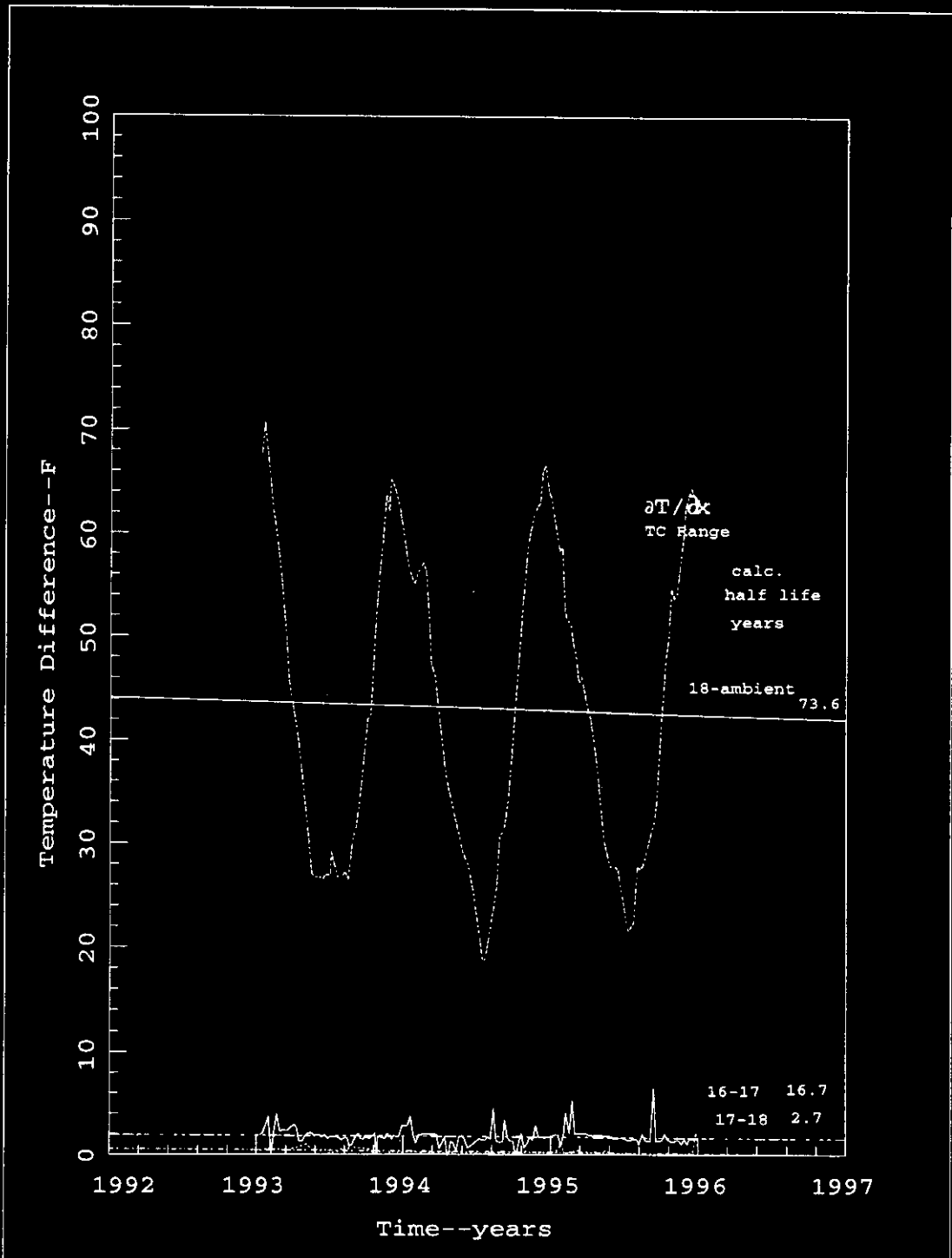


Figure 4.26 Temperature Difference vrs Time, Linear Fits, and Half Lives

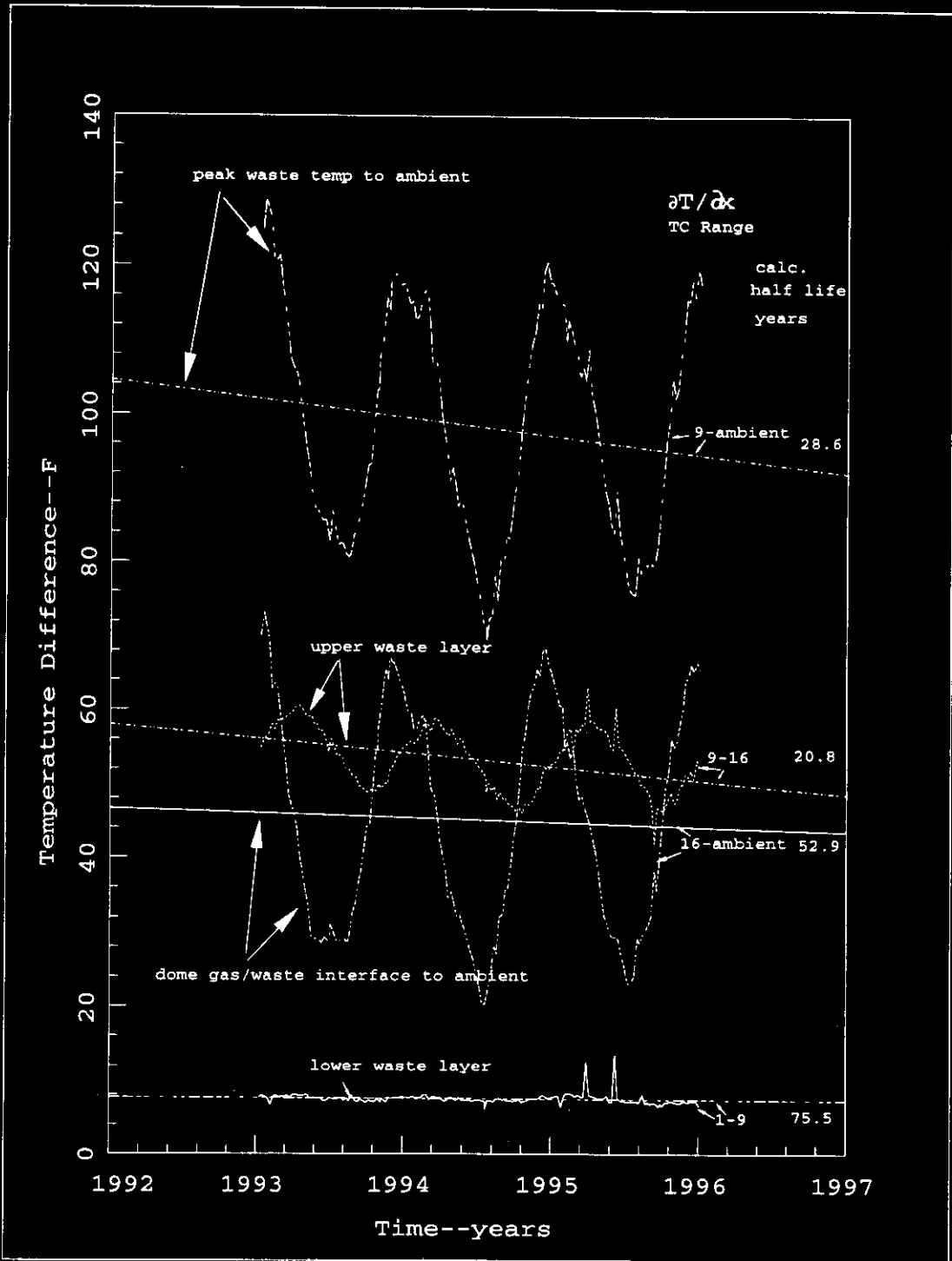


Figure 4.27 Temperature Difference vrs Time, Linear Fits, and Half Lives

4.3.2.3. Time Rate of Change in Heat Generation Rate  
Based on First Order Spatial Temperature  
Differences

Volumetric heat generation rate versus time and axial location, linear fits of these rates, and half lives were calculated based on differences in temperature between thermocouple locations. The results are graphed in Figures 4.23-4.26. Based on this method heat generation in the upper regions of the tank is decreasing with roughly the half life expected. In the lower regions of the tank the power generation level is significantly reduced and its rate of decay is more difficult to ascertain with this method. Although it appears by visual observation that the power is decreasing in the bottom of the tank linear fits of the data have a positive slope at some locations. This appears to be due to the "hash" problem discussed earlier. Clearly there is nothing in these calculated results that would indicate any significant increase in heat load at any location within the waste.

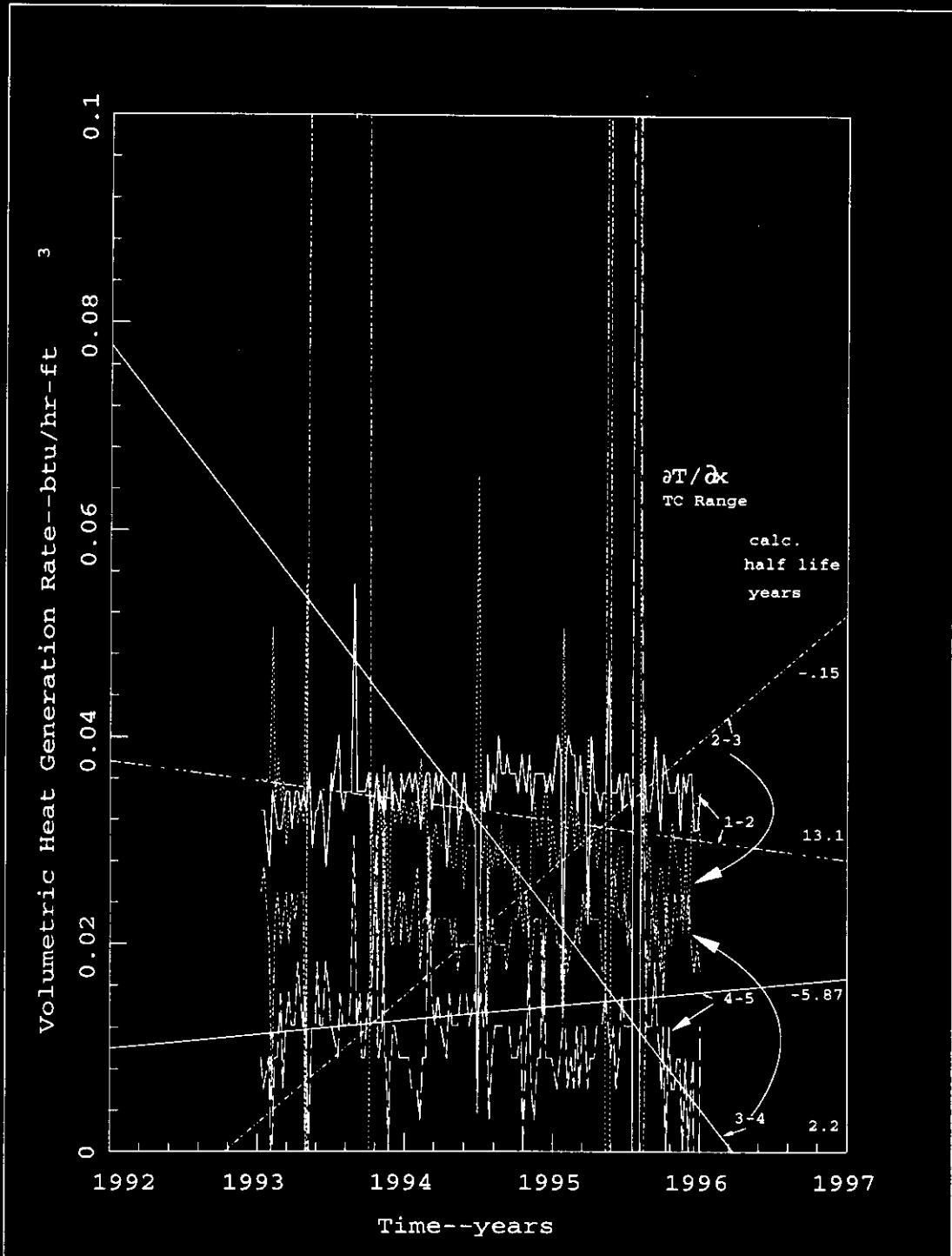


Figure 4.28 Volumetric Heat Generation Rates vrs Time, Linear Fits, and Half Lives

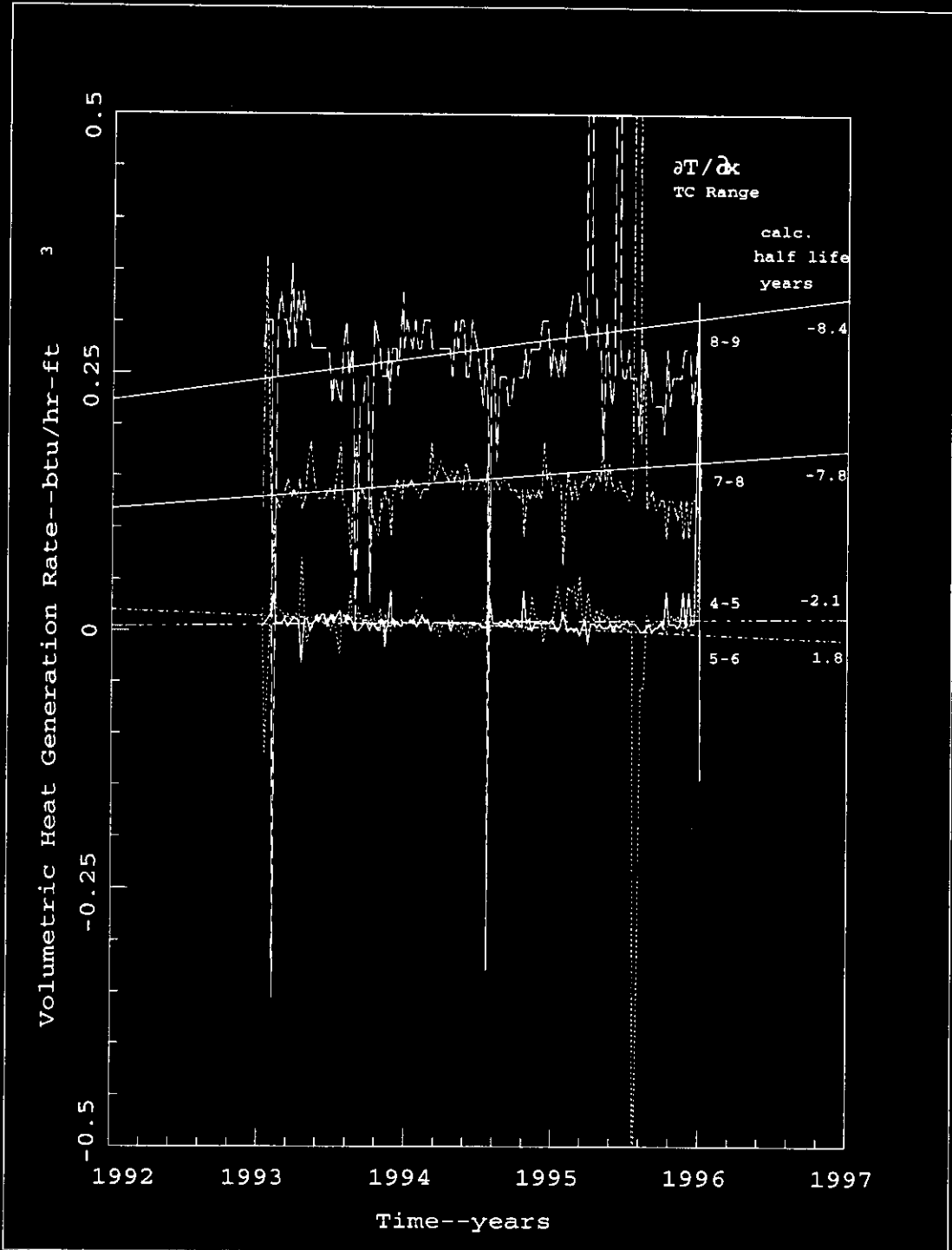


Figure 4.29 Volumetric Heat Generation Rates vrs Time, Linear Fits, and Half Lifes

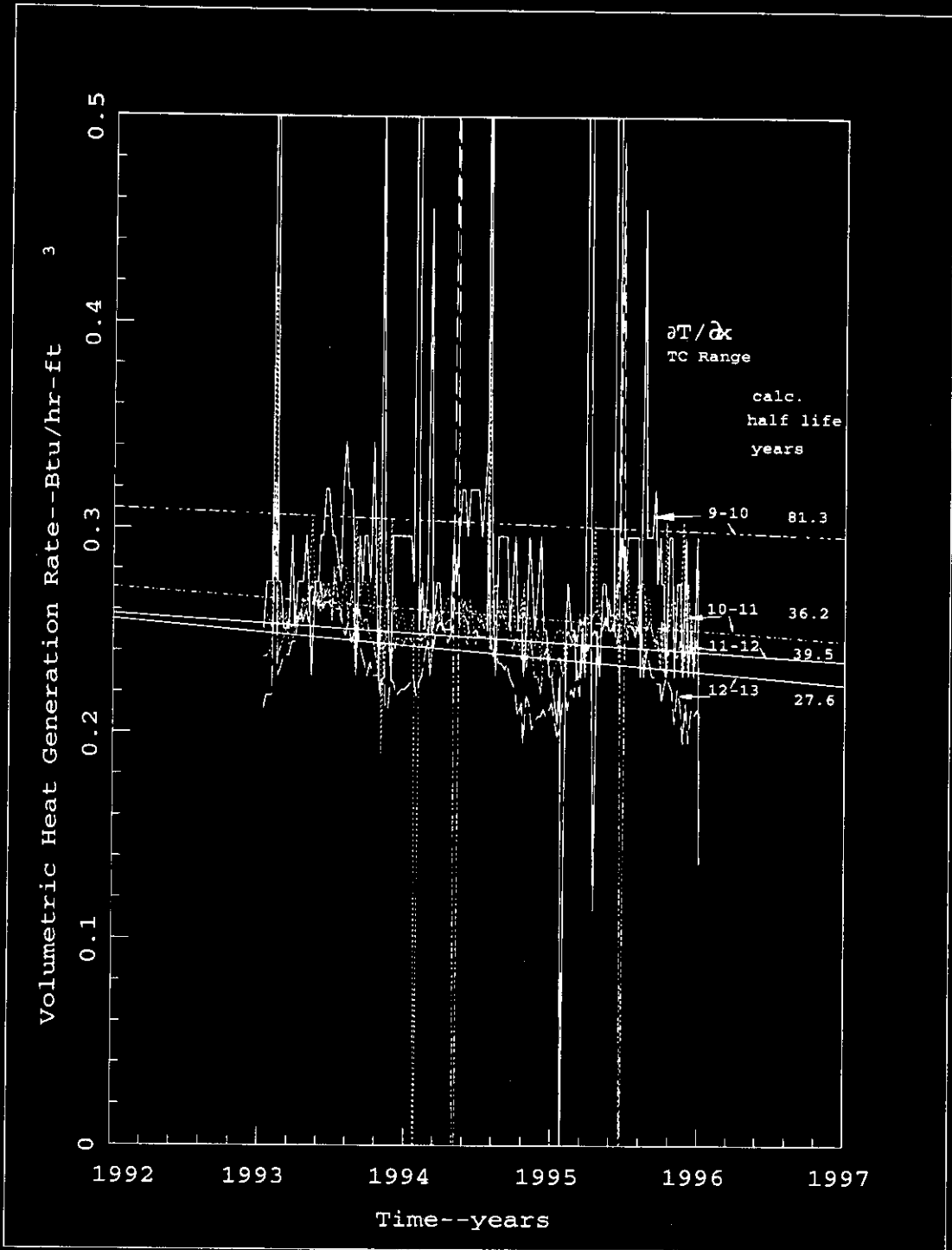


Figure 4.30 Volumetric Heat Generation Rates vrs Time, Linear Fits, and Half Lives

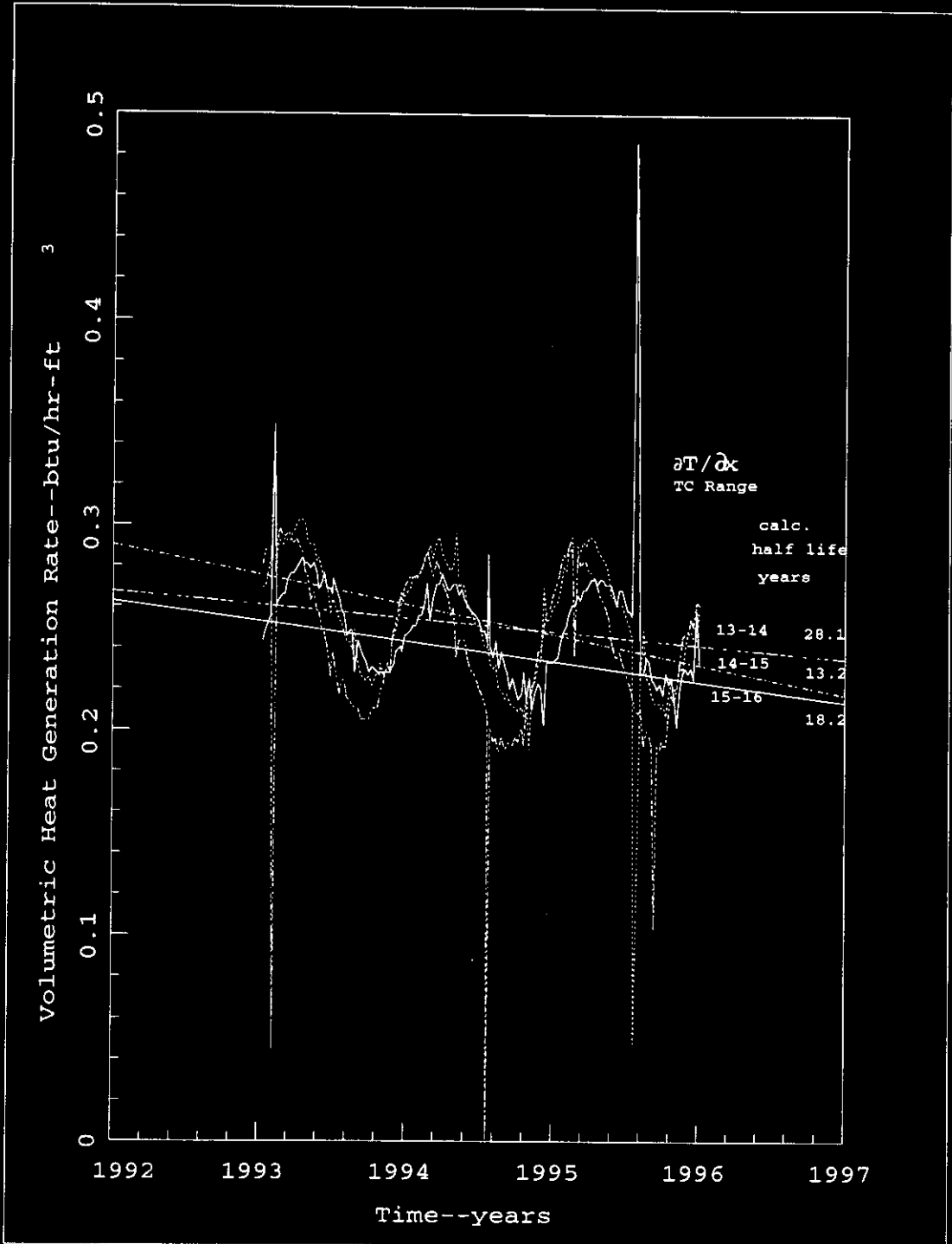


Figure 4.31 Volumetric Heat Generation Rate vrs Time, Linear Fits, and Half Lives

## 5. MODELING AND ANALYSIS METHODOLOGY AND GOTH MODEL DESCRIPTIONS

Steady state and transient thermal hydraulic simulation of the dome gas, waste, and soil temperature for Tank A-101 depends on making reasonable assumptions for the soil and sludge layers' thermal physical properties, the tank heat load and distribution, and the natural and forced ventilation air flow rates, and periods of operation of forced ventilation. Although data for none of these parameters is available, their quantitative values have to lie within certain reasonable ranges based either on data for similar materials, overall energy balances and transport rates through the sludge and soil, and the temperature data available from the one active thermocouple tree located in Tank A-101.

Estimates for soil and sludge conductivity, and the power and power distribution, were developed in this analysis and this development is described below. The process was an iterative one based first on the use of HUB<sup>2</sup> classical conduction heat transfer analysis, and evaporation and dryout analysis. This was followed by GOTH steady state and transient analysis. Comparison of results from both of these methods were made to temperature data.

The GOTH model is first described. This is followed by a description of the method used to estimate thermophysical parameters. The methodology utilized in the HUB classical heat transfer analysis is described in the same sections in which the results are presented.

### 5.1. GOTH MODEL DESCRIPTION

A 1-D GOTH thermal hydraulic model based on the nodalization diagram in Figure 5.1 was used for this analysis. There are multi-dimensional thermal effects present in Tank A-101, however, at the vicinity of the

---

<sup>2</sup>HUB is a trademark of Numerical Applications, Inc., Richland, WA.

thermocouple tree they are not large. Comparison of the 1-D model transient simulation results to the temperature history data indicates that for purposes of understanding the thermal hydraulic behavior of this tank a 1-D model appears adequate. The 1-D model consists of the waste, the dome space and gas, soil above and below the tank, and inleakage and/or forced ventilation air flow. The waste is modeled as two separate layers with different conductivity and volumetric heat generation rates in each layer. The selection of the thickness of the layers and estimation of their physical properties is discussed below. The soil layers above and below the tank are assumed to extend in diameter to the mid distance between tanks within the A tank farm.

With exception of thermocouple 1, the model's computation node centers within the waste are located midway between thermocouple locations. Comparisons of calculated temperatures to thermocouple data were made by averaging the temperatures between computation node centers for comparison with the appropriate thermocouple.

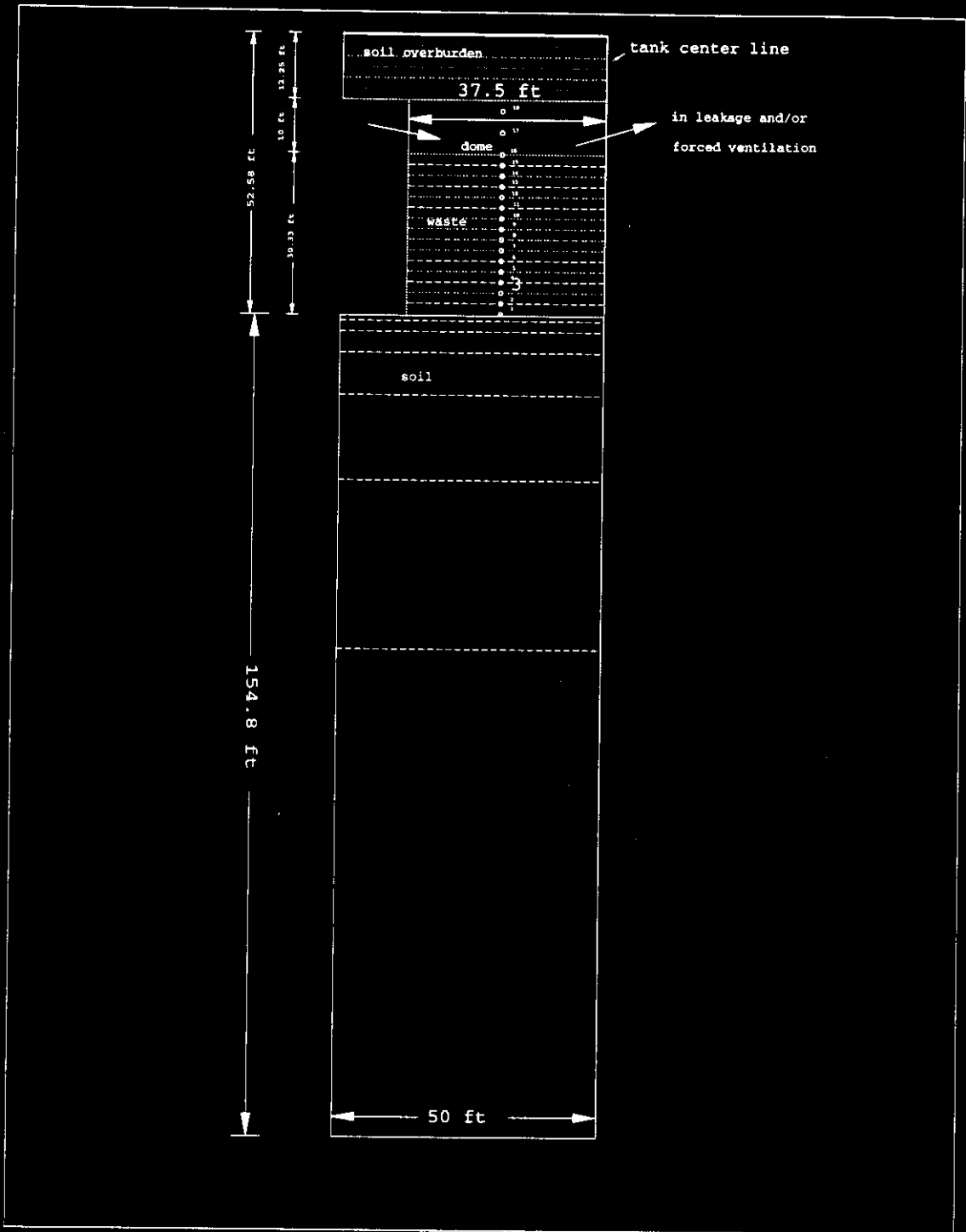


Figure 5.1 Tank A-101 1-D GOTH Nodalization Diagram

The GOTH model utilized two types of temperature boundary conditions for the soil surface and inlet ventilation flow. First a constant temperature of 53.3 F corresponding to the average temperature from 1945-1994 was used to eliminate the effects of time varying meteorological conditions and provide time average results. Second annual cyclic meteorological conditions were utilized. In this case the simulation was pre-conditioned with about 3 years of constant meteorological conditions, followed by 5 years of repeatable annual cycles based on the monthly averages for 1945-1994 to further condition the simulation. Beginning in 1990 the actual monthly average temperatures up to and including 12/1995 [Hoitink, 1994], [Burk, 1996] were utilized since this was the primary period of interest and there were significant changes from year to year--which are evident in both the data and the simulations. Finally 2 additional years based on the 1945-1994 monthly averages were used to extend the simulation results up to 1998. The time varying meteorological history assumed is illustrated in Figure 5.2. Future simulations should use the actual monthly temperatures beginning in 1980 to better represent the actual tank operation. Monthly average temperatures provide adequate resolution of ambient changes.

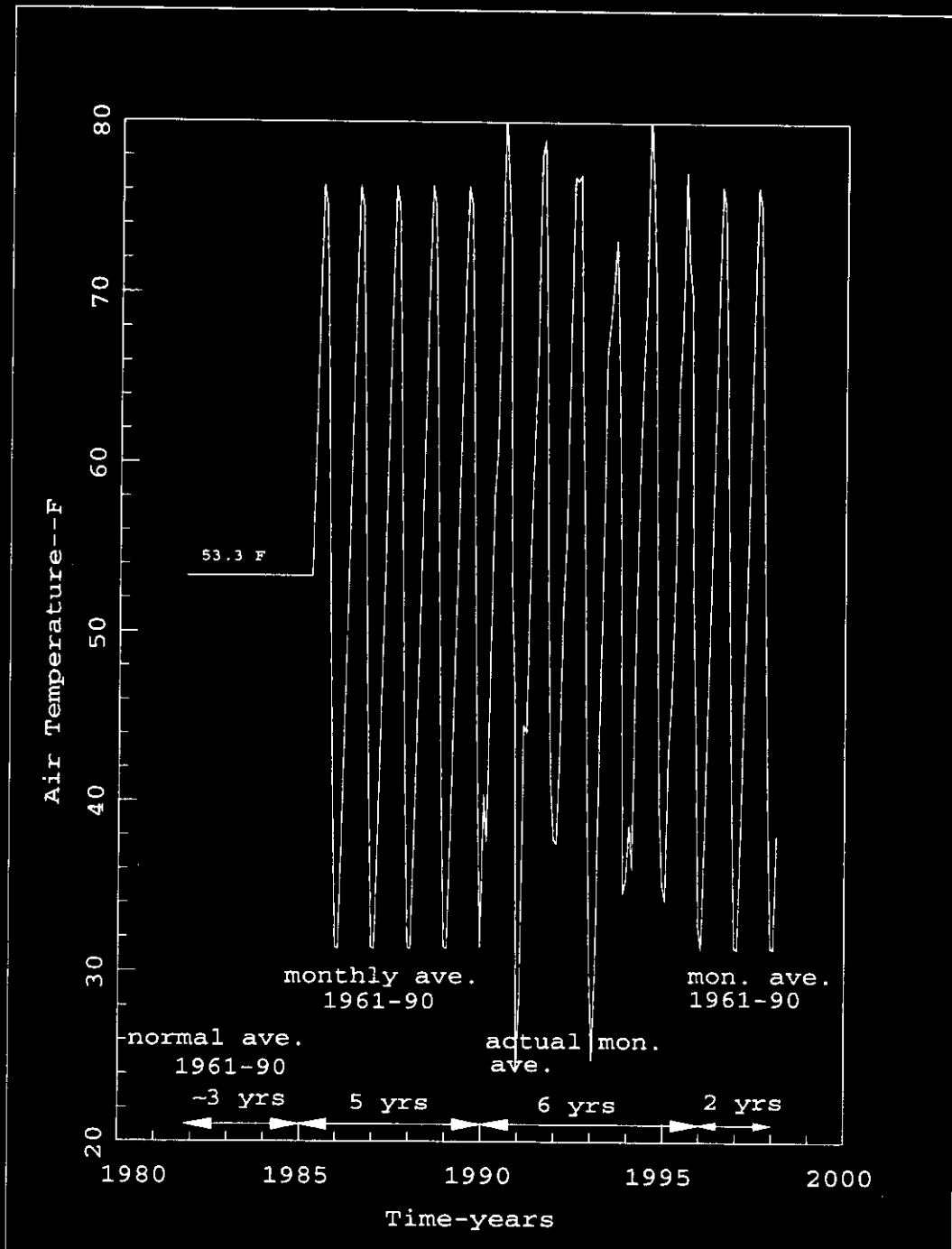


Figure 5.2 Variable Meteorology Dry Bulb Temperature History Assumed

## 5.2. ESTIMATES OF THERMOPHYSICAL PROPERTIES AND OPERATING CONDITION PARAMETERS

Estimates for the thermophysical properties and operating parameters were made by the following step by step process. The process involves generation of a consistent set of soil and waste conductivities, and power generation levels for each waste layer, which are compatible with the time averaged temperature distribution of Figure 4.6. Explanation of this process is aided with Figures 5.3-5.8.

First a distinction is made in the following between parameter sets based on the assumption of whether inleakage via natural convection is assumed present or not. Air flow through the dome due to inleakage will remove heat in direct proportion to the flow. At air flow rates considered in this evaluation the air will heat from inlet temperature to almost the temperature at the surface of the waste. The same quasi-steady temperature distribution can be maintained within the waste and dome gas for different inleakage air flow rates by increasing the heat generation rate in the upper waste layer, and simultaneously increasing the upper waste layer conductivity by the same proportion. The ratio of volumetric heat generation rate to conductivity in the upper layer remains the same as for the zero leakage case. The increase in heat generation must match the amount of heat removed by sensible air temperature change due to inleakage to maintain the same temperature distribution. (The same effect could also be achieved changing the amount of evaporation assumed to occur as a result of inleakage, or the amount of chemical heating assumed to be occurring at the waste surface. Only heat removal due to sensible air temperature change was modeled with GOTH in this analysis).

Figures 5.3 and 5.4 provide compatible sets of thermophysical properties and conditions for the case of no air inleakage, and for the case of an assumed air

inleakage rate of 1 ft<sup>3</sup>/sec, respectively. A decreasing rate of in leakage is one possible cause of the thermal behavior observed in Tank A-101. Other leakage values are possible. However, 1 ft<sup>3</sup>/sec was selected since it is about the minimum that must have been present in 1990, which if it decreased at the rate required to match the decrease in heat generation in the tank due to radiolytic decay would reach zero flow by 1997. Higher flow rates beginning in 1990 are possible, but lower values, say .5 ft<sup>3</sup>/sec starting in 1990 and decreasing at the required rate would have reached zero flow in 1993, and then the tank waste and dome temperatures would have started to decrease at a rate faster than has been observed.

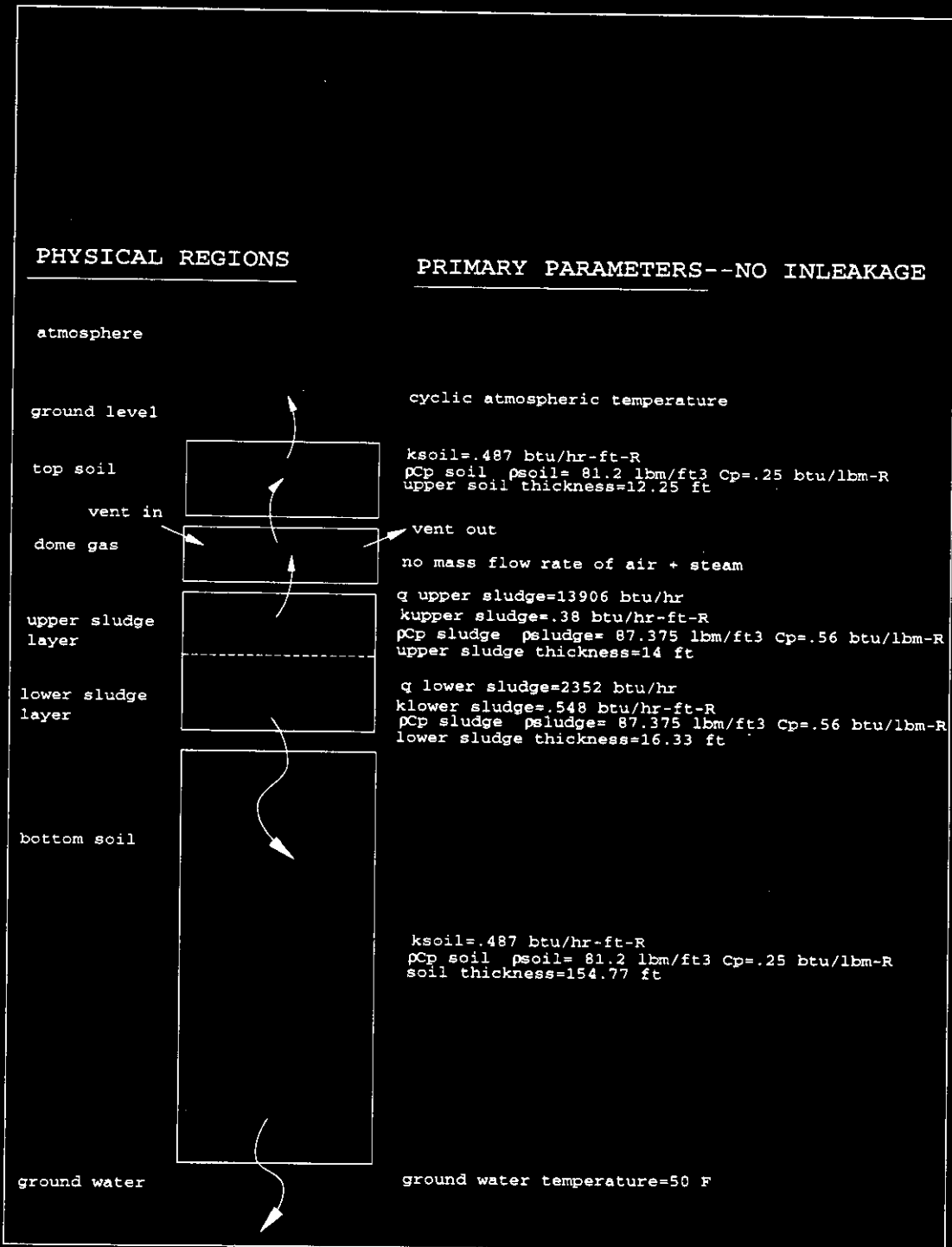


Figure 5.3 Energy Transport Processes and Parameters Under No Air Inleakage Conditions

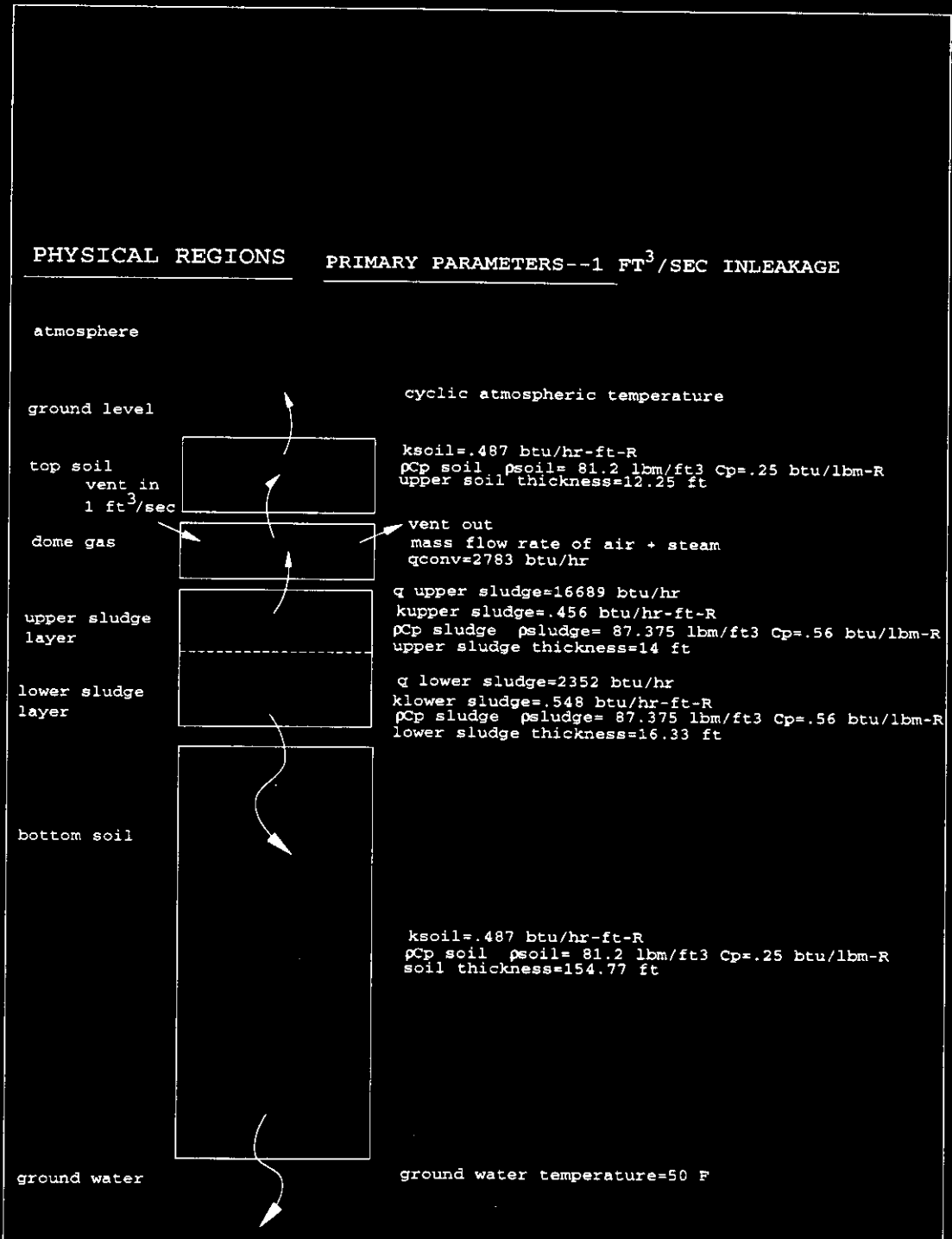


Figure 5.4 Energy Transport Processes and Parameters Under Air Inleakage Conditions

Combinations of thermophysical properties, such as those described in Figures 5.3 and 5.4 above, must meet certain time averaged and dynamic compatibility requirements. The time averaged compatibility requirements are illustrated in Figure 5.5 and the dynamic compatibility requirements are provided in Figure 5.6.

On a time averaged basis the radiolytic heat generated in the waste must be accounted for by conduction through the soil plus convection via ventilation air (or evaporation to ventilation air). If there are other heat sources such as heat of solution due to precipitation of salts or chemical reaction this must be added to the heat load at the appropriate location in the thermal system. The time averaged temperature distribution in the waste must be compatible with heat generation, its distribution, and the waste conductivity.

In addition to the time averaged compatibility requirements certain dynamic requirements must be met. The propagation of the annual meteorological cycle effects into the soil and waste is a dynamic process. The amplitude attenuation and phase shift associated with this process is dependent upon the thermal diffusivity of the soil and waste, and the magnitude of convective/evaporative cooling of the dome space, relative to conduction through the tank overburden soil. Increasing the cooling due to in leakage, decreases both the amplitude attenuation and the phase shift of the annual meteorological cycle temperature effects into the soil, dome, and waste. To match the temperature data, simulations must include the amount of cooling due to inleakage or equivalent evaporation.

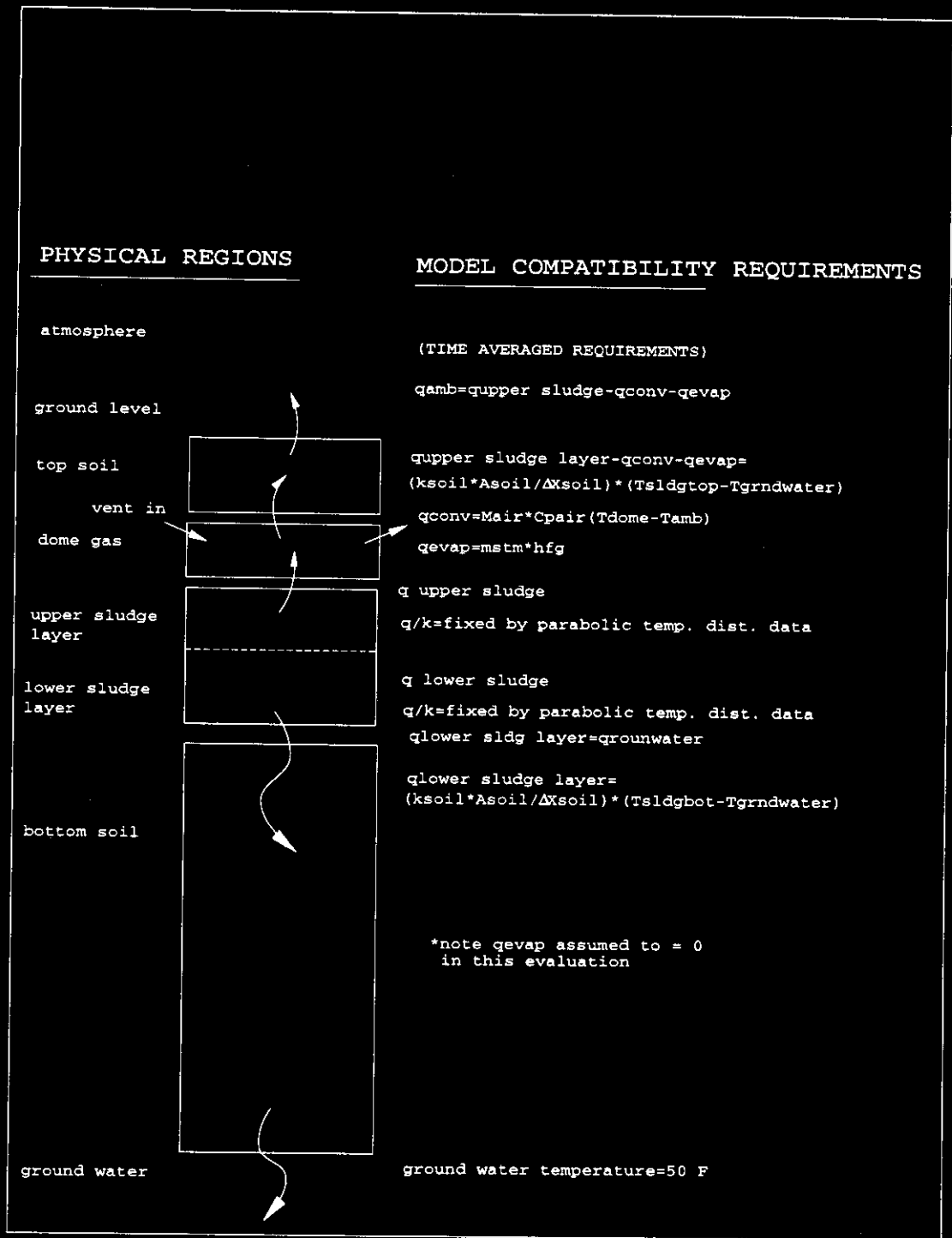


Figure 5.5 Time Averaged Parameter Compatibility Requirements

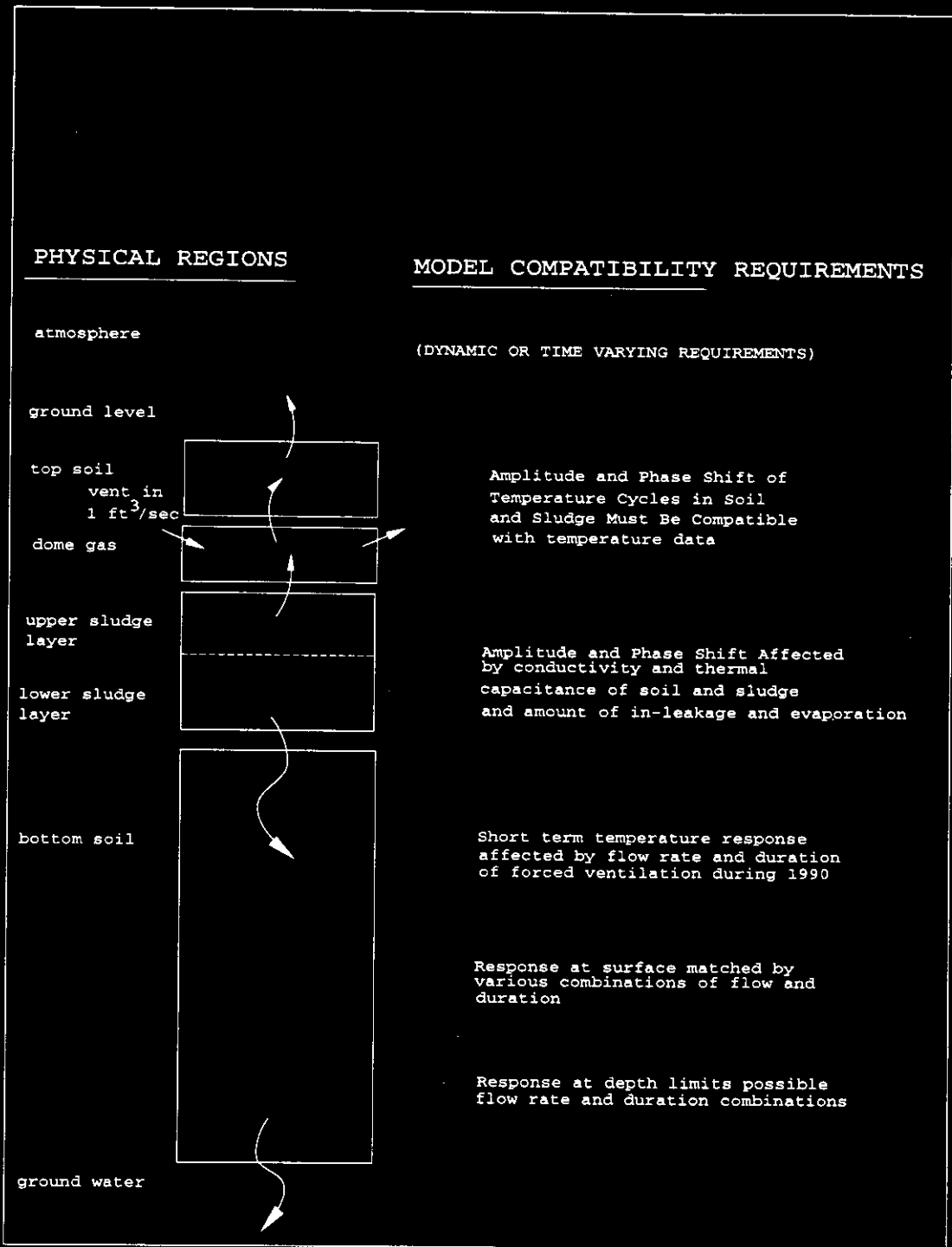


Figure 5.6 Dynamic Parameter Compatibility Requirements

Soil and waste density and specific heat values were estimated based on values used for other thermal analyses. The conductivity of the two different waste layers and soil, and the volumetric heat generation rate within each layer was developed by the following process.

First the waste was partitioned into two layers as shown in Figure 5.7. Second the ratios of volumetric heat generation to conductivity were calculated for each layer assuming the temperature distribution approximated the classical 1-D conduction solution.

For any three data points the following can be derived:

$$T(x) = - \left( \frac{\left( \frac{Q_m}{k_m} \right) (x - x_b)^2}{2} \right) + \left( \frac{T_t - T_b + \frac{\left( \frac{Q_m}{k_m} \right) (x_t - x_b)^2}{2}}{x_t - x_b} \right) (x - x_b) + T_b \quad (5.1)$$

where,

x = vertical distance from tank floor, at some location between points b and t

b = bottom of general sludge layer (point 1)

t = top of general sludge layer (point 3)

x<sub>b</sub> = distance from tank bottom to bottom of general sludge layer (point 1)

x<sub>t</sub> = distance from tank bottom to top of general sludge

layer (point 3)

T<sub>b</sub>= temperature at bottom of general sludge layer, x<sub>b</sub>  
(point 1)

T<sub>t</sub>= temperature at top of general sludge layer, x<sub>t</sub>  
(point 3)

Q= uniform volumetric heat generation rate in general  
layer

k= sludge conductivity in general layer

From this, by specifying the third data point the ratio of  
q/k can be calculated:

$$\frac{Q}{k} =$$

$$\frac{(T_m - T_b) - (T_t - T_b) \left( \frac{x_m - x_b}{x_t - x_b} \right)}{\frac{-(x_m - x_b)^2}{2} + \frac{(x_t - x_b)^2 (x_m - x_b)}{2 (x_t - x_b)}} \quad (5.2)$$

where,

m = middle of general sludge layer (point 2)

x<sub>m</sub>= distance from tank bottom to any point between the  
top and bottom of general sludge layer (point 2)

T<sub>m</sub>= temperature at any point between top and bottom of  
general sludge layer, x<sub>m</sub> (point 2)

This requires any three data points within each layer.  
The two end points and intermediate point within each

layer were used for this purpose. Next, based on experience as a first approximation the conductivity of the upper and lower slurry/salt cake layers was assumed to be that of water. Estimates of the heat generation in each layer were then computed.

The horizontal plane defined by the time averaged peak waste temperature is an adiabatic plane with heat generated in the upper layer assumed to be conducted through the upper soil, or convected out by ventilation flow. Heat generated in the lower layer is assumed to be conducted to groundwater. Therefore, with estimates for the heat flow upwards and downwards, soil conductivity can be calculated since time average dome temperature, ambient, and ground water temperatures are known.

This process results in the calculated classical temperature distributions shown in Figure 5.7. This process must be further iterated upon due to the following. First different values for soil conductivity above and below the tank result from this process. Second, the initial estimates of slurry conductivity are independent of temperature, but the conductivity of the slurry is treated in GOTH as a multiple of water conductivity, and the conductivity of water in GOTH is temperature dependent. The conductivity of slurry is likely highly coupled to the conductivity of water and likely temperature dependent so this conductivity treatment is reasonable. However, this effects the resultant calculated temperature distribution in GOTH and therefore in order to calculate a more correct distribution, adjustments were made in the top waste layer conductivity to produce the correct temperature distribution in the GOTH model. The lower soil conductivity was next set to that calculated for the top layer, and proportional adjustments were then made in the lower slurry layer conductivity. The resultant calculated temperature distribution in GOTH is provided in Figure 5.8.

Note that the above process of calculating the  $Q/k$  ratio using the temperatures at the bottom and top of each layer, combined with the classical conduction relationship, does not necessarily result in an adiabatic condition at the interface between the two layers. In addition the spatial temperature gradients or slopes,  $jT/\partial x$ 's, are not equal from the right and left hand sides of the temperature distribution at the peak temperature point. It does however result in a reasonable estimate of  $Q/k$  for the top and bottom waste layers, and when adjustments in  $k$  for the top and bottom layers are made for the reasons explained above, the process results in a calculated steady state temperature distribution in GOTH which closely approximates the actual time averaged distribution in the tank as shown in Figure 5.8.

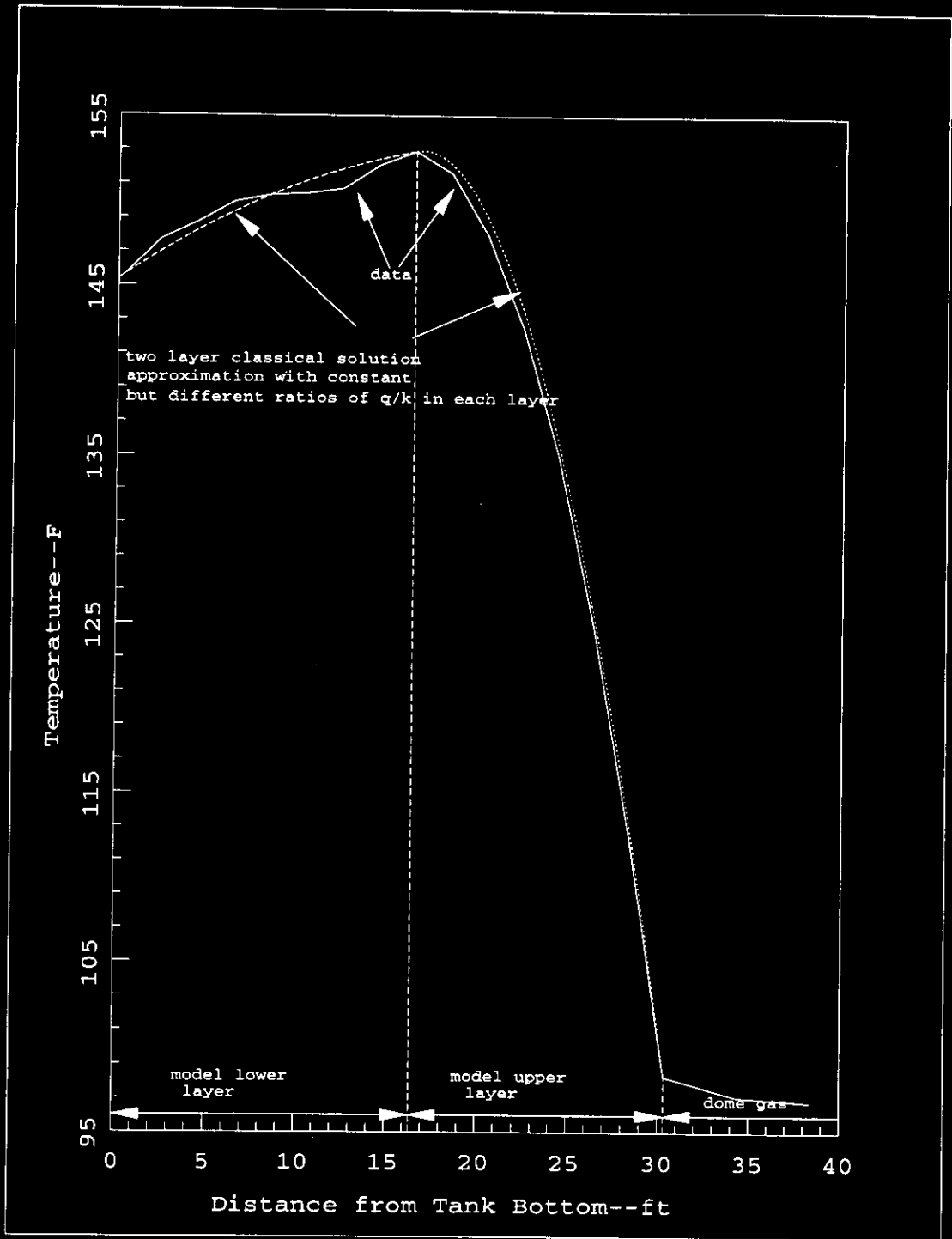


Figure 5.7 Two Layer Classical Conduction Solution Approximation for the Temperature Distribution

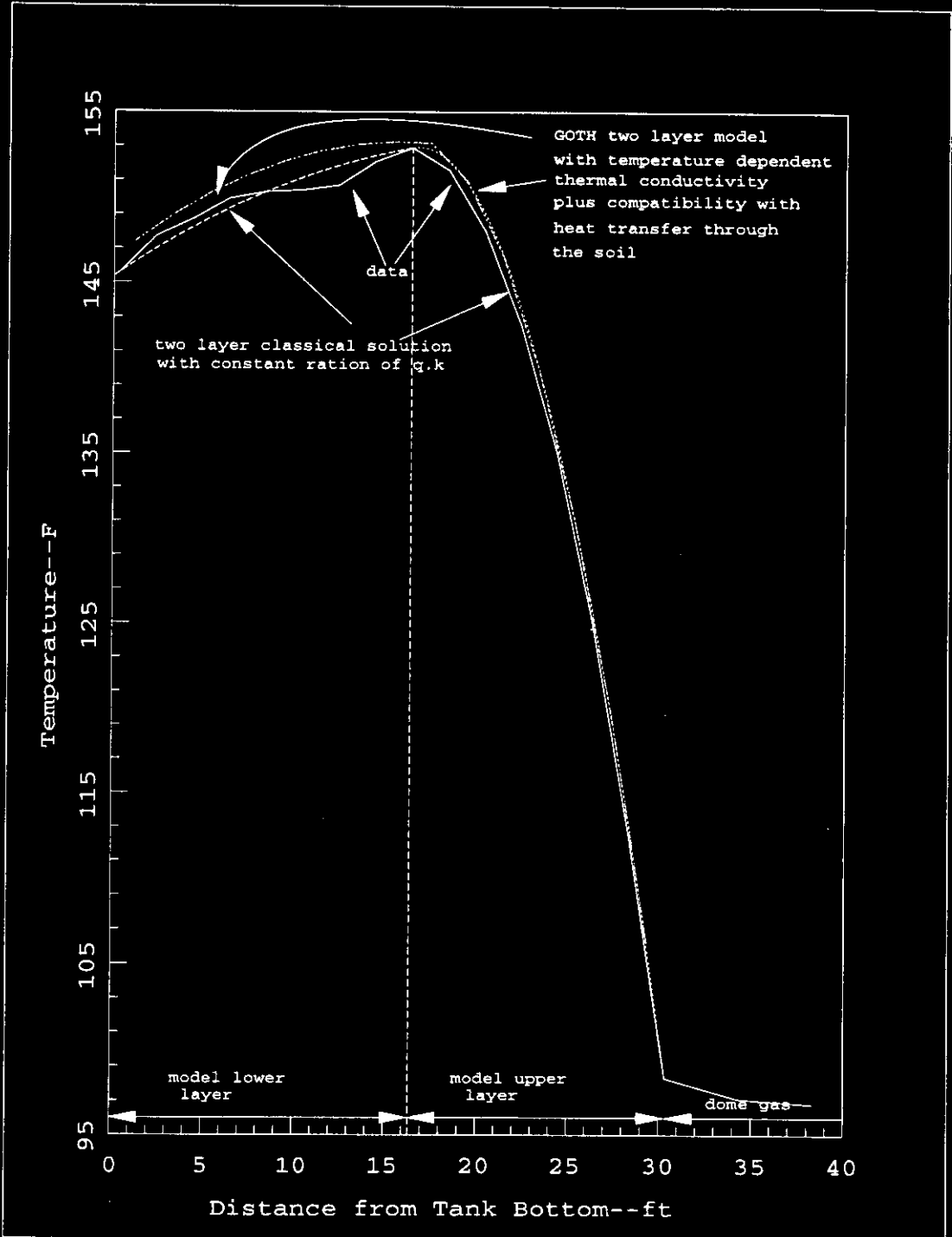


Figure 5.8 Comparison of GOTH Steady State Temperature Distribution to Data and Classical Approximation

For the thermal hydraulic modeling conducted in this analysis the radiolytic heat load within the waste is assumed to decay with a 30 year half life. The tank heat load as a function of time assumed in this analysis is provided in Figure 4.8. The January 1, 1996 heat load is estimated to be 16600 btu/hr for the case with air inleakage. If the time varying radiolytic heat load were based on the half lives for either Strontium 90 or Cesium 137 rather than the 30 years assumed then the result would be as shown (i.e. very little difference).

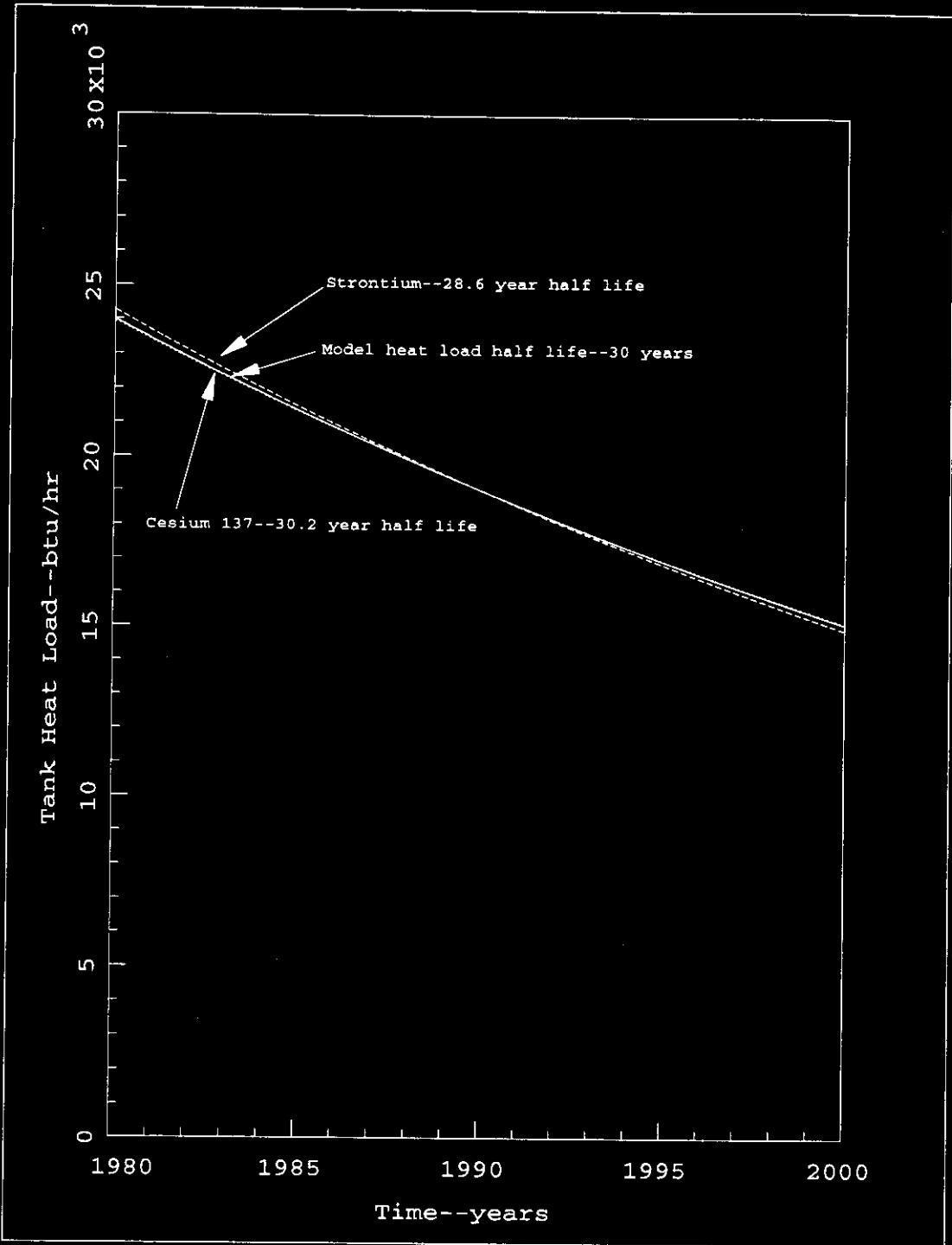


Figure 5.9 Estimated Tank A-101 Radiolytic Heat Load Versus Year for 30 Year Half Life

Dynamic thermal hydraulic simulations indicate that dome gas and waste/dome gas interface temperatures are being maintained at their current measured levels as a result of decreases in dome cooling, or increases in surface heating. The amount of decreased cooling or increased heating must be approximately equal to the change in the radiolytic heat load. This is illustrated in Figure 5.10. Currently this would correspond to turning on an additional 100 watt light bulb each year at the surface of the waste, or alternatively decreasing the cooling by decreasing inleakage, evaporation, or soil conductivity such that its effect is reduced by ~100 watts of cooling/year. It is not a large quantity, but over time the effect is noticeable.

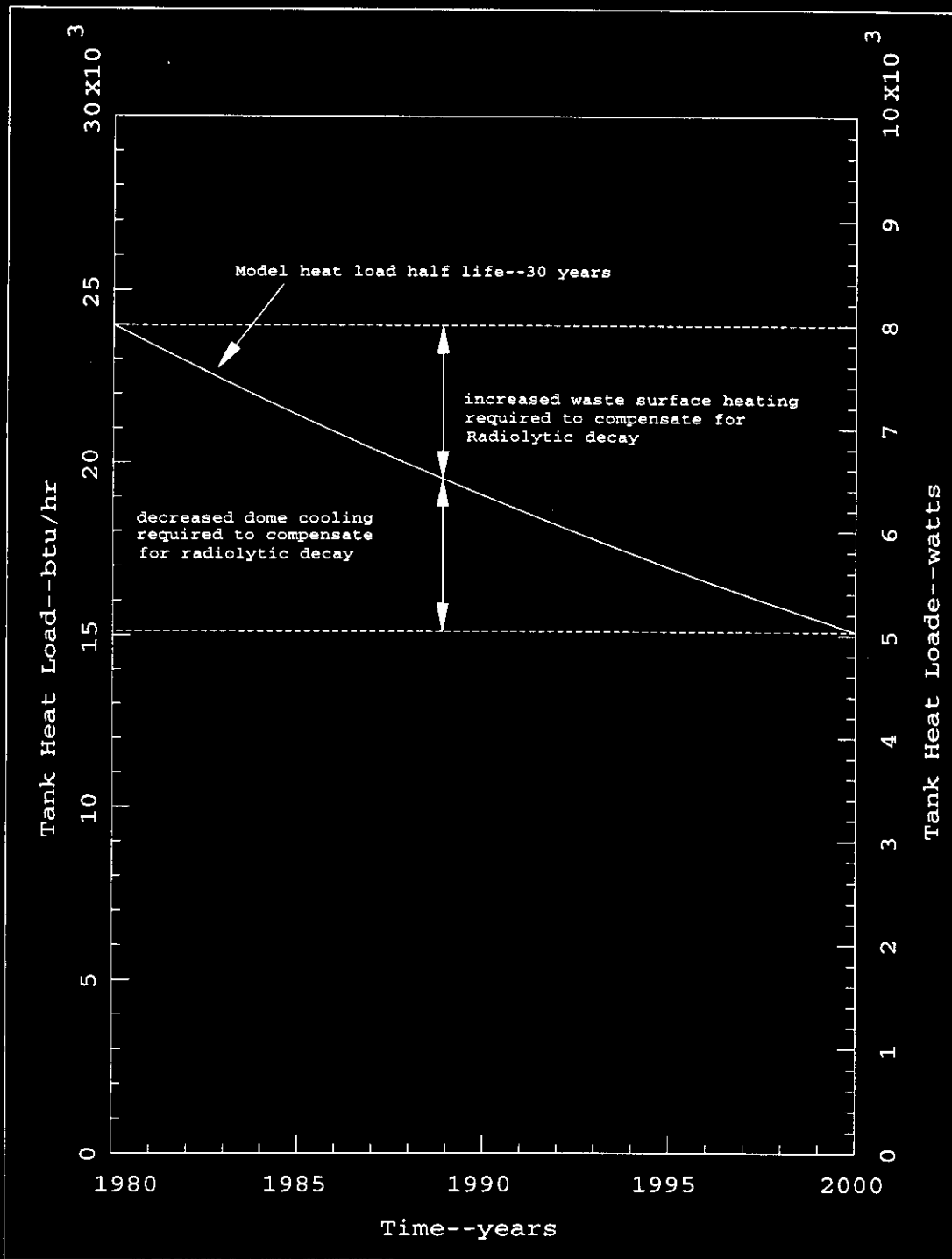


Figure 5.10 Decreased Dome Cooling or Increased Waste Surface Heating Required to Compensate for Radiolytic Heat Load Decay

## 6. HUB SCOPEING AND ANALYTICAL CALCULATION RESULTS

Two types of calculations were conducted during this thermal hydraulic evaluation. Scopeing and analytical calculations based on classical methods were conducted in parallel with GOTH thermal hydraulic numerical computer code simulations. The scopeing and analytical calculations conducted with the HUB engineering notebook software tool are discussed below.

### 6.1. SIMPLE ANALYTICAL MODEL ESTIMATE OF THERMAL CHARACTERISTICS

The temperature response of the upper layer of waste subsequent to being placed in Tank A-101 can be estimated by combining the following analytical relationships [Carslaw, 1959].

The first term provides the transient temperature within the upper waste layer, initially at a uniform temperature of 125 F, but subjected to a step change in temperature at the surface, 98.3, and with an adiabatic surface at the bottom. Turning the ventilation on intermittently between 1980 and the present, plus conduction through the soil has resulted in roughly a constant temperature at the dome space/waste interface. The axial gradients in the sludge suggest the interface between the lower layer and the upper layer is approximately adiabatic.

$$\begin{aligned}
 & \text{sv1}(x, t, nt, Tf, Ti) = (Tf - Ti) \left( 1 - \left( \frac{4}{\pi} \right) \right. \\
 & \left. \sum_{n=0}^{nt} \left( \left( \frac{(-1)^n}{2n+1} \right) e^{\frac{-\kappa (2n+1)^2 \pi^2 t}{4l^2}} \cos \left( (2n+1) \frac{\pi x}{2l} \right) \right) \right) \quad (6.1)
 \end{aligned}$$

The second expression provides the temperature response of the upper layer initially at a uniform temperature, 125 F, with an exponentially decaying radiolytic heat load, a constant temperature upper surface equal to the initial temperature, 125 F, and an adiabatic surface at the bottom of the upper layer.

$$e^{v\lambda_1(x, t, \tau, nt, T_i)} =$$

$$\left( \frac{\kappa Ad}{\lambda_1(\tau) K} \right) \left( \frac{\cos \left( x \left( \frac{\lambda_1(\tau)}{\kappa} \right)^{\frac{1}{2}} \right)}{\cos \left( 1 \left( \frac{\lambda_1(\tau)}{\kappa} \right)^{\frac{1}{2}} \right)} - 1 \right) e^{-\lambda_1(\tau) t} + \left( \frac{4 \kappa Ad}{\pi \lambda_1(\tau) K} \right) \tag{6.2}$$

$$\sum_{n=0}^{nt} \frac{(-1)^n e^{-\frac{\kappa (2n+1)^2 \pi^2 t}{4 l^2}} \cos \left( (2n+1) \frac{\pi x}{2 l} \right)}{(2n+1) \left( 1 - \left( \frac{\kappa (2n+1)^2 \pi^2}{4 \lambda_1(\tau) l^2} \right) \right)} + T_i$$

Combining the terms provides the complete solution:

$$se_{u1}(x, t, nt, T_f, T_i, \tau) =$$

$$s_{u1}(x, t, nt, T_f, T_i) + e_{u1}\lambda_1(x, t, \tau, nt, T_i)$$
(6.3)

Where,

$t$  = time

$x$  = distance from the bottom of the upper waste layer

$\tau$  = half life of the radiolytic heat load decay

$\kappa$  = thermal diffusivity of upper waste layer

$K$  = thermal conductivity of upper waste layer

$$\lambda_1(\tau) = \frac{-\log_e(.5)}{\tau}$$
(6.4)

$A_d$  = volumetric heat generation rate of upper waste layer

$T_i$  = 125 F

$T_f$  = 98.3 F

The results are graphed in Figure 6.1 and an overlay of the analytic solution results together with the data is provided in Figure 6.2.

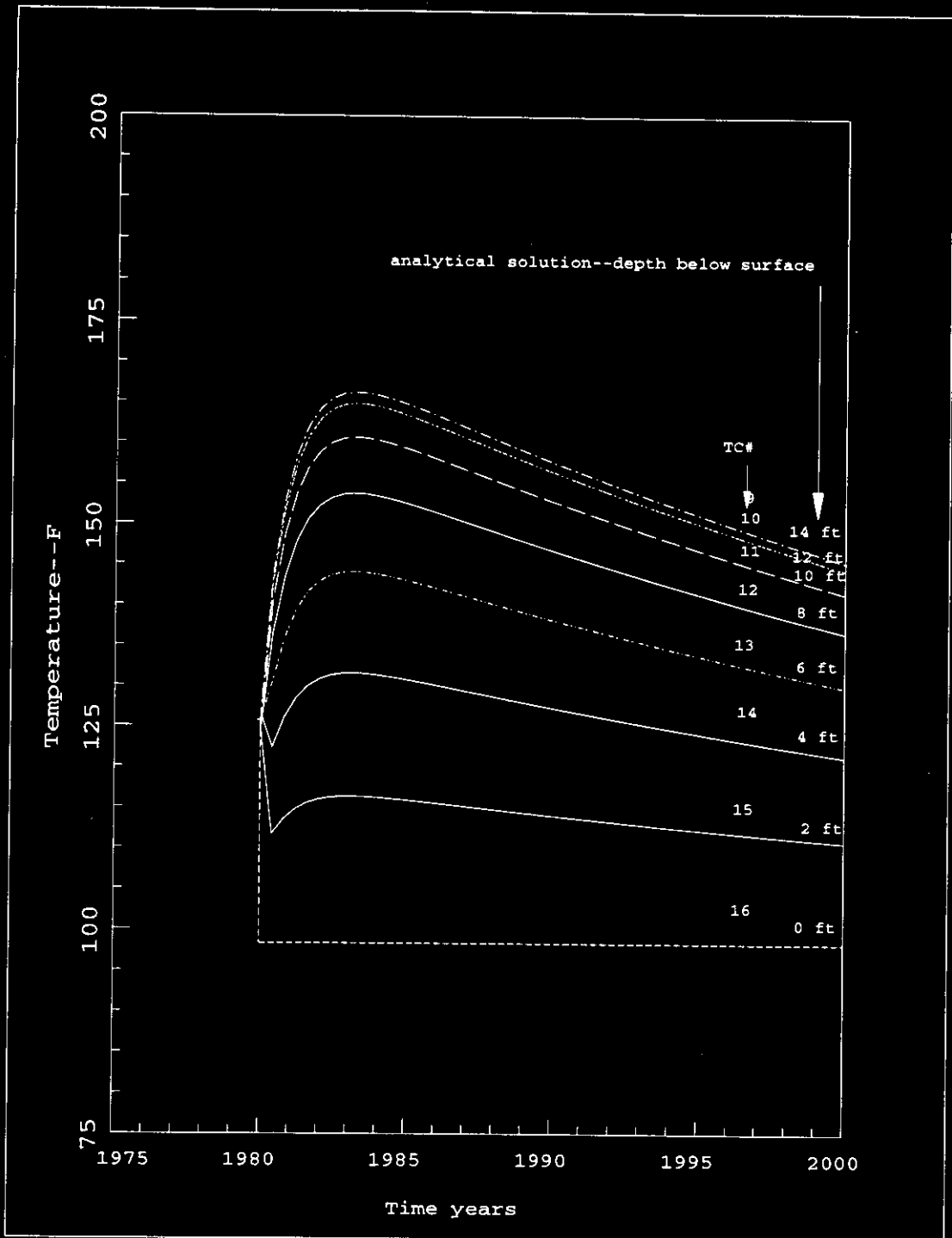


Figure 6.1 Simple Analytical Thermal Model--Estimate of Temperature Response of Upper Waste Layer

The analytic solution results compare reasonably well to the time averaged temperature data when consideration is given to the fact that the data reflects the intermittent operation of the forced ventilation system, changes in annual average temperature year to year, and soil and lower waste layer thermal inertia effects, while the analytical solution does not.

If the ventilation system had not operated at all, then the data would have been closer to the analytical solution, provided some means were present to maintain the dome space at a constant temperature. An additional increasing heat source at the surface of the waste, or continual decreased cooling from inleakage or inleakge combined with evaporation could maintain the dome temperature constant by compensating for the decay in radiolytic heat load. However, the periodic oscillations due to the annual meteorological cycle would have still been present in the data. If the thermocouple reference junction were stable then much of the "hash" in the data would be non-existent.

If the cooling mechanisms in the dome did not degrade, or if an increasing heat source at the waste surface were not present to maintain dome temperature at an approximately constant value, then actual dome and waste temperatures would be expected to decrease faster than calculated by this analytical method, provided the thermal inertia effects of the soil beside and below the tank is ignored. When these soil inertia effects are included it is unclear whether the cooldown rate would be faster, or slower than calculated with this simplistic analytical model.

Although this simple model provides some useful insight into the general expected thermal response of Tank A-101, it cannot explain fine subtleties of the detailed thermal behavior. The thermal behavior is a result of past tank history including slurry filling, heatup of the slurry and surrounding soil, intermittent operation of the ventilation system from 1980-1990, changes in meteorology

from 1980 to the present, varying evaporation rates and slurry dryout, varying inleakage flow rates, soil dryout, and possible additional heat sources due to chemical reaction, or heat release due to salt precipitation.

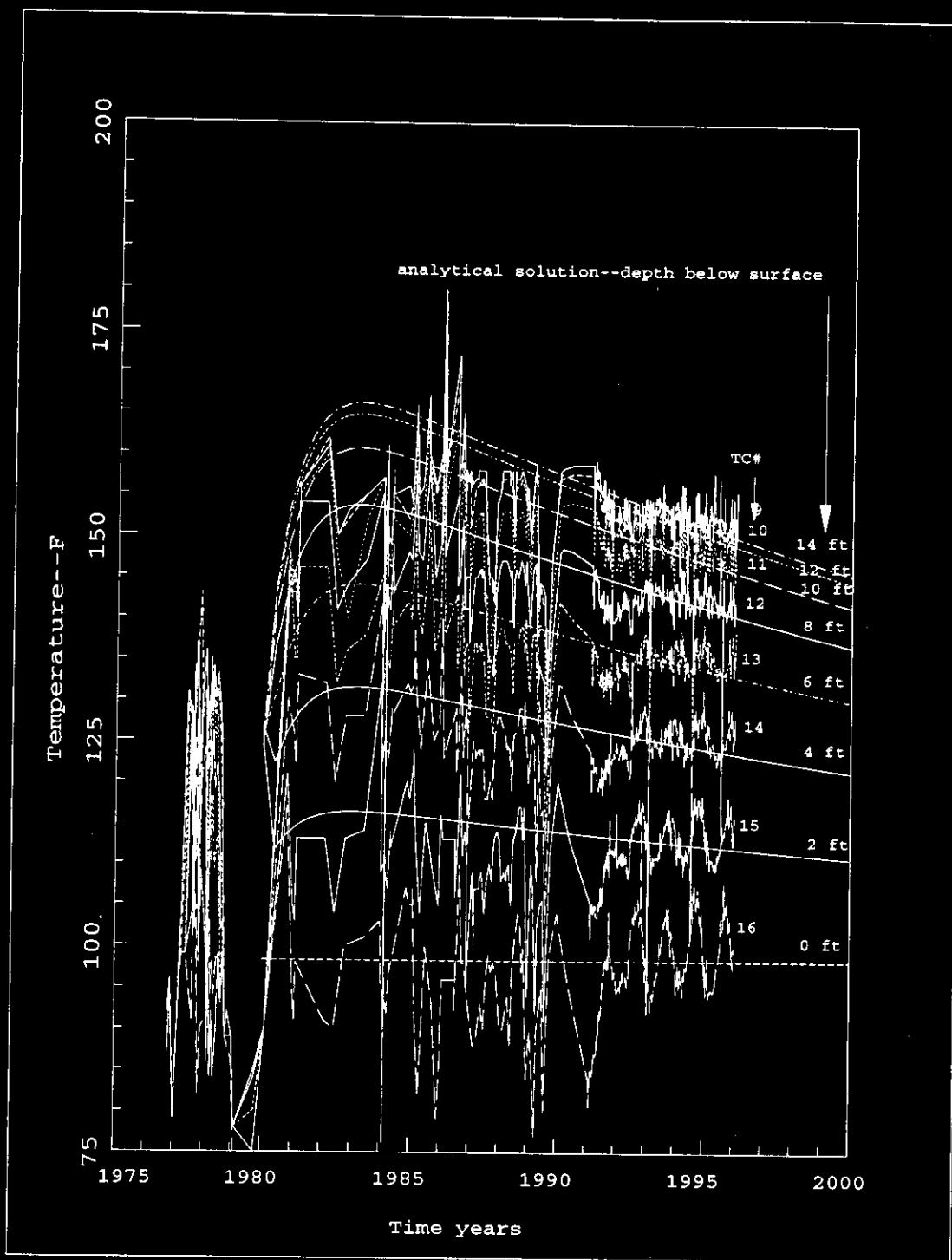


Figure 6.2 Comparison of Temperature Data and Simple Analytical Model Calculated Temperatures

## 6.2. EFFECT OF ANNUAL METEOROLOGICAL CYCLE ON WASTE AND DOME GAS TEMPERATURE

The annual meteorological cycle increases and decreases the temperature of the soil at the surface in a periodic and oscillatory way. This cyclic variation is propagated through the soil to the dome gas and waste. The amplitude of the temperature swing is decreased the further the soil and/or waste are below the soil surface due to thermal diffusivity effects. The oscillation at depth in the soil or waste is phase shifted relative to the oscillation in temperature at the surface, also due to thermal diffusivity effects. The time averaged temperature gradient through the soil and waste, due to the net time average conduction of the tank heat load, is superimposed upon the thermal wave propagation effects due to the annual meteorological cycle. The analytical solution for these combined effects in the soil between the soil surface and the dome is provided below [Carslaw, 1959], [Crowe, 1993].

Propagation of the soil surface temperature oscillation into a semi-infinite unheated soil slab:

$$v(t, z) = A_0 e^{-b z} \cos(\omega t - b z - \epsilon_0) \quad (6.5)$$

Steady state temperature gradient within a soil layer with a constant heat flux through the layer adequate to produce a temperature difference of  $T_{dind} - T_{ssind}$ .

$$u(z) = T_{ssind} + \left( \frac{z}{z_{max}} \right) (T_{dind} - T_{ssind}) \quad (6.6)$$

Combining these solutions:

$$T_{it}(t, z) = u(z) + v(t, z) \quad (6.7)$$

Where:

t = time

z = distance below soil surface

zmax = distance from soil surface to tank dome

Tdind = time averaged temperature at dome, 98.3 F

Tssind = time average temperature at soil surface, 53.3 F.

Ao = amplitude of the temperature oscillation at soil surface

$$b = \sqrt{\frac{w}{2 \alpha}} \quad (6.8)$$

alpha = soil thermal diffusivity

w = frequency of the oscillation

eo = 0.0

The resulting temperature oscillation is propagated from the top of the soil to various depths with amplitude attenuation and phase shift as shown in Figures 6.3-6.5.

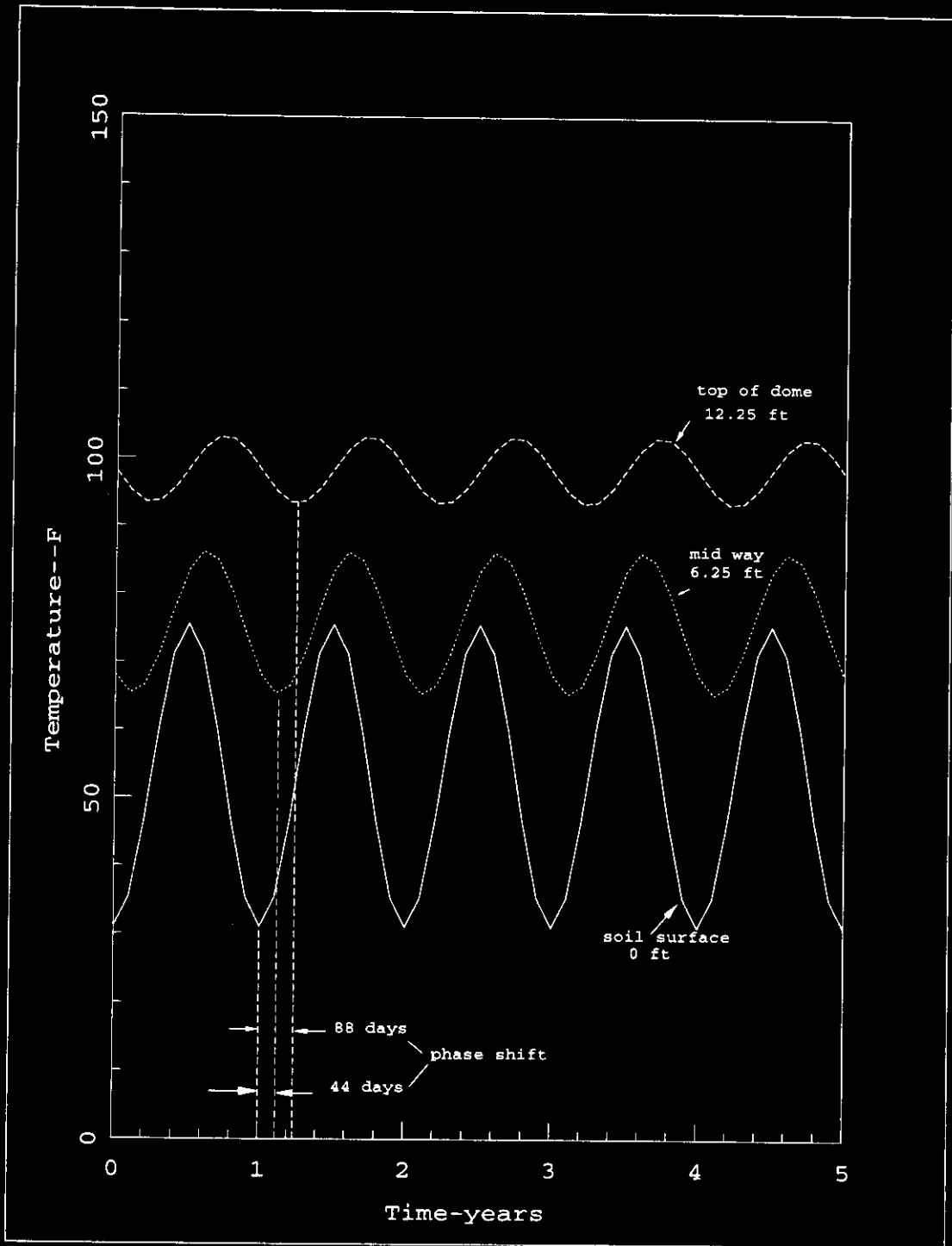


Figure 6.3 1-D Classical Solution to Temperature versus time and distance from soil surface

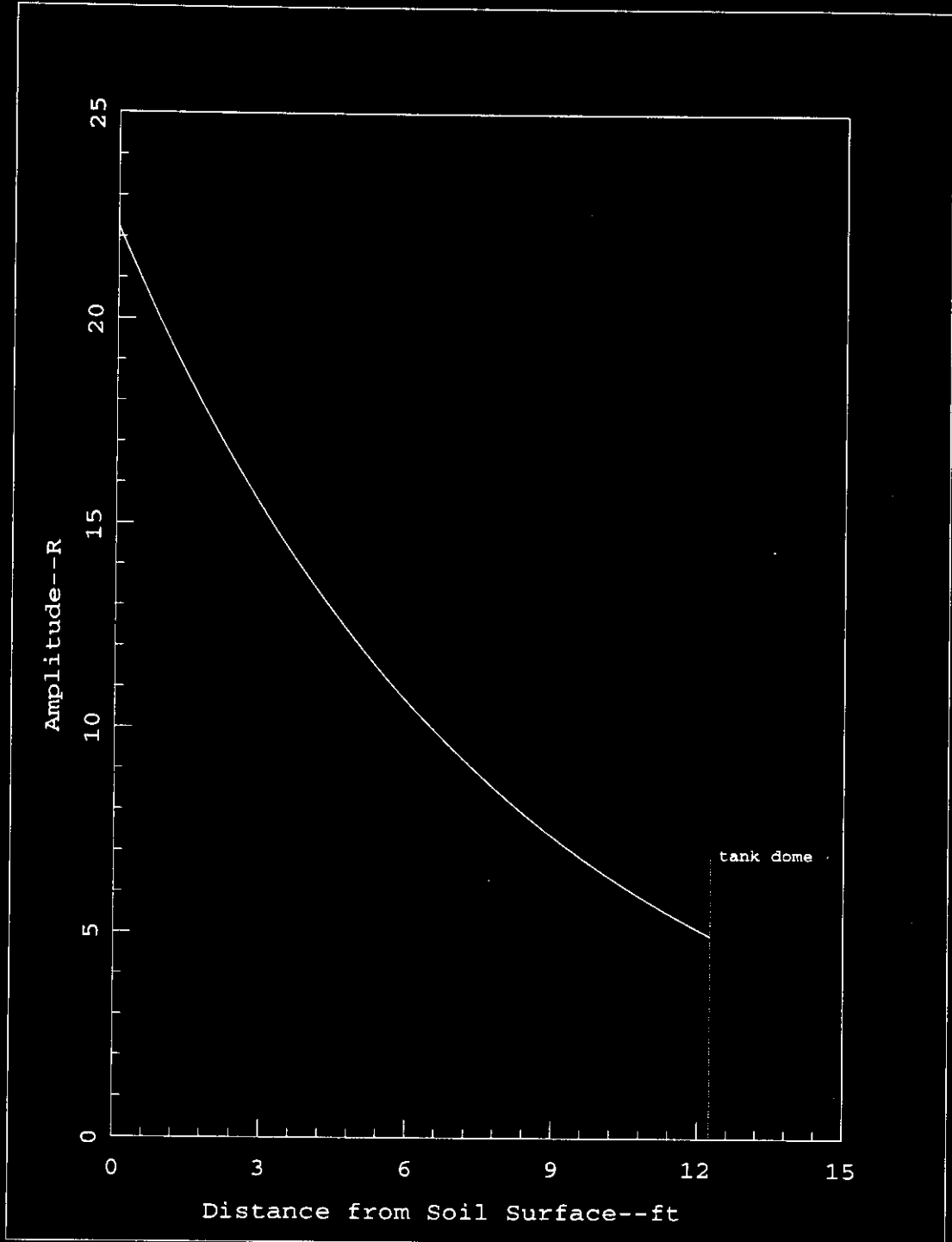


Figure 6.4 Amplitude of Temperature Oscillation versus Distance Downward from the Soil Surface

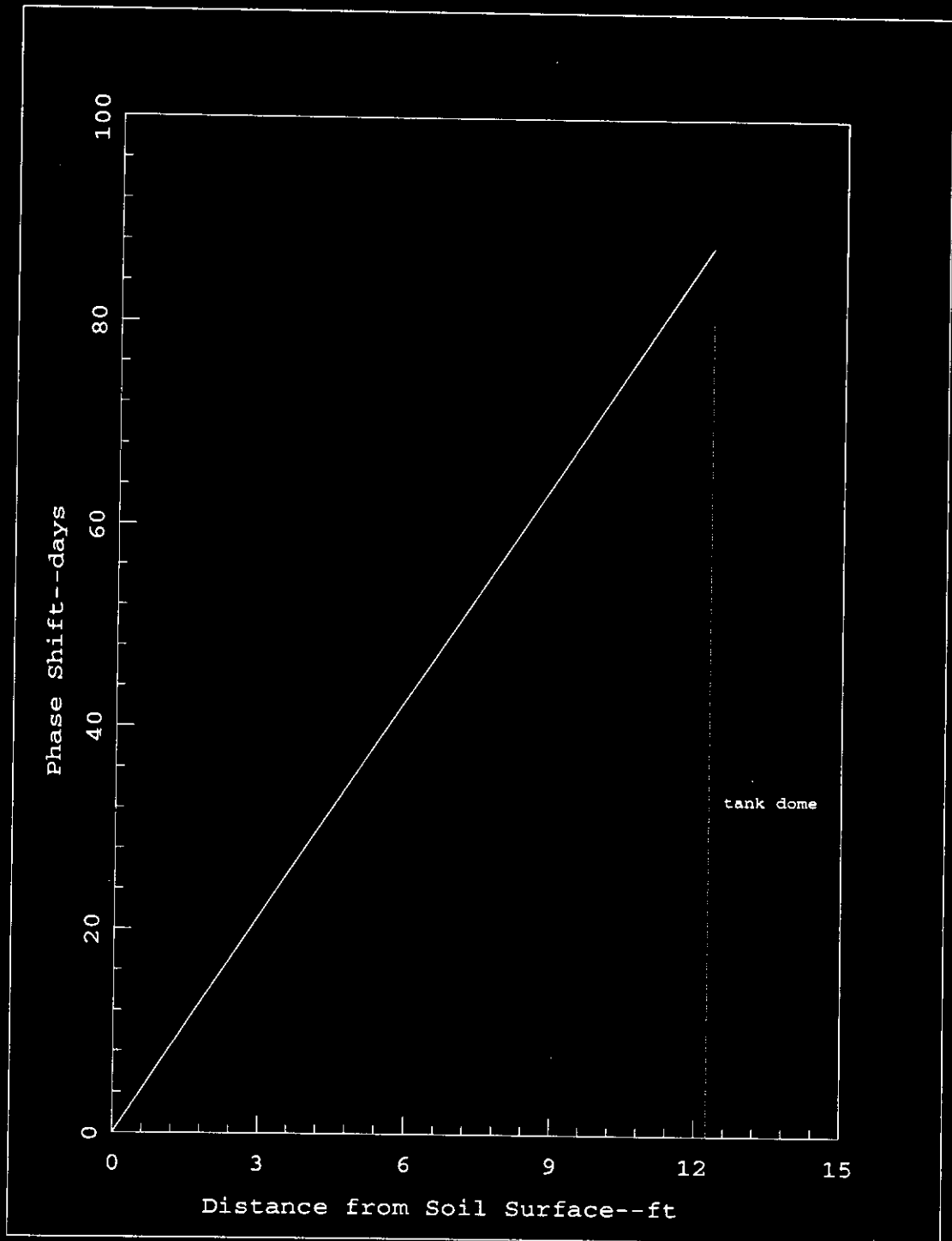


Figure 6.5 Phase Shift of Temperature Oscillation versus Distance Downward from the Soil Surface

Figure 6.6 provides a comparison of the actual ambient monthly average temperature and the ambient assumed for the simple analytical model. Also shown is the comparison of the waste/dome gas interface temperature data to that calculated with this simple analytical model. The calculated result for the dome gas/waste interface temperature is quite remarkable both in terms of the amplitude and the phase shift. The results however include some compensating errors or modeling omissions, in the following sense. First it does not include the effect of a decaying radiolytic heat load, the heat flux through the soil is assumed to be constant. Second, since the radiolytic heat load is decreasing, and the actual dome temperature data is remaining relatively constant when annual average ambient temperature changes are considered, no accounting is made in the simple analytical model for: (1) either the reduction in cooling of the dome; or, (2) the increase in heat supplied to the dome. Third, variations in the actual annual meteorological cycle are not included, fourth, operation of the forced ventilation during late 1990 are not included.

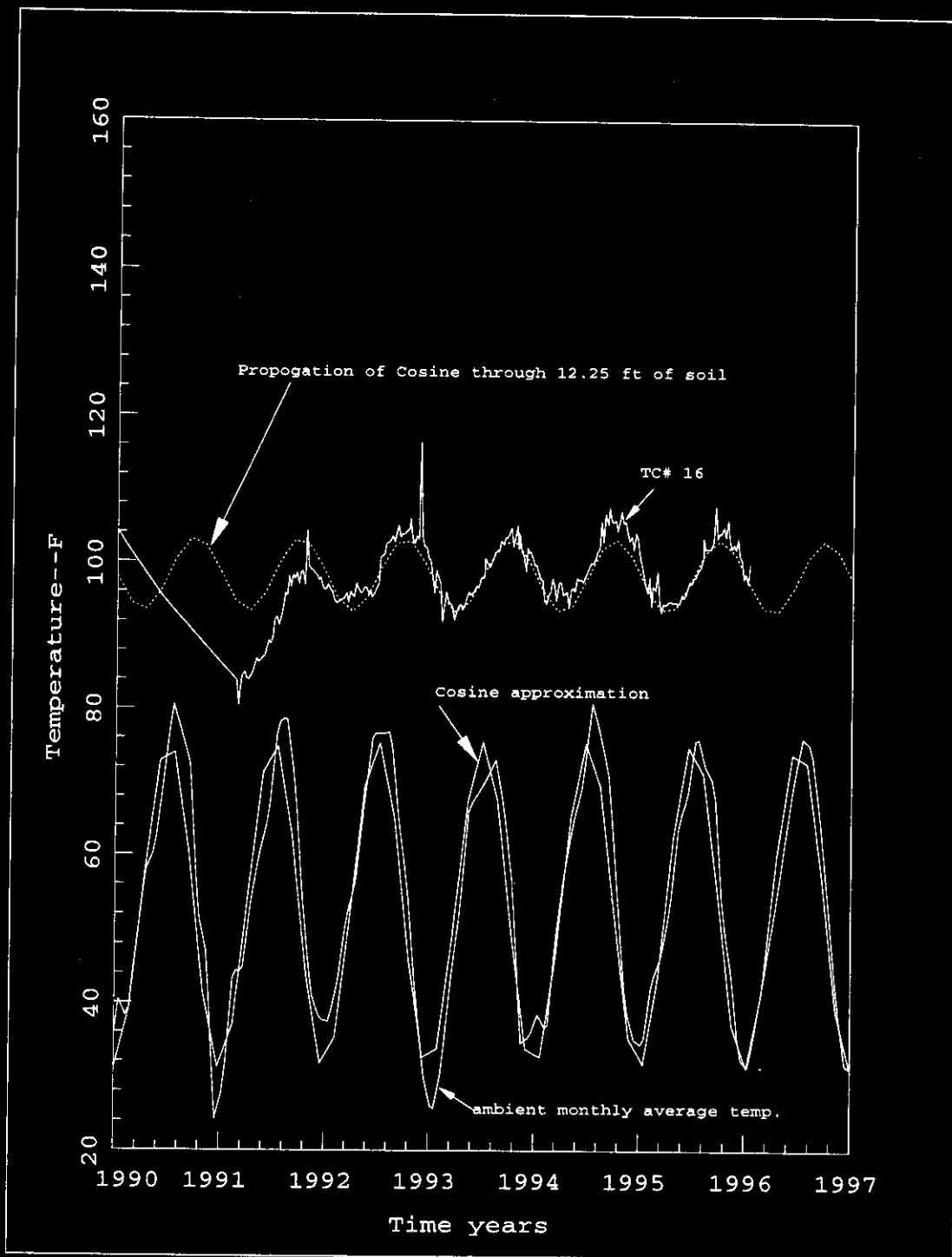


Figure 6.6 Comparison of Simple Analytical Solution to Data--Ambient and Dome Gas Temperature

### 6.3. ESTIMATED EFFECT OF ADJACENT TANKS

Tanks A-102, A-104, and A-105 are adjacent to Tank A-101 as shown in Figure 6.7. Tank A-105 dome gas temperature oscillates between 130-150 F following the annual meteorological cycle. Temperatures below the tank are 220-240 F at some locations and increases and decreases of 20 F have occurred over periods of 2-3 years. Tank A-104 dome gas temperature oscillates between 185-195 following the annual meteorological cycle. Tank A-102 dome gas temperature is about 90-95 F. The influence of changes in temperature in these tanks upon Tank A-101 was evaluated using analytical solutions to a 1-Dimensional semi-infinite horizontal soil slab being driven on the finite side (i.e. wall of adjacent tank) with temperature oscillations, and also a step change in temperature [Carslaw, 1959]. The calculations assume the propagation of the thermal oscillation or step change in temperature was through soil and waste, both having the properties of waste.

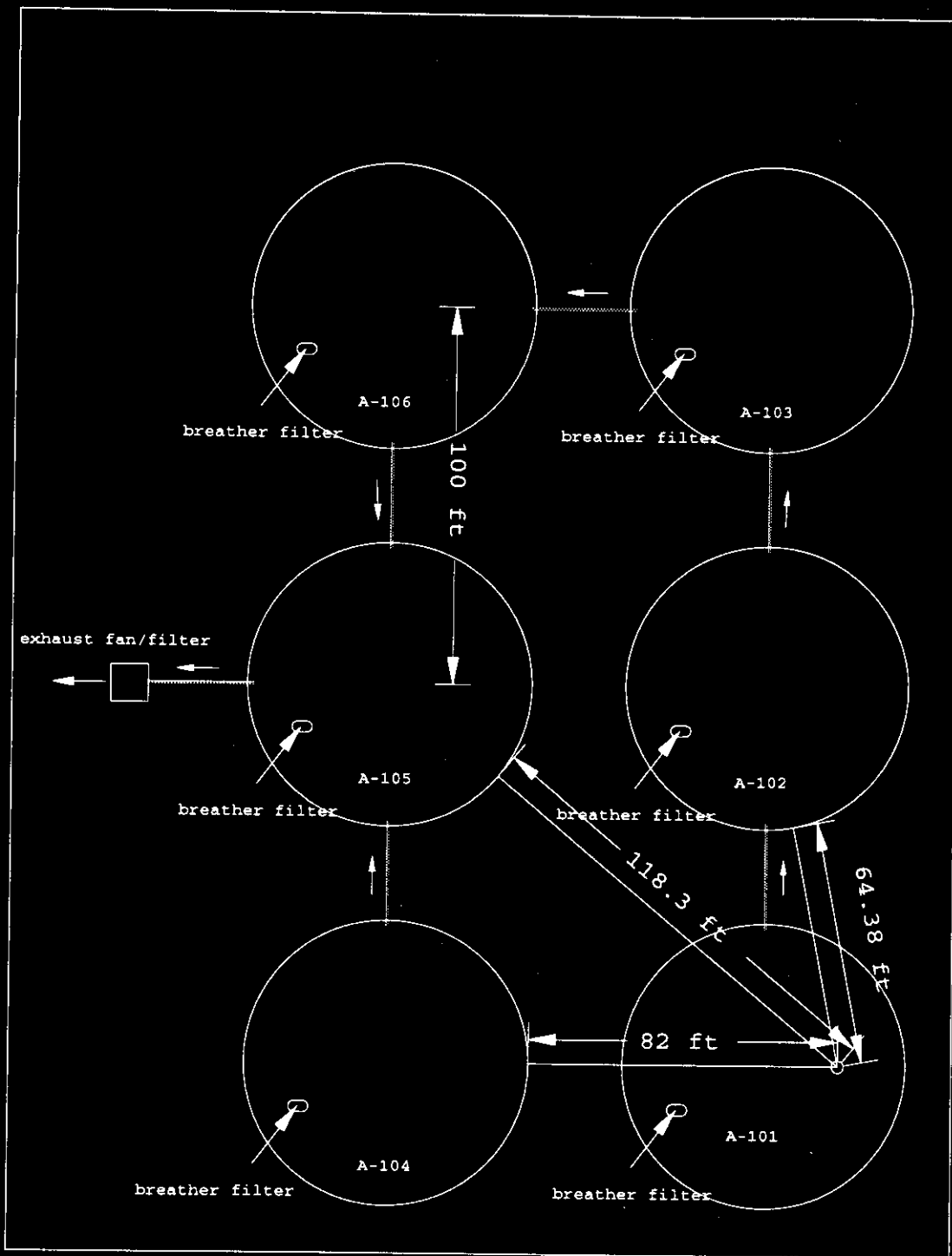


Figure 6.7 A Tank Farm--Relative Location of Tanks and Thermocouple Tree in Tank A-101

The amplitude attenuation and phase shift at the Tank A-101 thermocouple tree resulting from a temperature oscillation of amplitude 10 F at adjacent tanks is provided in Figures 6.8 and 6.9. This suggests that the effects of oscillatory increases and decreases in temperature at Tanks A-104 and A-105 upon Tank A-101 would be negligible and lagged in phase by 2-3 years. In addition, multi-dimensional cooling effects in the soil would further reduce these effects.

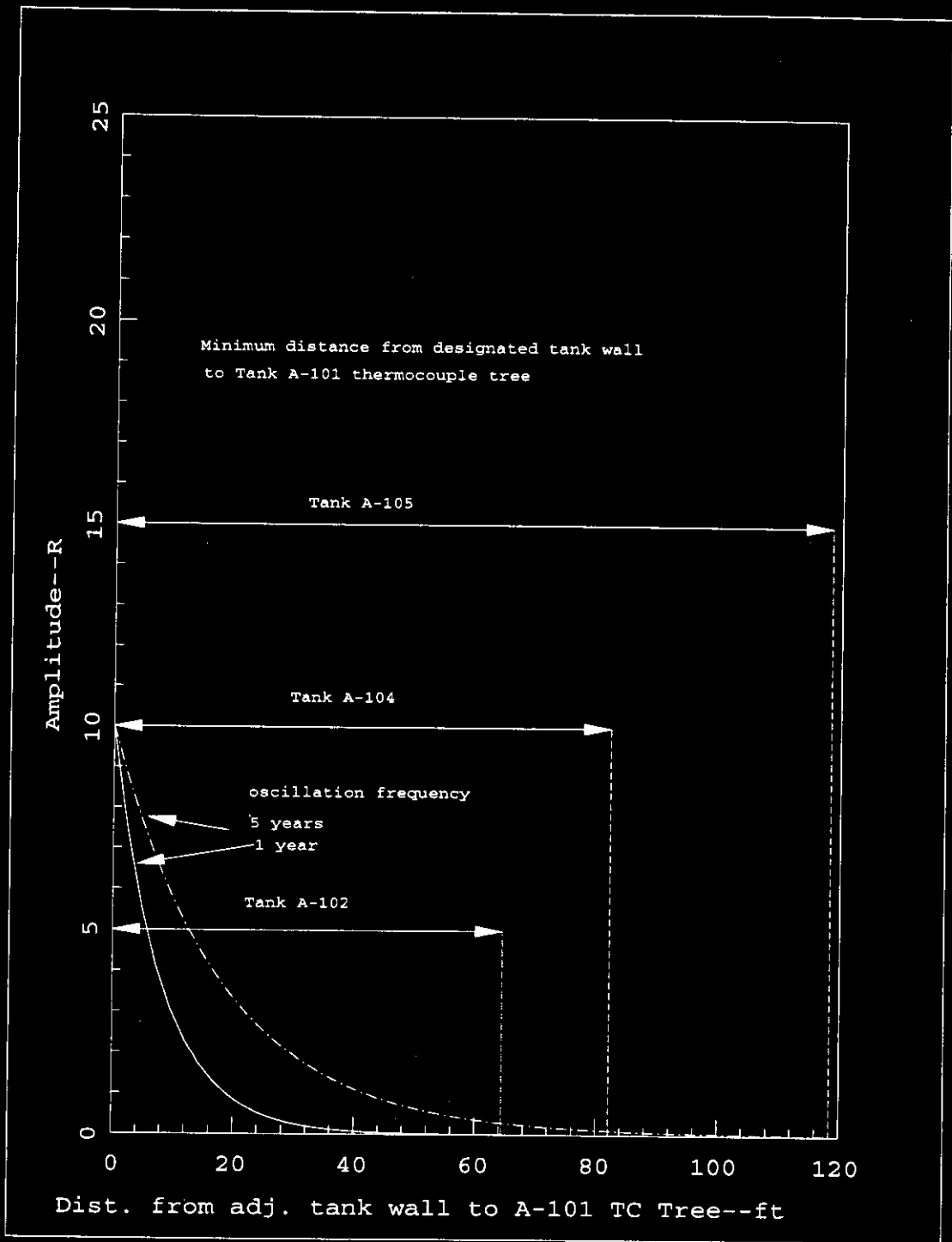


Figure 6.8 Amplitude of Temperature Oscillation versus Horizontal Distance from the Soil Surface

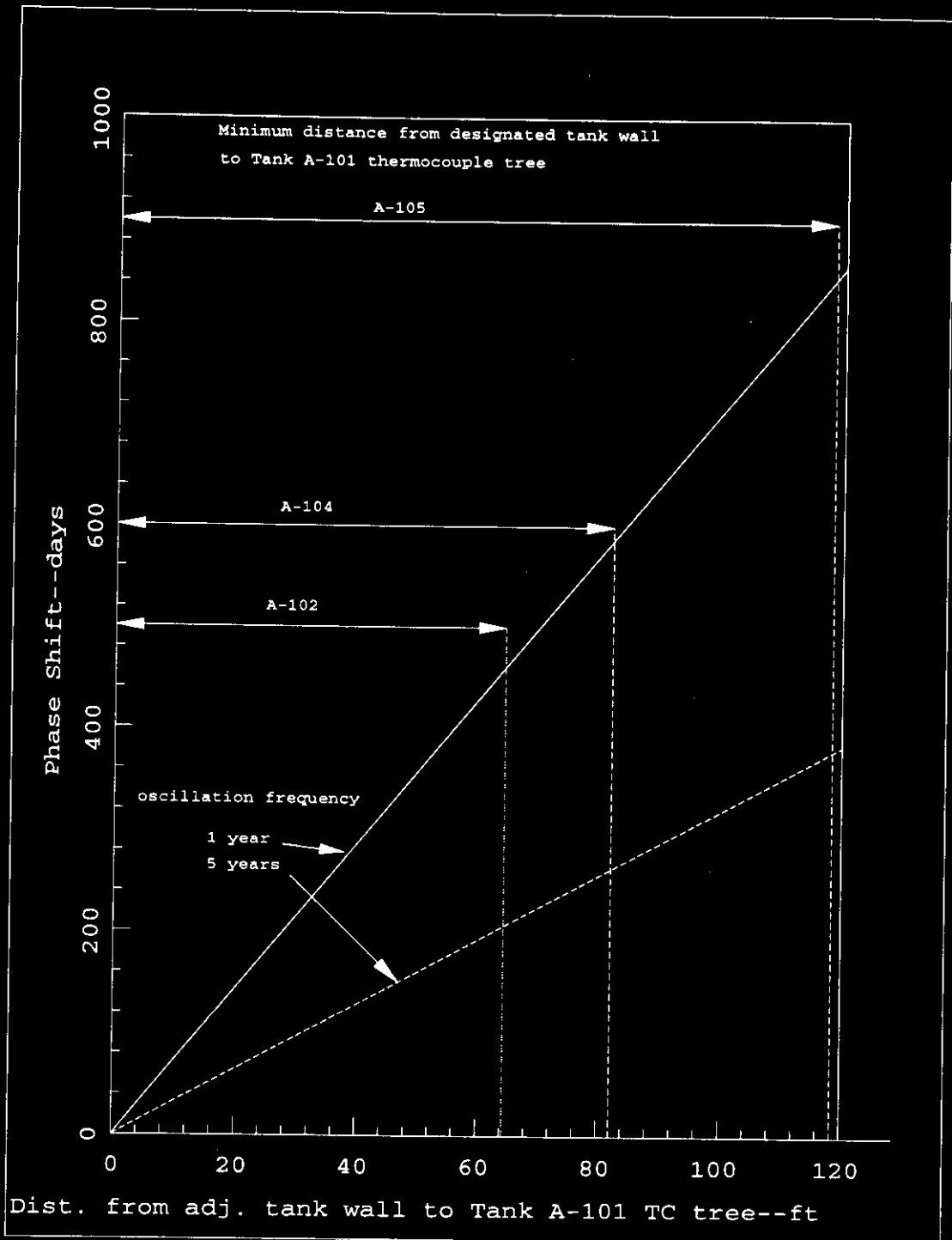


Figure 6.9 Phase Shift of Temperature Oscillation versus Horizontal Distance from the Soil Surface

The time required for a 20 F step change in temperature at an adjacent tank to increase the temperature at Tank A-101 thermocouple tree is shown in Figure 6.10. This result is based on the temperature transient in a horizontal 1-Dimensional semi-infinite slab subjected to a step change in temperature at the finite end (i.e. adjacent tank wall):

$$T(x, t) = (T_i - T_o) \operatorname{erf}\left(\frac{x}{2\sqrt{\alpha t}}\right) + T_o \quad (6.9)$$

Where:

$T_i$  = initial temperature in the soil and waste field prior to the temperature change at the adjacent tank wall

$T_o$  = temperature at adjacent tank wall after the step change

$t$  = time after the step change

$\alpha$  = thermal diffusivity of the soil

Although the rate of temperature increase at Tank A-101 may be significant due to a 20 F step change at an adjacent tank, multi-dimensional cooling effects would reduce this effect significantly below that calculated with the semi-infinite slab assumption. The tank with the largest temperature change during recent times is Tank A-105. It however is the furthest away and the rate of temperature change occurring at Tank A-101 due to a 20 F increase at Tank A-105 under this simple, but conservative analytical approach is on the order of .2 F/year.

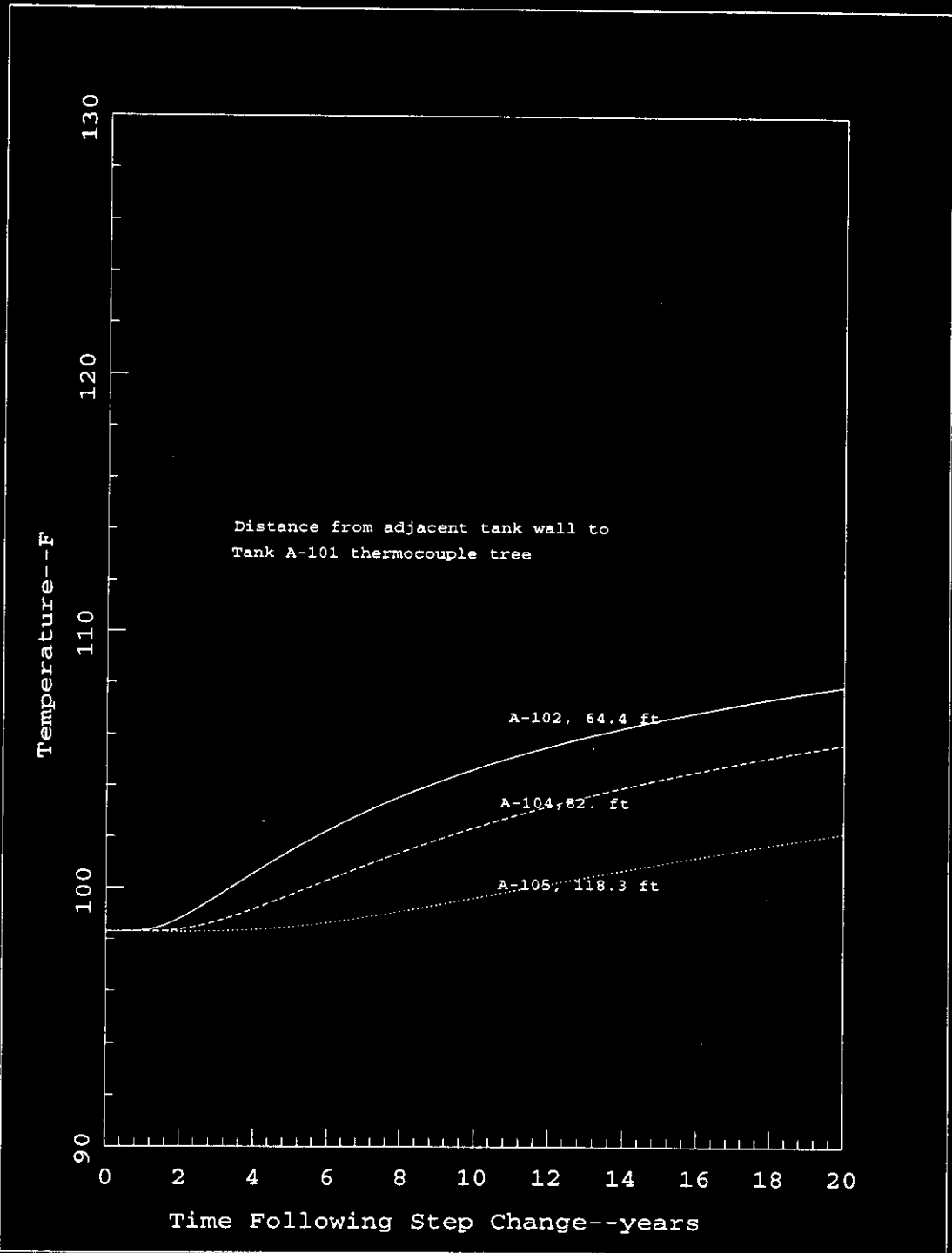


Figure 6.10 Temperature Versus Location and Time

Although adjacent tanks temperatures and their transient effects will have some finite effect on the thermal behavior of Tank A-101, the effects would appear to be small. In addition, the largest recorded temperature changes have occurred in the soil below Tank A-105. Temperature changes at this location would seem to have an effect on the bottom of Tank A-101 as well as in the dome space. Therefore, the possibility that adjacent tanks' thermal behavior is responsible for the decreasing temperatures in the bottom and constant or slightly increasing temperatures in the upper waste and dome gas at Tank A-101 appears remote.

Additional 3-D analysis would be required to further refine the impact of adjacent tanks on Tank A-101.

#### **6.4. HEAT REMOVAL AND SLURRY DRYOUT RATES VIA EVAPORATION**

One possible explanation for the thermal hydraulic behavior of Tank A-101 is that there is air inleakage into the tank, and evaporation of water from the waste plus heat up of the inleaking air has been augmenting the cooling of the waste/dome gas interface. This effect would be decreasing in time due to dryout thereby compensating for the decreasing radiolytic heat load. Air inleakage without evaporation is also a possibly explanation, but in this case the air flow must be decreasing to compensate for the decreasing heat load.

Shown below in Figure 6.11 are two, of many, possibilities involving decreasing evaporation, either of which could explain tank behavior. The first possibility is that air inleakage at the rate of about 48 ft<sup>3</sup>/min has been leaking into the tank since the beginning of 1981 and this has been evaporating water from the waste at a decreasing rate. Initially the air was leaving saturated at 98.3 F, but now is leaving at a steam partial pressure slightly above the inlet steam partial pressure. Another possibility ignores

what occurred before 1990. In this case at the beginning of 1990, 25 ft<sup>3</sup>/min enters and leaves saturated. Now however the evaporation rate has decreased and the air is leaving nearly at the same partial pressure at which it enters. The partitioning of the heat removal due to evaporation and sensible air temperature change as a function of flow rate for the case where air leaves saturated, versus at the steam partial pressure at which it enters are provided in Figures 6.12 and 6.13 respectively. The amount of water evaporated in lbm/hr, equivalent inches of level drop/year, and total equivalent level drop since filling the tank at the beginning of 1981 are shown in Figures 6.14-1.16.

Although it is not known how much liquid has been evaporated from Tank A-101 since filling it at the beginning of 1981, nor how much was evaporated due to forced ventilation at flow rates likely well above those that might be possible with inleakage, a review of these graphs leads to the conclusion that this explanation is plausible.

For example with an inleakage rate of 48 ft<sup>3</sup>/min and an exit relative humidity of 100%, 46 equivalent inches of liquid would have been removed from Tank A-101 since 1981. If the evaporation rate had been decreasing significantly since then to essentially nothing, then 23 equivalent inches might be the total that has been evaporated. If the resultant waste solids without moisture has a 50% volume fraction, then the waste would be dried out down to 46 inches.

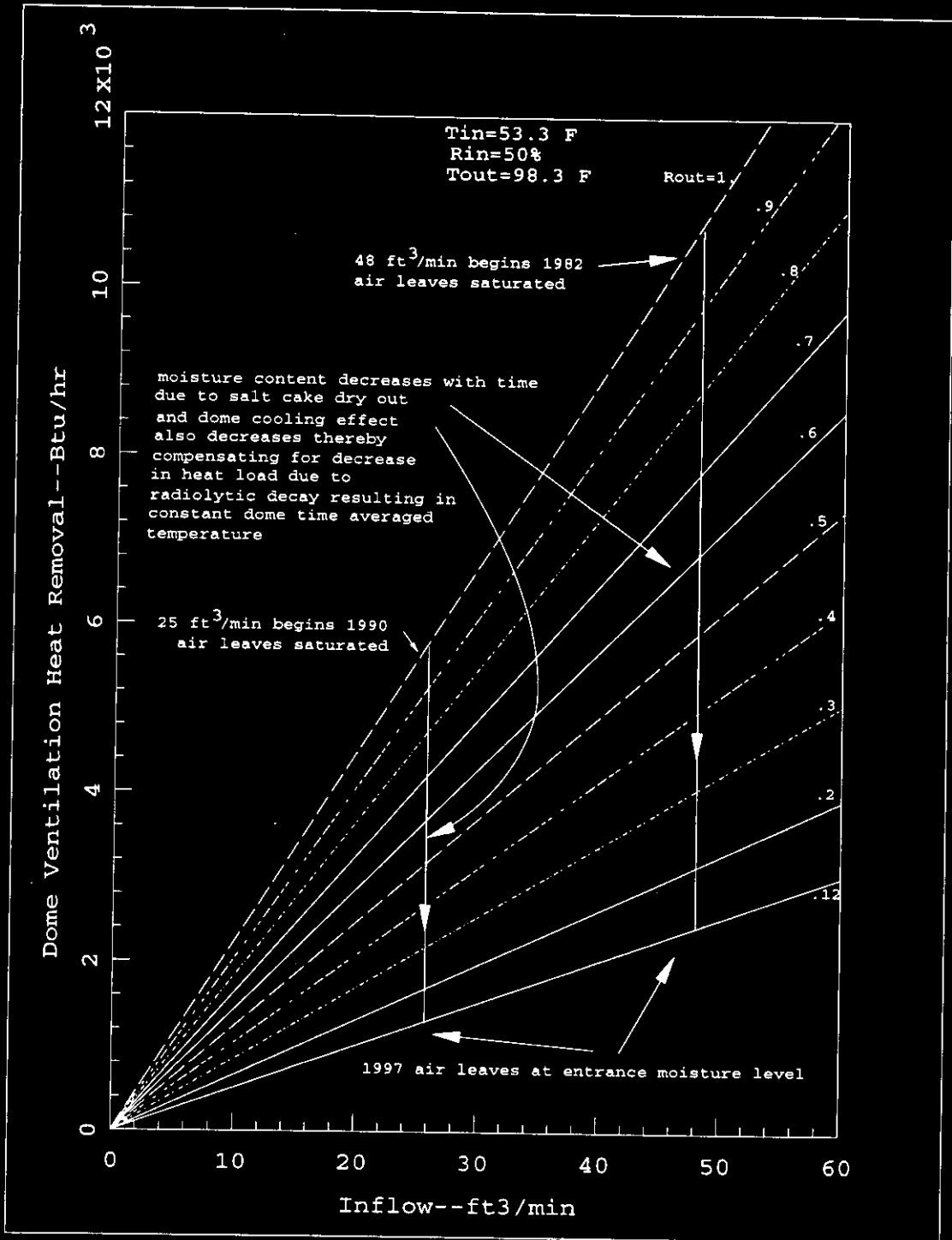


Figure 6.11 Low Heat Tanks with Natural Inflow Leakage--Dome Ventilation Heat Removal versus Inflow and Outlet Relative Humidity at 98.3 F Outlet Temperature

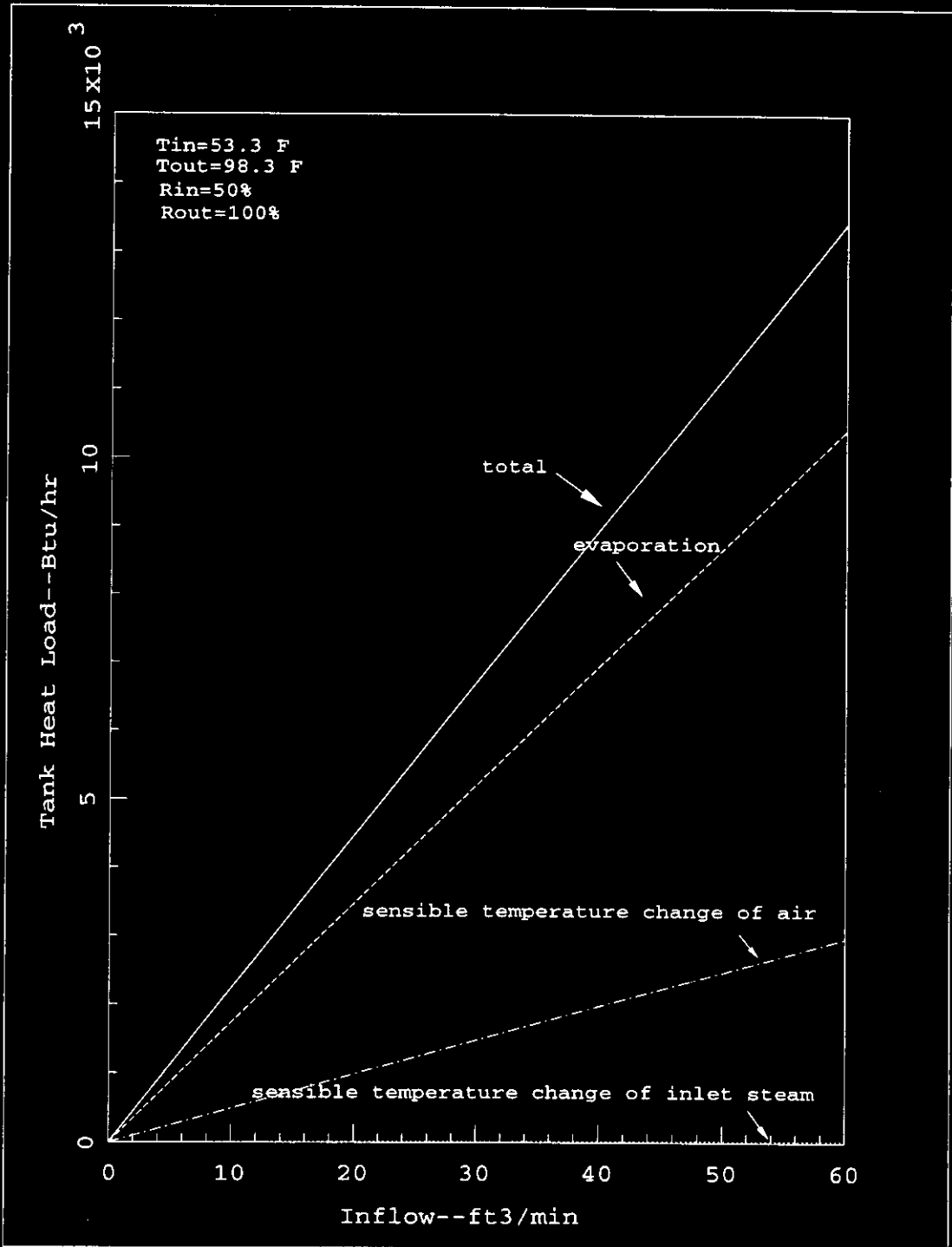


Figure 6.12 Low Heat Tanks with Natural Inflow Leakage--Tank Heat Load Partitioning versus Inflow and at 98.3 F Outlet Temperature and 100% Relative Humidity

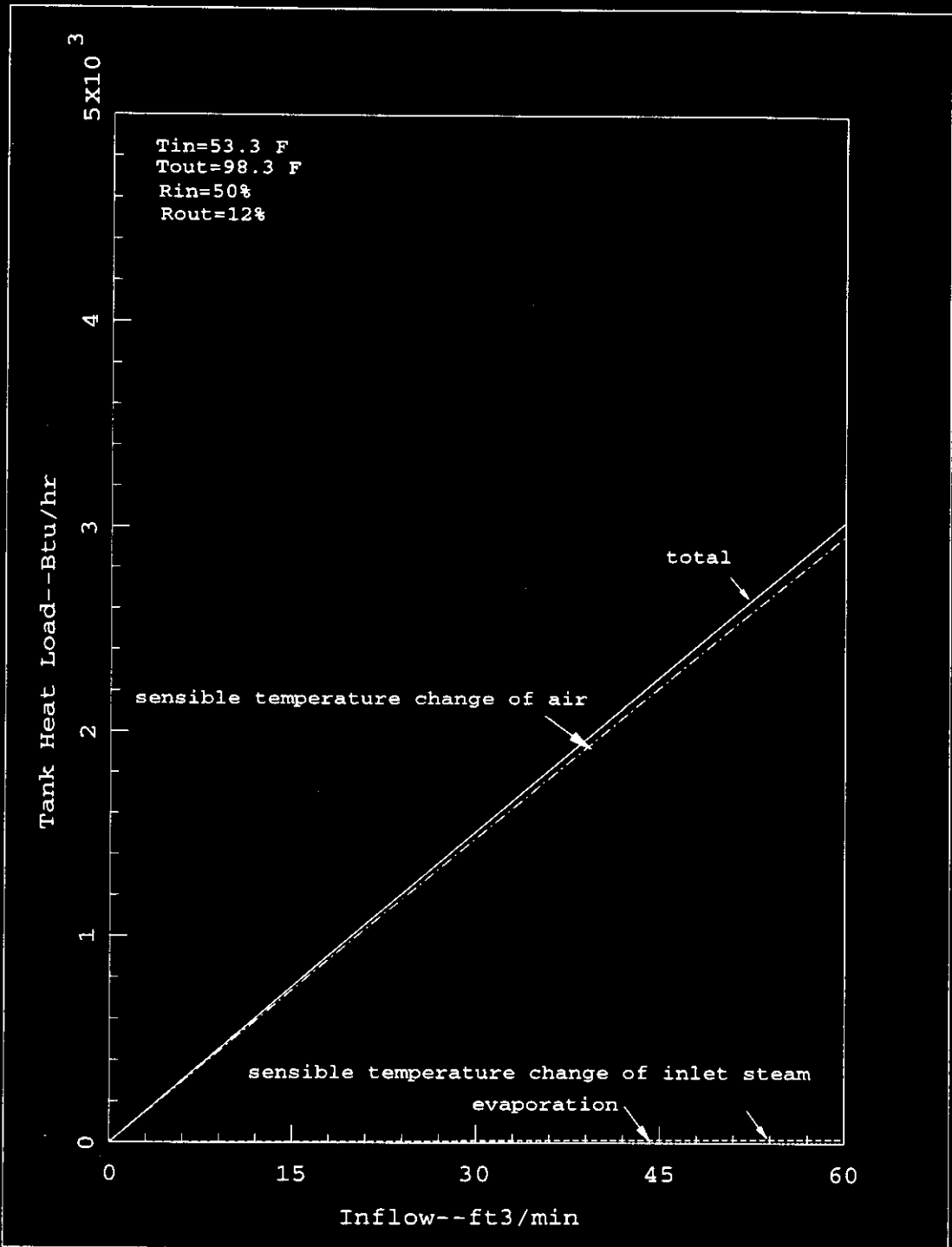


Figure 6.13 Low Heat Tanks with Natural Inflow Leakage--Tank Heat Load Partitioning versus Inflow and at 98.3 F Outlet Temperature and 100% Relative Humidity

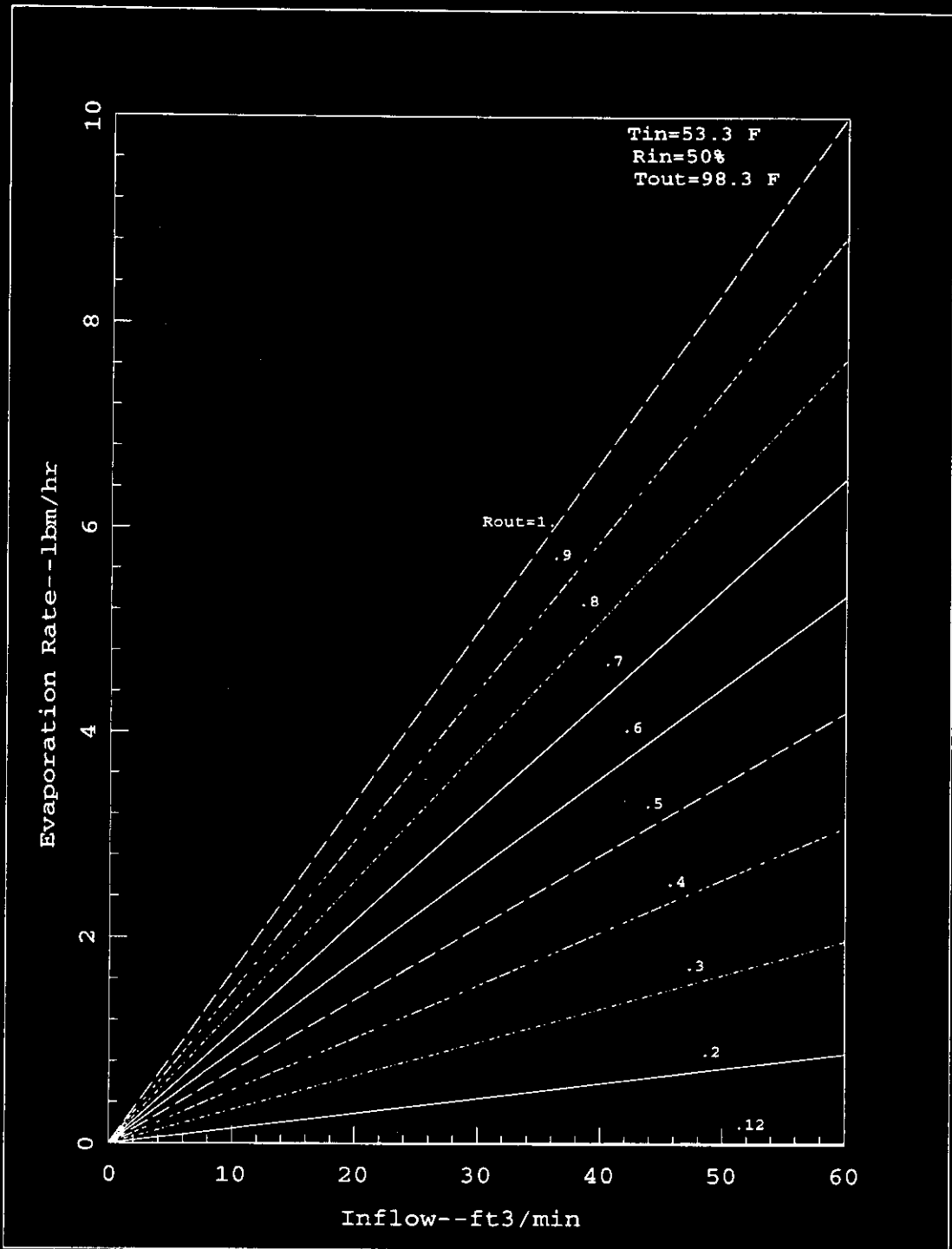


Figure 6.14 Low Heat Tanks with Natural Inflow Leakage--Tank Evaporation Rate versus Inflow Rate and Outlet Relative Humidity at a 98.7 F Outlet Temperature

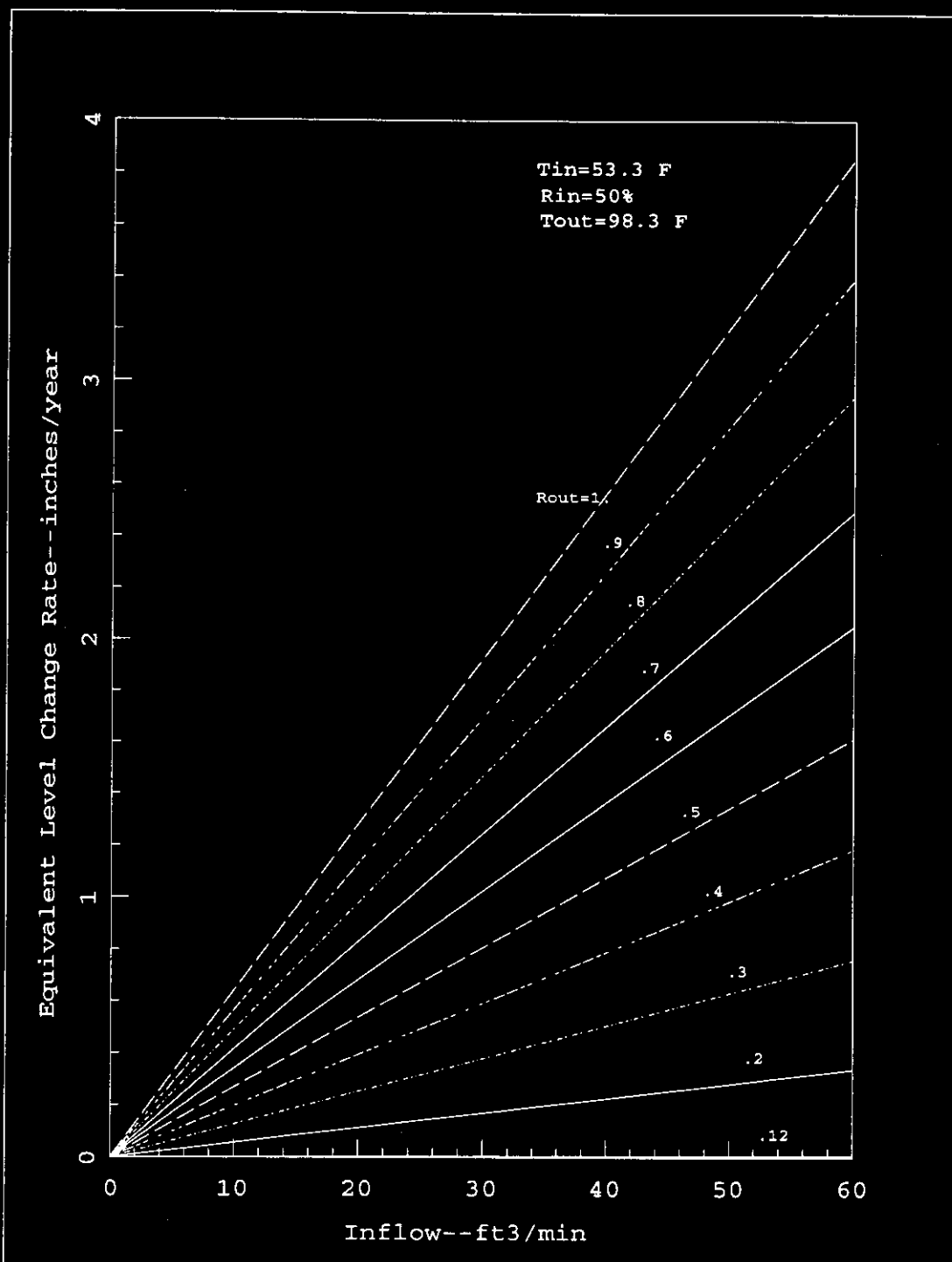


Figure 6.15 Low Heat Tanks with Natural Inflow Leakage--Tank Level Change Rate Due to Evaporation Versus Inflow and Outlet Relative Humidity

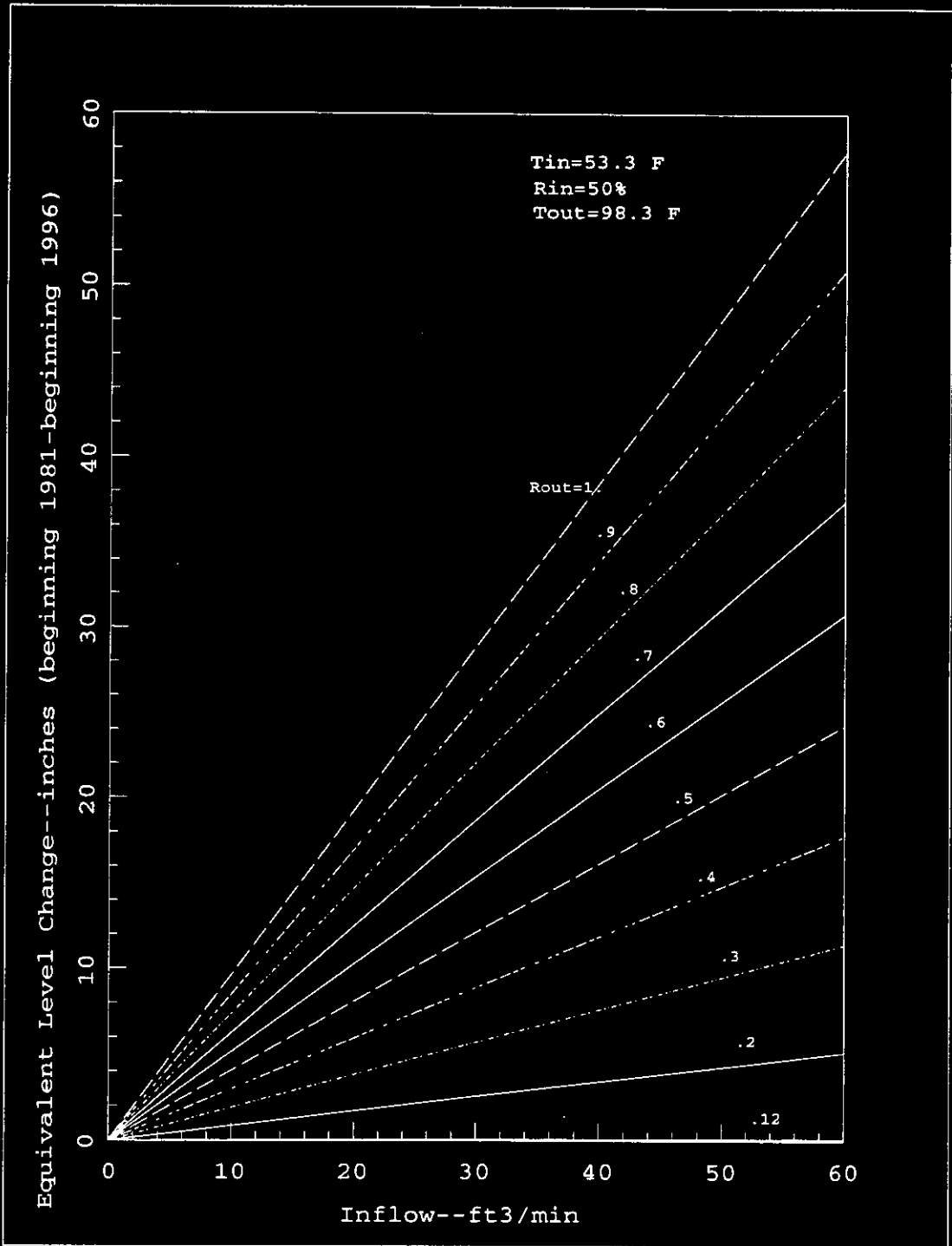


Figure 6.16 Low Heat Tanks with Natural Inflow Leakage--Tank Level Change Due to Evaporation Versus Inflow and Outlet Relative Humidity

## 7. GOTH SIMULATION RESULTS

Many GOTH thermal hydraulic code simulations were conducted in this analysis to help understand the thermal hydraulic history or behavior of Tank A-101. Initially these simulations were directed towards the 1991-1996 time period since the quality and quantity of temperature data was better and the forced ventilation system was off. Between completing filling of the tank with slurry in early 1981 and early 1991 temperature data acquisition was infrequent, ventilation flow data was not available, and forced ventilation operating periods were obviously erratic which in turn lead to erratic temperature behavior.

At the beginning of this evaluation, quasi-steady or repetitive periodic thermal history for the tank prior to 1990 was synthesized to provide a rational 1990 thermal starting condition for simulation of the 1990-1996 time period. Constant radiolytic heat load and constant or periodic cooling conditions were assumed. Later it was determined that the thermal history for the 1980-1990 time period could be roughly approximated by varying the radiolytic heat load rather than holding it constant. An initial guessed temperature distribution for the waste based on the previously described time averaged distribution for the 1993 time period was used for the beginning of the simulation, which was initiated near the beginning of 1982. Future simulations should initiate the thermal conditions beginning in 1981 with uniform temperature of 125 F and soil at near its annual average temperature of 50-55 F. This should be followed by periodic periods of forced ventilation flow to synthesize a temperature behavior from 1981-1991 similar to the data.

Although there are improvements that could be made in the model for the 1981-1990 time period, the period of time between 1991 and 1996 has been quite well simulated based

on the above described model, model assumptions, and preconditioning 1982-1990 approach.

Three sets of simulations are described below. Two simulations are presented within each of the three sets, one for constant average meteorological conditions, and one for the meteorological history described in Figure 5.2 (i.e. annual cyclic meteorology). The constant meteorological condition assumption provides insight on what is essentially the time averaged thermal behavior, whereas the other case simulates the effect of the actual annual meteorological cycle.

The first set of two simulations assumes constant cooling conditions (i.e. fixed air inleakage). The second set assumes decreasing cooling conditions (i.e. decreasing air inleakage). The third set assumes both decreasing inleakage, plus a period of forced ventilation in late 1990 to create the temperature decreases and reheat seen in the data.

These simulations include the effects of soil thermal inertia, two separate layers with different thermal conductivities and volumetric heat generation rates, constant and variable inleakage, a forced ventilation period, and the annual cyclic meteorology from 1990-96 based on actual monthly average temperatures. In comparison to Figures 6.1-6.2, which are based on a much simpler assumptions, the general temperature trends are similar. However, in the GOTH simulations the heat up and cool down trends are slower due to thermal inertia effects of the lower sludge layer and soil, and temperature time variation effects due to cyclic meteorological effects and operation of the forced ventilation are present. The cyclic effect of the ambient oscillations on the dome gas/waste interface are similar to that for the results of the simple analytical model of Figures 6.3 and 6.6, however, the more complex model dynamic simulation results trend up or down on a time averaged basis depending

on the amount of air inleakage present. Only under decreasing air inleakage conditions do the complex model results match well with the data.

## **7.1. CONSTANT DOME COOLING MECHANISM**

The effects of radiological heat decay combined with constant dome cooling mechanisms for both constant and annual cyclic meteorological conditions are described below. The dome cooling mechanisms were assumed to be conduction through the soil to the atmosphere and cooling via inleakage with sensible air temperature change only. In leakage air flow rate was held constant at 1 ft<sup>3</sup>/sec and no evaporation was assumed. Soil conductivity was assumed not to change due to dryout.

### **7.1.1. Constant Meteorological Conditions**

The simulation assumptions and results based on radiolytic heating with a 30 year half life, constant inleakage of 1 ft<sup>3</sup>/sec, constant ambient temperature of 53.3 F and no forced ventilation period is illustrated in Figure 7.1. The constant meteorological assumption produces essentially time average results relative to the data. Simulation cooldown rates during the 1993-1996 period are faster than for the data, particularly in the upper regions of the waste. From 1982 until 1990 the simulation temperature results roughly approximate the actual temperatures. The difference is due primarily to the operation of the forced ventilation system which intermittently cooled the waste relative to the simulation which assumed inleakage flow, but not forced ventilation adequate to intermittently cool the waste to the temperature levels observed.

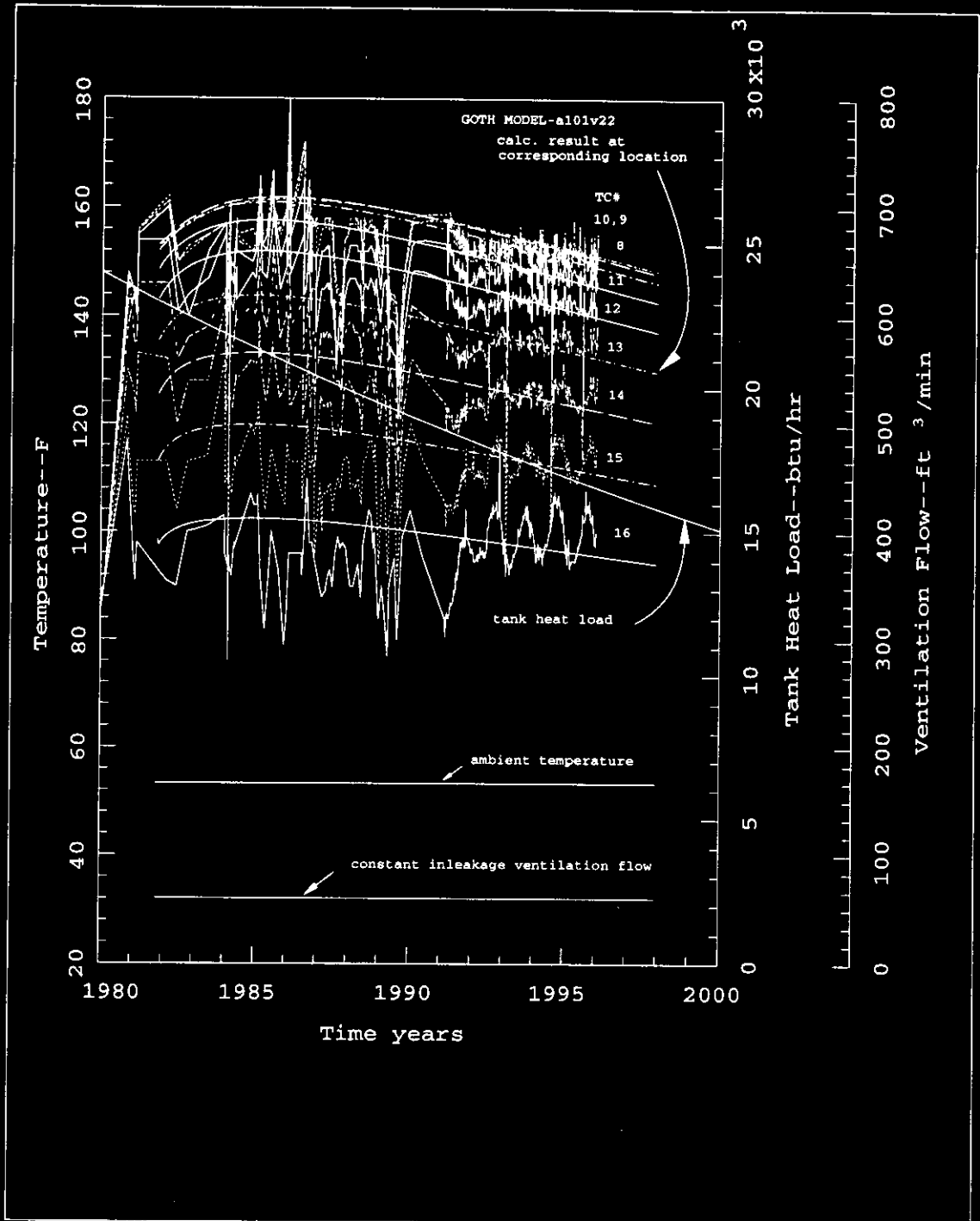


Figure 7.1 Data versus Model--Historical Average Meteorology, Fixed Inleakage Flow, 30 Year Half Life Radiological Heat Load

### 7.1.2. Annual Cyclic Meteorological Conditions

When annual cyclic meteorological conditions are superimposed upon the simulation described in Figure 7.1 cyclic behavior similar to the data results as shown in Figure 7.2. Rates of temperature decrease from 1993-1996 remain faster than the data however, but somewhat slower on a time averaged basis than for Figure 6.1. This is due to the increase in the time averaged ambient temperature during this time period which is incorporated in the meteorological cycle. This small increase in the ambient average temperature can have noticeable effects on the dome and waste temperature. By comparing Figure 7.2 to Figure 7.1 it can be observed that the intermittent decreases in waste temperature during the 1980-1990 time period are primarily due to forced ventilation being on intermittently, but to a lesser extent these intermittent decreases are also due to the actual annual cyclic ambient temperatures.

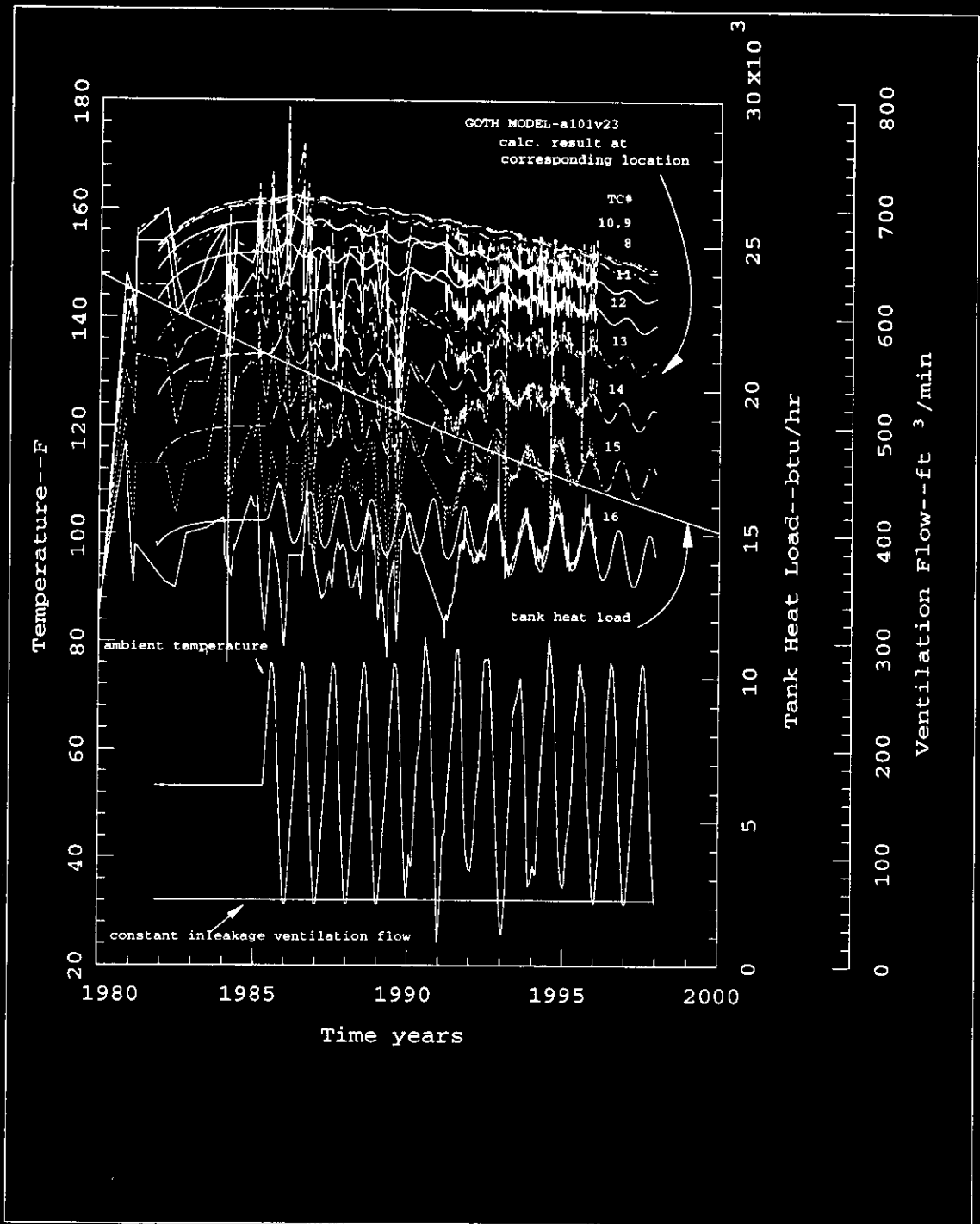


Figure 7.2 Data versus Model--Annual Cycle Meteorological Conditions, Fixed Inleakage Flow, 30 Year Half Life Radiological Heat Load

## **7.2. DECREASING DOME COOLING MECHANISM**

The effects of radiological heat decay combined with a decreasing dome cooling mechanism for both constant and annual cyclic meteorological conditions are described below. The dome cooling mechanisms were assumed to be conduction through the soil to the atmosphere and cooling via inleakage with sensible air temperature change only. In leakage flow rate was set to 1 ft<sup>3</sup>/sec in 1990 and no evaporation was assumed. Soil conductivity was assumed not to change due to dryout. The inleakage was decreased linearly from 1 ft<sup>3</sup>/min in 1990 to 0 ft<sup>3</sup>/min in 1997. This linear ramp was increased backwards in time to 1982, the beginning of the transient simulation. The decrease in cooling was essentially compensated for by the decrease in radiolytic heat load due to decay, thereby maintaining the time average dome temperature in both simulations nearly constant.

### **7.2.1. Constant Meteorological Conditions**

By decreasing the inleakage ventilation flow cooling by the same amount as the decaying radiolytic heat load the dome gas temperature can be maintained constant on a time averaged basis. Maintaining the dome temperature constant will slow the rate of temperature change in the waste--but the waste temperature will continue to decrease, albeit at a slower rate. Decreasing the inleakage at a faster rate than the equilibrium decrease rate will result in increasing the temperature of the dome over time. Decreasing the inleakage rate even further will ultimately cause the waste at progressively deeper and deeper levels to begin increasing in temperature--even though the radiolytic heat load is decaying.

The simulation in Figure 7.3 assumes a decreasing inleakage flow cooling rate that almost approximates the decrease in radiolytic heat load. The rate of decrease

is slightly higher than the equilibrium flow rate decrease and the net result is a slightly increasing dome temperature. However after the initial waste heat up which ends in the 1984-85 time period, calculated waste temperature 4 feet below the surface (TC#14) continually decrease as do all waste locations below this level.

The simulation temperatures approximate the time averaged temperatures in the 1993-1996 time period. During the 1991-93 time period the effects of the force ventilation period are not included in the simulation. As a result simulations temperatures are higher than the time averaged data.

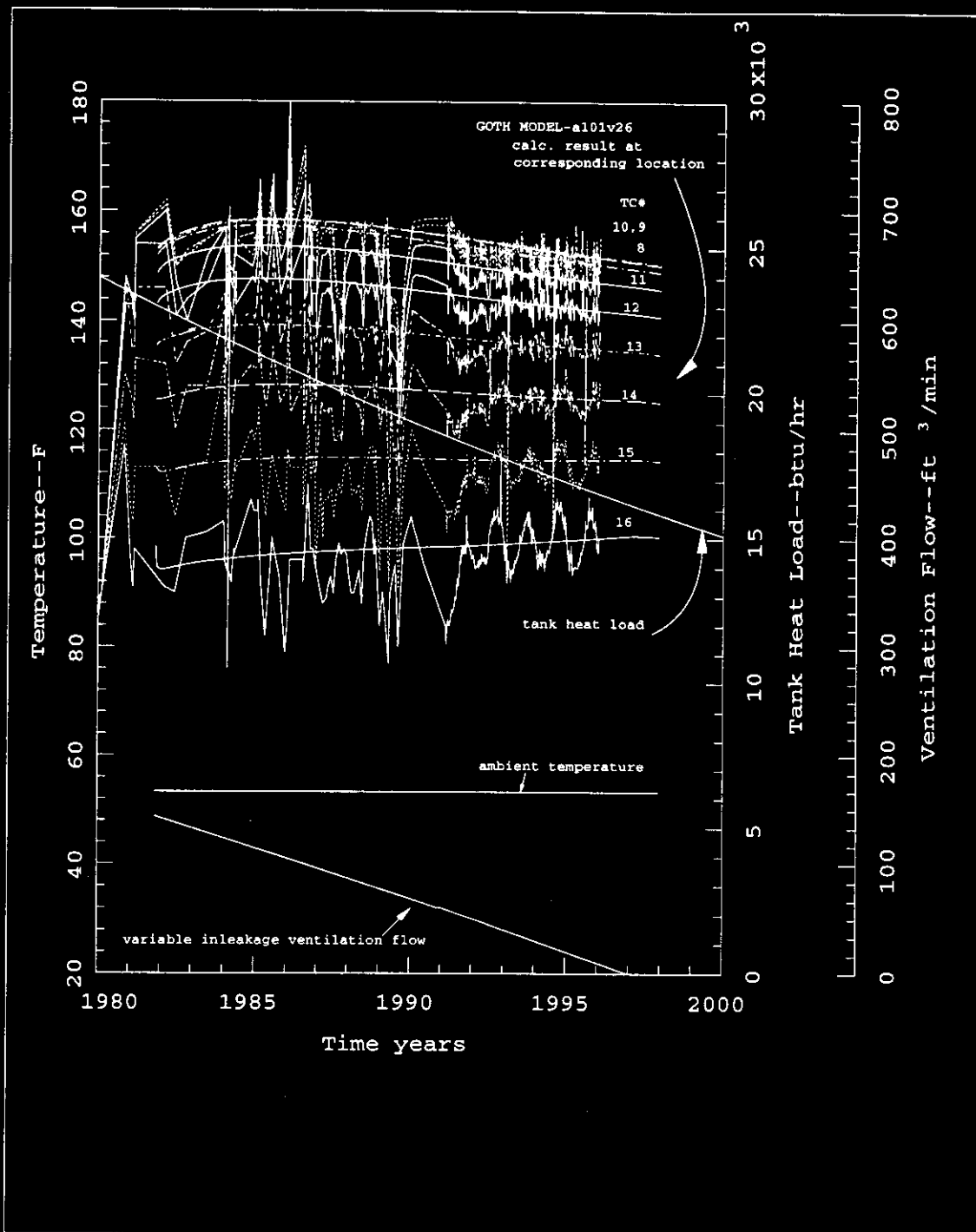


Figure 7.3 Data versus Model--Historical Average Meteorology, Variable Inleakage Flow, 30 Year Half Life Radiological Heat Load

### **7.2.2. Annual Cyclic Meteorological Conditions**

Figure 7.4 presents the results of superimposing the annual cyclic meteorology upon the simulation described in Figure 7.3, or equivalently superimposing the effect of decreasing ventilation inleakage on the simulation described in Figure 7.2. As shown there the simulation compares favorably with the data except for the 1990-92 time period when the waste was cooled by operation of the forced ventilation system for a short period of time, then reheated when the forced ventilation was turned off.

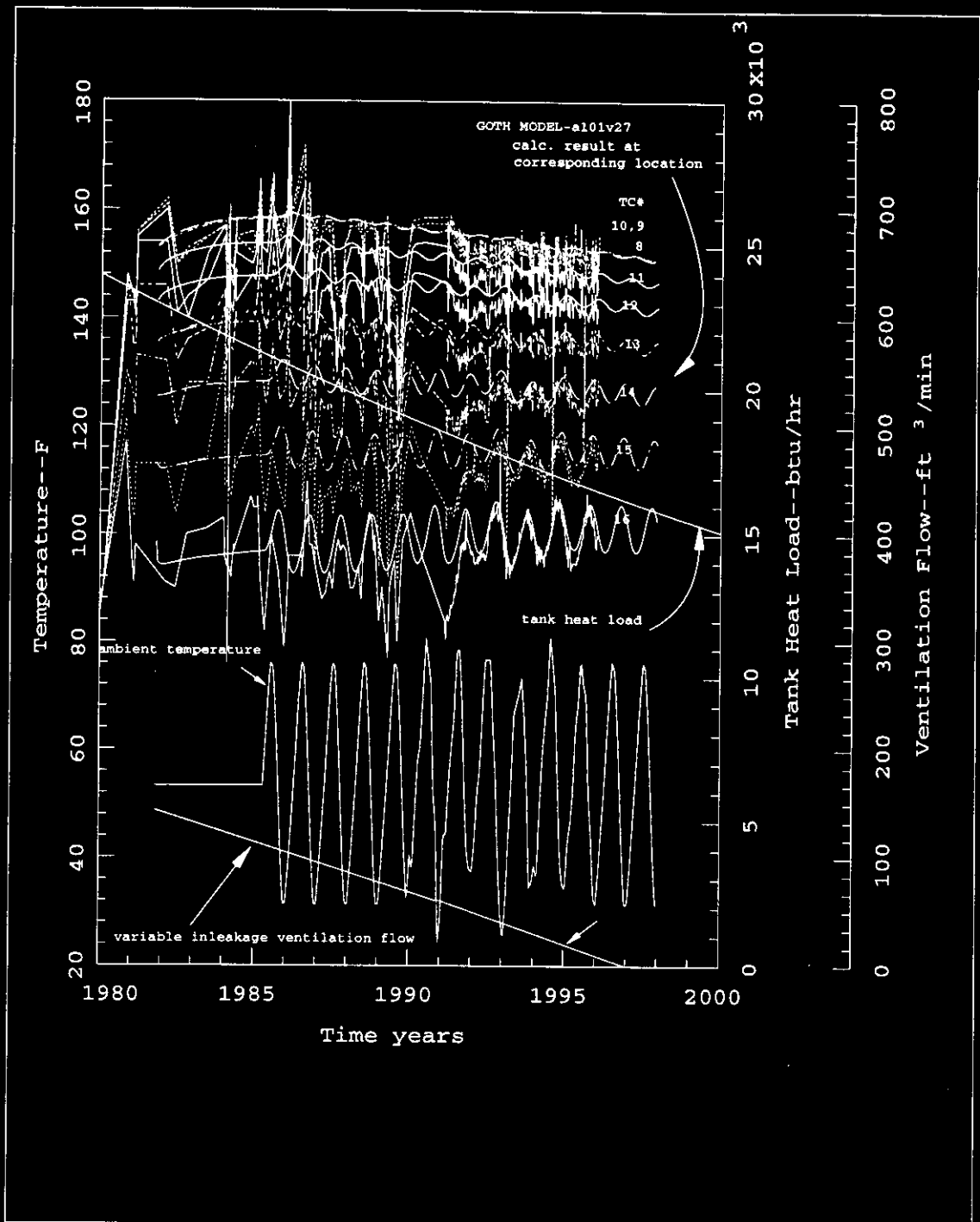


Figure 7.4 Data versus Model--Annual Cycle Meteorological Conditions, Variable Inleakage Flow, 30 Year Half Life Radiological Heat Load

### **7.3. DECREASING DOME COOLING MECHANISM COMBINED WITH FORCED VENTILATION PERIOD IN 1990**

The temperature data indicates the forced ventilation system was operable towards the end of 1990 or the beginning of 1991 for a short period of time. To simulate this period, a total forced plus inleakage ventilation flow of 780 ft<sup>3</sup>/min for a period of 1.5 months was assumed. The forced ventilation flow was initiated on November 15, 1990 and terminated on January 1, 1991. This effect is described below.

#### **7.3.1. Constant Meteorological Conditions**

If the effects of the late 1990 forced ventilation period are superimposed upon the simulation described in Figure 7.3, the time averaged resultant cooldown and heatup effects are simulated as shown in Figure 7.5. A comparison of Figures 7.5 and 7.3 shows the effects of the outage have essentially been eliminated by the beginning of 1996.

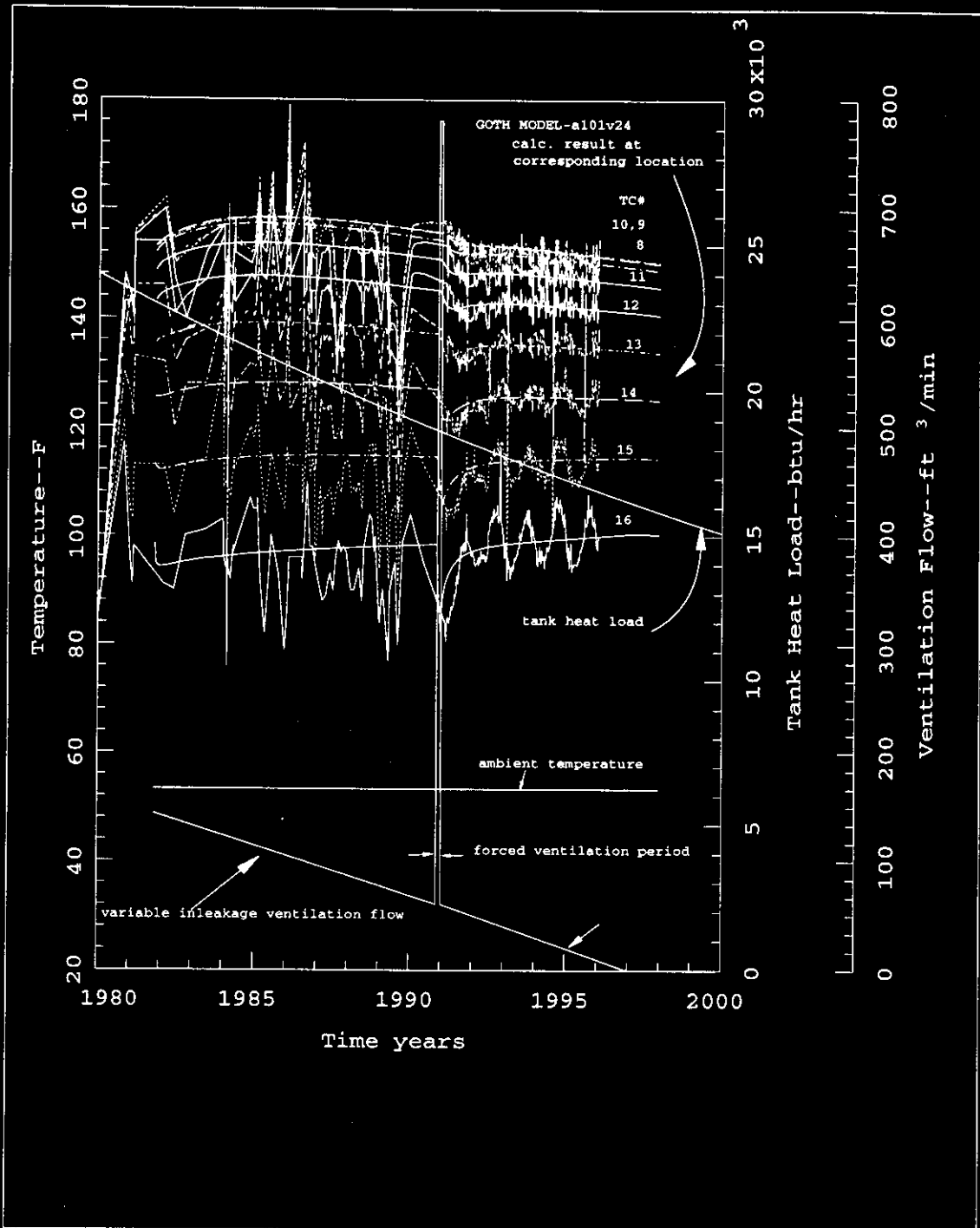


Figure 7.5 Data versus Model--Historical Average Meteorology, Variable Inleakage Flow, 30 Year Half Life Radiological Heat Load, Late 1990 Forced Ventilation Period

### 7.3.2. Annual Cyclic Meteorological Conditions

Superimposing the effects of the ventilation outage on the simulation described in Figure 7.4, or equivalently the annual cyclic meteorology upon the simulation described in Figure 7.5, provides the most complete simulation developed during this evaluation. The results are provided in Figure 7.6. As shown there the calculated temperatures agree quite well with the data.

The inleakage air provides cooling by sensible air temperature change, but assumes there is not evaporation from the waste to the inleakage air. As noted earlier a similar result could be achieved with constant inleakage, but with decreasing evaporative cooling, or by adding an increasing non-radiolytic heat source at the surface due to chemical reaction, or possibility heat of precipitation. If additional heating were substituted for inleakage, then the propagation of surface temperature oscillations into the waste would be more attenuated and more out of phase. Although inleakage of  $1 \text{ ft}^3/\text{sec}$  does reduce the attenuation and phase lag and bring simulation results into reasonable agreement with the data, this much flow does not produce a large effect in this regard. Additional analysis would be necessary to determine if it is possible differentiate between additional cooling or additional heating as the best explanation for tank thermal behavior.

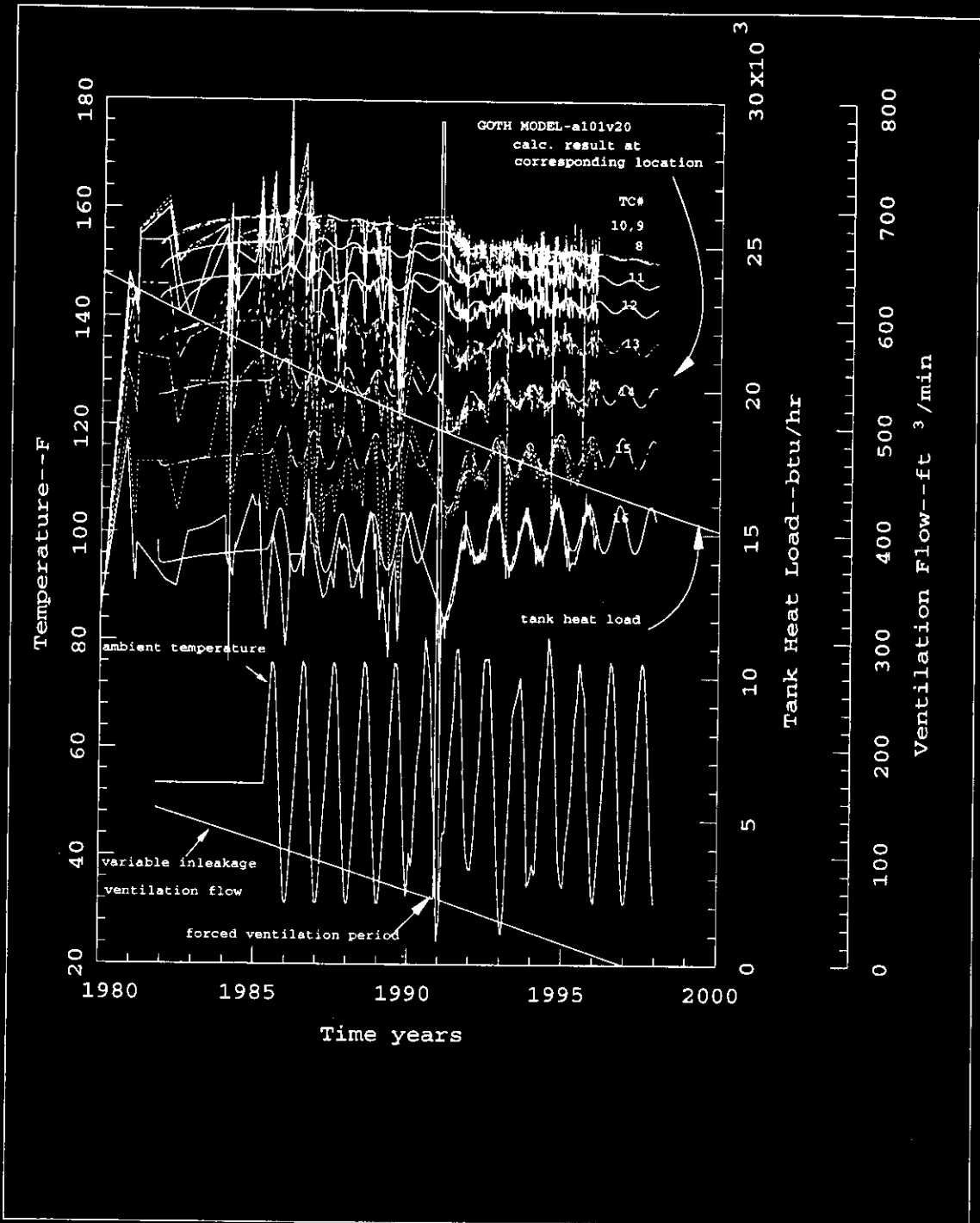


Figure 7.6 Data versus Model--Annual Cycle Meteorology, Variable Inleakage Flow, 30 Year Half Life Radiological Heat Load, Late 1990 Forced Ventilation Period

Simulation versus data comparison at a higher resolution for this case is presented in Figure 7.6. Although the comparison is quite good some adjustments during the time when the forced ventilation system was on would improve the results. In addition changing the assumptions used for the 1980-1990 time period may improve the simulation during the 1990-92 time period due to thermal history effects.

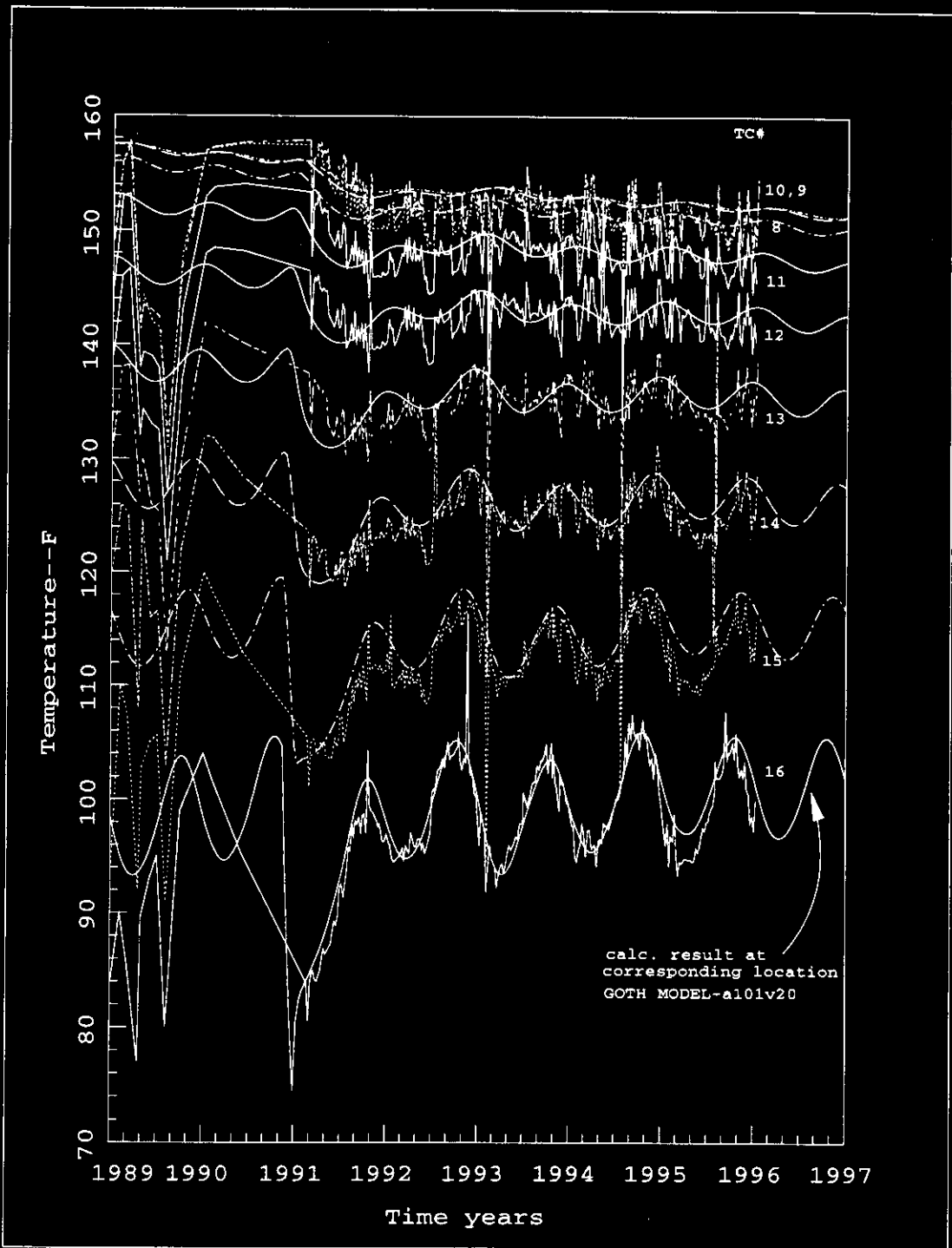


Figure 7.7 Data versus Model--1989 to present, upper axial waste region.

Previous figures did not include waste temperatures below TC# 8. This region of waste is included in Figures 7.7 for TC#6-10 and Figure 7.8 for TC# 1-5. As noted there the calculated temperatures are a little high, but the cool down rates compare reasonably well to the data.

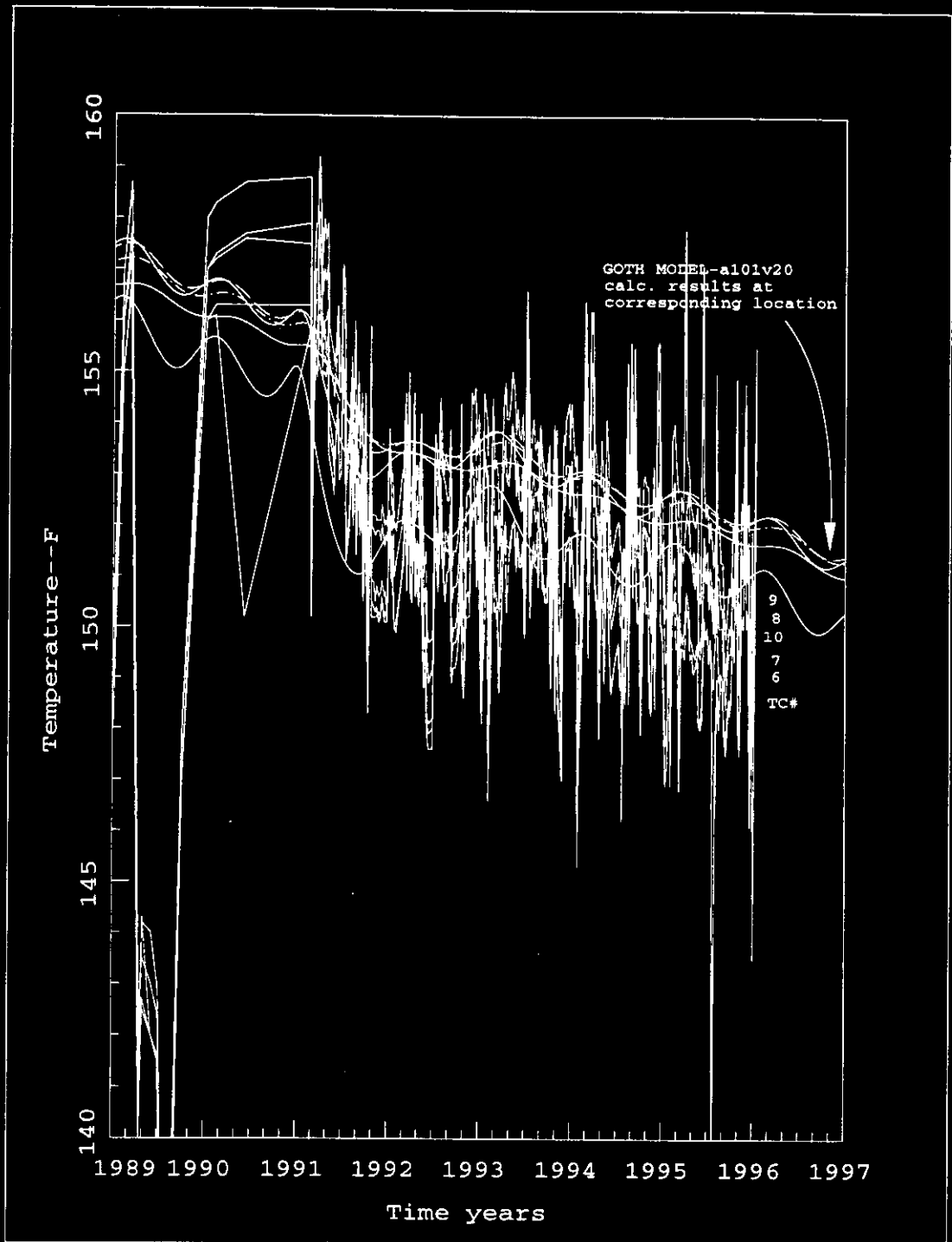


Figure 7.8 Data versus Model--1989 to present, intermediate lower axial waste region

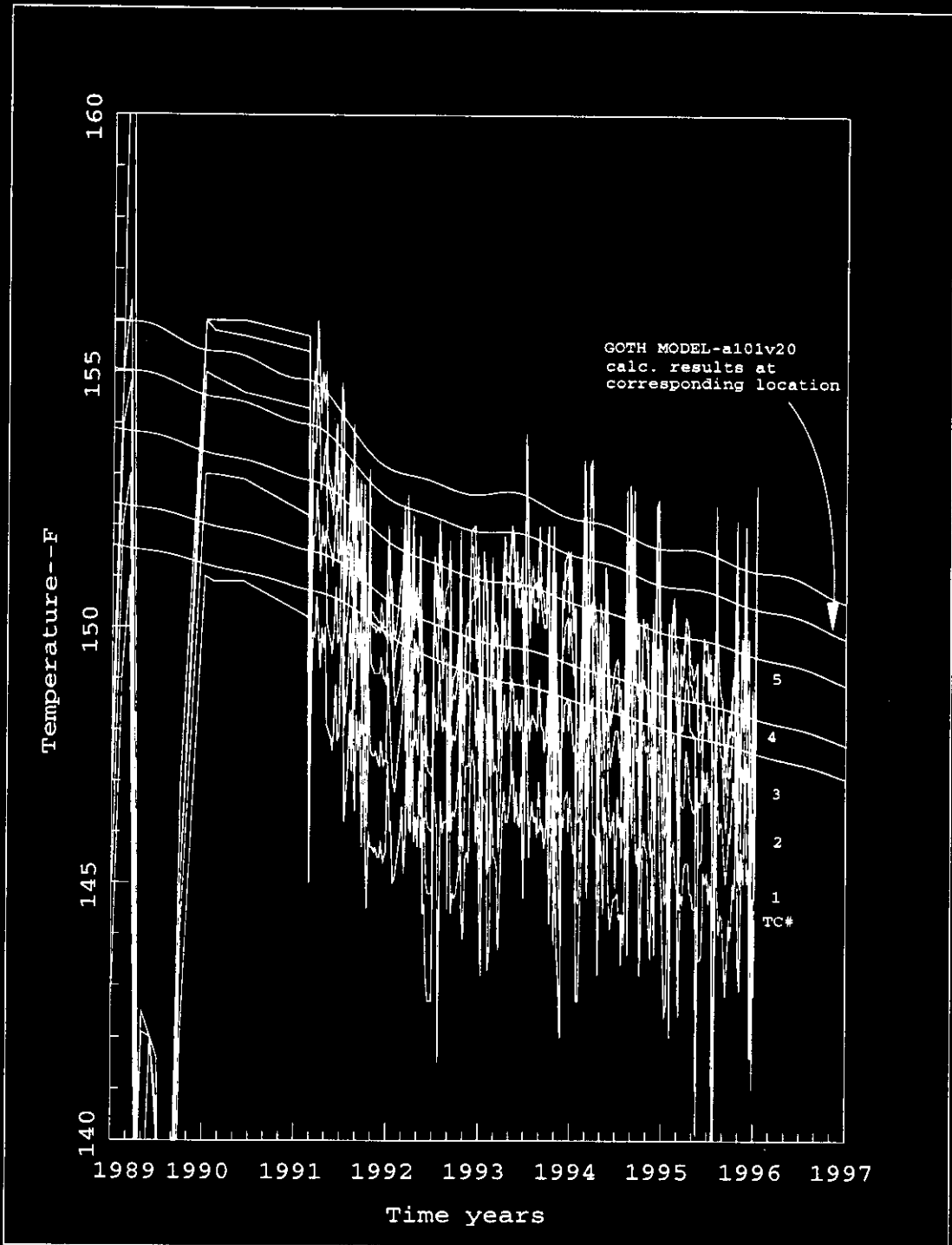


Figure 7.9 Data versus Model--1989 to present, bottom axial waste region

## 8. CONCLUSIONS

The following can be concluded from this thermal hydraulic evaluation:

1. With possible exception of waste near the surface, Tank A-101 waste appears to be slowly cooling based on temperature data, analysis of that data, and comparison to dynamic thermal hydraulic simulations. Consideration of the operation of forced ventilation during 1990, and changes in annual cyclic meteorological conditions, and possible degrading cooling conditions in the dome or increasing heating at the waste surface were considered to arrive at this conclusion.

2. When increasing annual average temperatures are considered, the dome space does not appear to be heating up, neither however is it cooling at any significant rate.

3. Cooling trends within the waste, combined with the lack of an identifiable cooling trend at the surface of the waste/dome space, and a 30 year half life for radiolytic decay, suggests one of two possible phenomena. One possibility is that considerable in-leakage of air occurs at Tank A-101 when the forced ventilation is off. However, if this in-leakage exists, but has been decreasing for some time, then heat removal due to this mechanism will have been decreasing thereby compensating for the decrease in heat load, and thereby keeping time averaged temperatures in the dome relatively steady. A decreasing evaporation rate at the waste surface due to dryout will have the same effect.

Another possibility is that there is increasing heat production at the surface due to chemical reaction at the surface, or heat of salt precipitation. The chemical reaction heat load or heat of precipitation would have to be increasing to compensate for the decrease in

radiolytic decay. The additional heat production would have to be at or near the surface since axial temperature gradients within the sludge are decreasing suggesting decreasing heat generation within the sludge. A third possibility is that as the salt solution concentrates and precipitates heat is given off due to an endothermic heat of solution characteristic. It is not clear what would cause an increase in waste surface chemical reaction, particularly if reactants are being consumed, or what would cause an increase in the heat of solution as evaporation rates decrease with slurry dryout.

4. As a minimum, for Tanks like A-101, thermal hydraulic models which account for forced and natural ventilation and changes in meteorology are required to investigate the potential for heat up.

5. Tank A-101 should be monitored and GOTH simulations based on the actual future meteorology should be compared to the actual future temperature data. If the thermal hydraulic behavior of Tank A-101 is due to decreasing cooling (either sensible air temperature change or evaporation) resulting from inleakage, then when this cooling mechanism is reduced to zero accelerated cooldown of the tank waste and dome space will begin. For inleakage rates of  $1 \text{ ft}^3/\text{sec}$  in 1990, and the rate of decrease required to maintain equilibrium with the radiolytic decay rate, this reduced cooling effect would end in 1997. At that time there would be small changes in the attenuation and phase shift of the temperature in the dome relative to that of the surface temperature oscillation. For higher assumed inleakage rates, the reduced cooling effect will end at a later date.

## 9. REFERENCES

Crowe, R.D., Kummerer, M., & Postma, A.K., 1993, Estimation of Heat Load in Waste Tanks Using Average Vapor Space Temperatures, WHC-EP-0709, Westinghouse Hanford Company, Richland, Washington.

Crowe, R.D., 1995. Internal Memo from R.D. Crowe to J. Meacham, 10/23/95. Subject: A101 Temperature Data, Westinghouse Hanford, Richland, Washington.

Gaddis, L.A., 1994, Supporting Document for the Historical Tank Content Estimate for A Tank Farm, Work Order ER4945, WHC-SD-WM-ER-308, Rev. 0., Prepared by ICF Kaiser Hanford Company for Westinghouse Hanford Company, Richland, WA.

Hoitink, D.J. & Burk, K.W., 1994, Climatological Data Summary 1994, With Historical Data, PNL-10553, UC-603, Pacific Northwest Laboratory, Richland, Washington

Burk, K.W., 1996. Fax 1995 Climatology Data Transmittal from Ken Burk, Pacific Northwest Laboratories, Hanford Meteorological Station, 1/5/96 & 1/10/96, to Don Ogden, Westinghouse Hanford Company, Richland, Washington.

Hanlon, B.M., 1995. Waste Tank Summary Report for Month Ending August 31, 1995. WHC-EP-0182-89, Westinghouse Hanford Company, Richland, Washington.

Drawing Set 1. Drawing H-2-55911, Waste Storage Tanks Composite Section, U.S. Atomic Energy Commission, Hanford Works, Richland, Washington

Drawing Set 2, Drawing H-2-64951 U.S. Research and Development Administration, H-2-62895 U.S. Department of Energy, H-2-69148 U.S. Atomic Energy Commission, Richland, Washington.

Kreith, F., 1973. Principles of Heat Transfer, Harper and Row, Publishers, Inc.

Carslaw, H.S. and Jeager, J.C., 1959. Conduction of Heat in Solids, Second Edition, Oxford University Press, New York.

## DISTRIBUTION SHEET

To Distribution	From D. M. Ogden	Page 1 of 1
		Date March 26, 1996
Project Title/Work Order Thermal Hydraulic Behavior Evaluation of Tank A-101/N2203		EDT No. 613544
		ECN No. N/A

Name	MSIN	Text With All Attach.	Text Only	Attach./ Appendix Only	EDT/ECN Only
H. Babad	S7-30	X			
R. J. Cash	S7-14	X			
R. D. Crowe	H0-38	X			
G. T. Dukelow	S7-14	X			
G. D. Johnson	S7-14	X			
E. J. Lipke	S7-14	X			
J. E. Meacham (10)	S7-14	X			
D. M. Ogden	H0-34				X
L. Stock	S7-14	X			
D. A. Turner	S7-14	X			
J. Zack	S7-14	X			
Central Files (Original + 2)	A3-88	X			
PEA File (Burstad 3)	H0-34	X			